RIVER BEND STATION

PLANT TRANSIENT ANALYSIS METHODOLOGY

EA-PT-91-0003-M

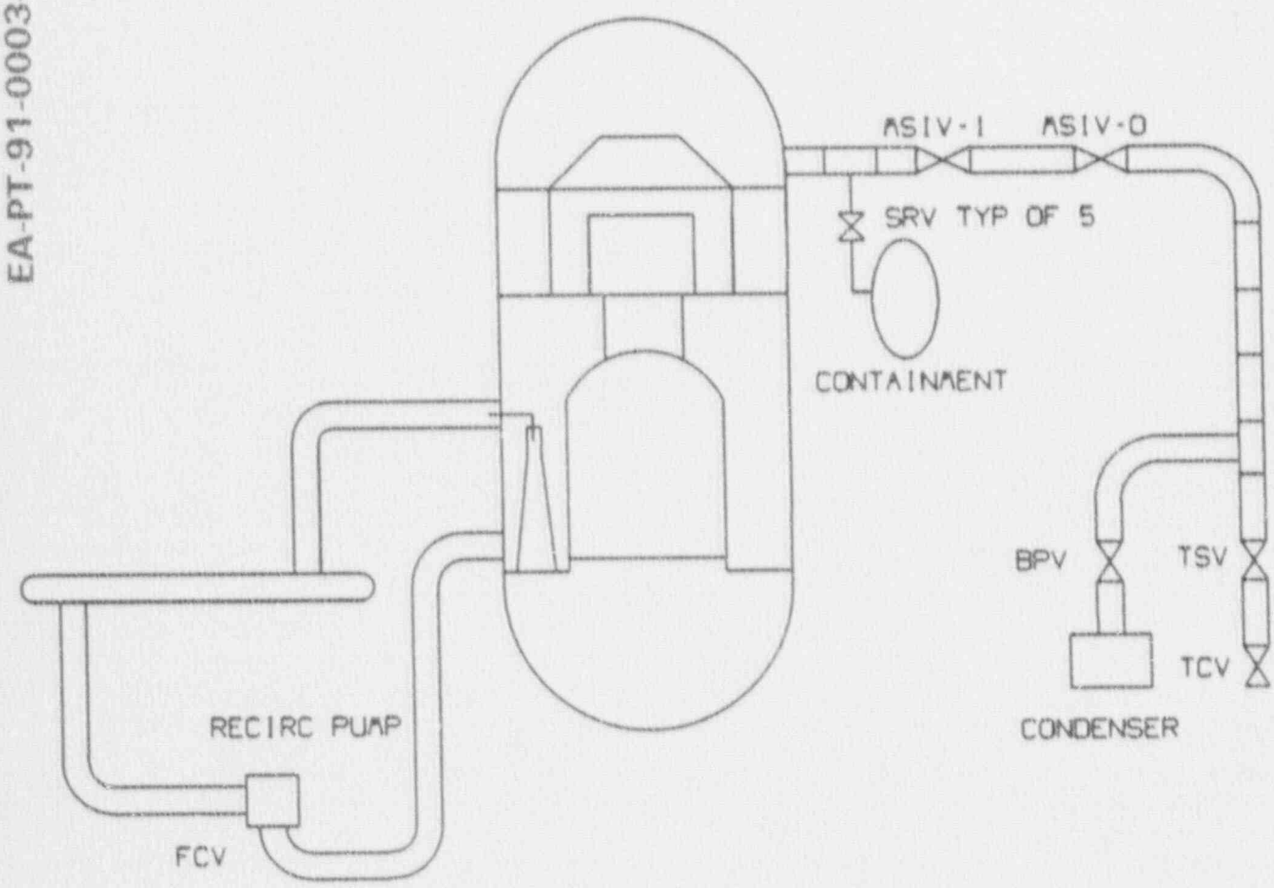

REVISION 0

APRIL 1991

EA-PT-91-0003-M

RIVER BEND STATION
PLANT TRANSIENT ANALYSIS METHODOLOGY

April 1991

Principal Engineer

Thomas W. Oliphant

Contributors

John P. Egan
Lynn A. Leatherwood
Stone S. Luo
David R. Swope

Reviewed: _____
James L. Thompson
Supervisor - Thermal-Hydraulic Analysis

Approved: _____
Joseph S. Miller
Director - Engineering Analysis

Gulf States Utilities Company
River Bend Station
P.O. Box 220
St. Francisville, LA 70775

IMPORTANT NOTICE REGARDING CONTENTS OF THIS DOCUMENT

PLEASE READ CAREFULLY

This document was prepared by Gulf States Utilities Company for the use of the U.S. Nuclear Regulatory Commission in matters regarding the operating license for the River Bend Station. To the best of the issuer's knowledge, this document contains work performed in accordance with sound engineering practice and is a true and accurate representation of the facts.

The work reported herein is the property of Gulf States Utilities Company, and any usage other than as described above is prohibited. Other than for the intended usage, neither Gulf States Utilities Company, nor any of its employees or officers, nor any other person acting on its behalf:

- Makes any warranty or representation, express or implied, with respect to the accuracy, completeness, or usefulness of the information contained in this report, or that the use of any information, apparatus, method, or process disclosed herein would not infringe privately owned rights; or
- Assumes any liabilities with respect to the use of, or for damages resulting from the use of, any information, apparatus, method, or process disclosed in this report.

Acknowledgements

The authors gratefully acknowledge the assistance of Dr. D.A. Prelewicz, B.J. Gitnick, and G.B. Peeler of SCIENTECH, Inc., Dr. A. Ancona of Ancona & Associates, and J.C. Chandler of John Elston Associates in the completion of this project and the preparation of this report.

The authors acknowledge the contribution of Gulf States Utilities (GSU) clerical employees Jerri Fontenot and Nancy Scott and of student engineers Kathy L. Hugle of the University of Louisville and Eric Ballon of the University of Florida.

In addition, the authors acknowledge the support provided by the Core Analysis Group, who provided input data for ESCORE and the one-dimensional reactor kinetics used by RETRAN.

The authors gratefully acknowledge the long-term financial support from Gulf States Utilities; in particular, Mr. Jim Deddens, Mr. Ken Suhrke, and Mr. Mel Sankovich.

Table of Contents

Table of Contents (Continued)

List of Tables

List of Figures

List of Figures (Continued)

List of Figures (Continued)

1.0 INTRODUCTION

This report describes the analytical tools and models to be used by Gulf States Utilities (GSU) for performing transient thermal-hydraulic analyses in support of River Bend Station (RBS). Methods for steady-state core physics analysis have been submitted previously[1].

RBS is a boiling water reactor plant located in West Feliciana Parish, Louisiana. The plant has a Boiling Water Reactor/6 (BWR) Nuclear Steam Supply System (NSSS) designed by General Electric (GE), who currently provides nuclear fuel and analytical services. The architect-engineer functions were performed by Stone & Webster Engineering Corporation. Design features of the plant are shown in Table 1.1.

1.1 SUMMARY

This report describes the computer programs and inputs used to perform analyses of rapid core wide Anticipated Operational Occurrences (AOOs) and the design

basis overpressurization event. These tools will be used in analyses of AOOs and the overpressurization event in support of reload licensing and plant operational changes such as increased core flow. Analyses of loss of feedwater heating, and control rod withdrawal error are performed using steady state methods previously submitted[1]. Analysis of loss of coolant accidents and local events such as control rod drop accidents are not included in this report.

These methods are qualified through benchmark analyses of plant data for RBS and Peach Bottom.

The computer codes used in the transient analysis are described in Section 2.0. This section provides a brief description of the calculations performed by the key software tools used in the GSU methodology.

The RBS RETRAN system model is described in Section 3.0. Basic characteristics of the RETRAN modeling and description of the major input segments are provided.

Supporting analyses covering nuclear cross sections and fuel rod gap conductance are described in Sections 4.0 and 5.0. The results of these analyses have a strong impact on the end result of the thermal-hydraulic transient analysis.

Sections 6.0 and 7.0 report benchmark analyses against data from RBS plant data and the Peach Bottom turbine trip tests. Benchmark analyses cover several RBS operational events, the Peach Bottom turbine trip tests, and a postulated License Basis Transient based on the Peach Bottom tests. These benchmarks demonstrate the capabilities of RETRAN and the GSU methodology to predict a broad spectrum of transient events.

The RETRAN hot channel model is described in Section 8.0. This model is used to predict the performance of potentially limiting assemblies in the core from system effects predicted by the system model.

1.2 METHODOLOGY APPLICATION

The methods described in this report will be used to meet licensing requirements for RBS. Additional information qualifying this application will be provided separately. The separate submittal will describe the methods used in determining an operating limit critical power ratio, calculation of uncertainty factors for the thermal

margin analysis, and applications of the GSU methodology.

1.3 CONCLUSIONS

The RBS RETRAN model provides acceptable representation of plant behavior during transient events within the capabilities of the coding. System phenomena are predicted consistently with measured data by the system model.

Based on the results of the benchmark analyses, it is concluded that the use of the RBS RETRAN model and associated code packages is acceptable for analyzing AOOs and the overpressurization event for reload safety analysis, licensing, and plant operational support activities.

Table 1.1 Design Features

Plant Name	River Bend Station
Plant Type	BWR/6
Rated Thermal Power (MW_t)	2894
Rated Core Flow (Mlbm/hr)	84.5
Rated Steam Flow (Mlbm/hr)	12.45
Recirculation Flow Control Method	Valve Flow Control
Number of Jet Pumps	20
Number of Recirculation Pumps	2
Number of Safety/Relief Valves	16
Number of Control Rods	145
Number of Fuel Bundles	624

2.0 DESCRIPTION OF COMPUTER PROGRAMS

The computer programs used at GSU for reactor transient analysis are described in this section. Figure 2.1 shows how the programs are linked together.

2.1 THE FIBWR STEADY-STATE CORE THERMAL-HYDRAULIC CODE

FIBWR[2,3] evaluates the steady-state thermal-hydraulic performance of BWR cores. FIBWR calculates the flow, void, and pressure distributions for multiple, parallel channels within the core by solving the one-dimensional equations for continuity, momentum, and energy. FIBWR was developed by Yankee Atomic Electric Company under a project sponsored by the Electric Power Research Institute (EPRI).

The GSU methodology uses FIBWR to develop initial core pressure and flow distributions for use in the RETRAN System Model and to develop a response surface to correlate hot bundle flow and core flow for hot channel analyses. FIBWR models have been developed for analyses

of Peach Bottom and RBS reported later in this report. Both models have been benchmarked to plant data.

2.2 THE SIMTRAN-E CROSS SECTION CODE

SIMTRAN-E[4] ("SIMTRAN") generates a one-dimensional cross sections file for use with the space-time kinetics option in RETRAN-02. SIMTRAN extracts nuclear data from restart files written by the three-dimensional nodal simulator code, SIMULATE-E. The nuclear data include macroscopic cross sections and pseudo-cross sections covering delayed neutron fractions and generation factors. Use of SIMULATE-E for core analysis is described in a separate report[1].

SIMTRAN reads three-dimensional, two-group partial cross sections from SIMULATE-E restart files for enough control rod states to characterize the RETRAN problem to be analyzed. Each SIMTRAN analysis requires a SIMULATE-E case with nominal control rod positions for the beginning of the problem. Whenever control rod movement is expected, additional SIMULATE-E cases with all control rods partially and fully inserted into the core are used.

SIMTRAN perturbs the SIMULATE statepoints according to user input to calculate the dependence of each cross section and pseudo-cross section on fuel temperature and moderator density. It then collapses the nuclear data from the SIMULATE three-dimensional representation to a one-dimensional axial cross section set using flux adjoint weighting. SIMTRAN spatially averages the fuel temperatures and moderator densities, correlating the SIMULATE tabular cross sections into polynomial functions of these independent variables at each axial node. These polynomials are of the form:

$$\Sigma_i = CF_{11} + CF_{21}dU + CF_{31}dU^2 + CF_{12}dT_f + CF_{22}dUdT_f + CF_{32}dT_fdU^2$$

where Σ_i = the fitted macroscopic cross section at node i;

CF_{nn} = coefficients calculated by SIMTRAN;

dU = the change in relative nodal moderator density; and

dT_f = the change in the square root of the nodal fuel temperature.

2.3 THE ESCORE FUEL ROD PERFORMANCE CODE

ESCORE[5] calculates the steady-state, thermal-mechanical performance characteristics of a fuel rod. The performance parameters calculated by ESCORE include fuel pellet temperature distribution, fission gas release, gap conductance, internal pressure, cladding stress and strain, power to melt, cladding corrosion, irradiation growth, pellet densification, and stored energy.

ESCORE is used in the GSU methodology to determine gap conductance values for use in the RETRAN system and hot channel analysis.

2.4 THE REBAL INITIALIZATION CODE

The REBAL computer code[6] was developed to facilitate the calculation of consistent thermal-hydraulic initial conditions for RETRAN models of BWR systems. REBAL is used to initialize the RBS RETRAN model for plant transients which are not initiated from rated power and flow conditions.

REBAL solves the steady-state pressure loss and heat balance equations for the reactor vessel, jet pump, and recirculation system, using an iterative procedure to solve for the reactor vessel water densities and pressures at rated conditions. Subsequent cases retain calculated pressure loss coefficients which are held constant as reactor operating conditions vary. These coefficients include the effective separator dryer loss coefficient, the upper downcomer loss coefficient, and a partial loss coefficient for the non-nozzle portion of the recirculation loop losses.

REBAL determines the separator and jet pump characteristics consistently with known component performance curves and measured plant data over a broad range of operating conditions. The jet pump M-N curve, core flow versus drive flow, and core and separator pressure drop versus flow relationships are preserved over a wide range of power and flow states.

2.5 THE RETRAN-02 ONE-DIMENSIONAL TRANSIENT CODE

RETRAN-02[7] ("RETRAN") is the transient thermal-hydraulic computer program used for analysis of AOOs at GSU. The GSU methodology uses RETRAN in two different modes. RETRAN is exercised in the core average mode to determine system response to transient events and in the hot channel mode to evaluate the change in thermal margins.

RETRAN was developed under EPRI sponsorship from RELAP4. RETRAN is a one-dimensional, homogenous equilibrium mixture thermal-hydraulic model with provisions for slip between the vapor and liquid phases. Power generation may be accomplished through a user controlled table of power as a function of time, through solution of the point kinetics equation, or through a more rigorous solution of the one-dimensional neutron diffusion equation. Other user-selectable options include a momentum mixing option for modeling of special components such as valves, separators, and jet pumps. RETRAN also has a capability for extensive modeling of control systems.

Development of RETRAN input is described in Section 3.0 of this report.

2.6 THE EDTRAN OUTPUT EDITOR

EDTRAN[8] is a post-processor code developed by Public Service Electric & Gas Company of New Jersey. EDTRAN reads restart files generated by RETRAN and performs simple output manipulation functions. The options available in EDTRAN are EDIT, LINK, and TCPR.

The EDIT option extracts minor edit information from the RETRAN restart file and prints it in a user-specified format.

The LINK option links the RETRAN system and hot channel models. It extracts the core power, pressure, and flow as functions of time from the restart file and calculates the hot channel power and flow characteristics from user input. The hot channel flow is determined from either a user supplied hot channel flow split as a function of time, or with a user supplied response surface. EDTRAN prints the results of this option in the format of RETRAN hot channel model input deck.

The TCPR option extracts power, flow, pressure, and enthalpy from the RETRAN hot channel restart file and uses the GEXL-Plus critical power correlation[9] to calculate Critical Power Ration (CPR) for specific transients.

Figure 2.1 Transient Analysis Calculational Flow

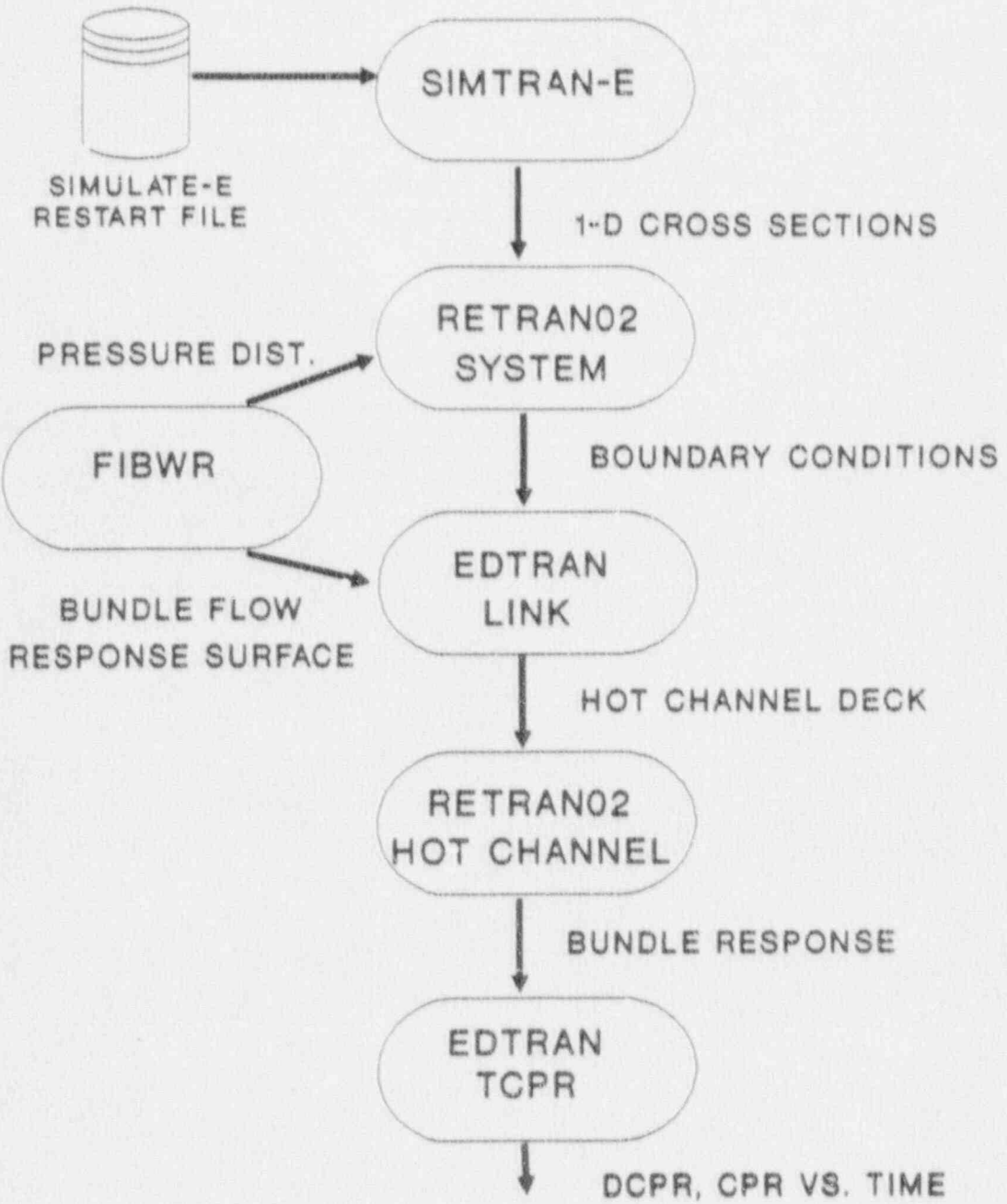

3.0 RBS SYSTEM MODELING

This section describes RETRAN conventions used in modeling the NSSS and connected systems for RBS. In preparing the input for RETRAN the authors familiarized themselves with the program limitations as outlined in the Safety Evaluation Report for RETRAN[7]. The separate hot channel model is described in Section 8.0.

3.1 SYSTEM NODALIZATION

The RBS system model encompasses the reactor core, recirculation loops, main steam lines, turbine control valves, condenser bypass line, and safety/relief valves. As-built geometric and performance data were the primary source for RETRAN input, where such data were unavailable, design information was used. System model nodalization is shown in Figure 3.1. Volume and junction data are given in Tables 3.1 and 3.2.

The system model nodalization was based on the results of a series of parametric studies. Separate studies were performed for the core region, the separa-

tor/dryer/downcomer region, the steam lines, and the recirculation lines. The nodalization shown in Figure 3.1 is sufficiently detailed to be in agreement with the results of finer nodalization schemes[10]. Other benchmark studies[11] also demonstrate agreement with plant data measurements of pressure, flow, and water level.

3.1.1 Vessel Internals

Feedwater enters the vessel via a rill junction located at the middle downcomer, which is consistent with the physical location of the feedwater sparger. Subcooled feedwater mixes with saturated water returning from the steam separators and dryers through the upper downcomer. The combined flow passes into the lower downcomer. The recirculation loops draw from this region, passing a portion of the flow through the recirculation pumps and returning it to the vessel as jet pump drive flow. The recombined fluid is driven through the jet pumps into the lower plenum, from which it proceeds upwards to the core. The flow is again split at the core inlet, where most of the flow enters the active

core. The remainder enters the bypass region. The active core flow cools the nuclear fuel.

These flow components again converge at the core exit and enter the upper plenum. The liquid-vapor mixture travels upwards through the standpipes to the steam separators, where most of the liquid is rejected to the upper downcomer. The steam dryers strip additional liquid from the flow, allowing predominantly dry steam to enter the steam dome. The last volume is a water annulus which connects the dome to the middle downcomer; this region corresponds to the fluid outside the dryer seal skirt. The water annulus and separator are modeled using the bubble rise option. The upper down comer is modeled using the nonequilibrium values option.

3.1.2 Core Region

The core consists of an active core region and a bypass region. Three volumes are used to model the bypass, with two junctions representing leakage flow paths around the lower tie plate and direct from the lower plenum. The active core region consists of 25

axial volumes. The algebraic slip option is used to provide for differences in the velocities of the vapor and liquid phases as they proceed up the channel. The slip option is used in the core region only, and is defeated elsewhere in the model. The profile fit option is used to provide for subcooled boiling for the neutronics calculations. Power is provided to the active core region volumes through heat conductors simulating the fuel cladding. Power generation within the fuel is calculated by solution of the time-dependent diffusion equation in one axial dimension. Power deposition to the bypass region is accomplished through a non-conducting heat exchanger. Heat conductors and power generation are described in Sections 3.2 and 3.3, respectively.

3.1.3 Recirculation Loops

The two physical recirculation loops are combined as a single analytical loop using six fluid volumes and seven junctions. The analytical loop consists of volumes and junctions representing a recirculation pump (with associated pump curves), a flow control valve, a dis-

charge line, the jet pump manifold, the jet pump risers, and the jet pumps. The recirculation pump suction and jet pump driven flow inlet are connected to the lower downcomer, while the jet pump drive flow is fed into the lower plenum. Valve position control and pump power supply (High Frequency Motor Generator [HFMG], Low Frequency Motor Generator [LFMG] or none) are accomplished by control systems. Manufacturer's data for pump performance was used to develop homologous pump curves.

3.1.4 Main Steam Lines

The four main steam lines are lumped into a single equivalent line using 11 fluid volumes and 12 junctions. The length of the longest steam line volume is approximately 50 feet. The line consists of an exit volume from the reactor vessel, a safety relief valve volume, a flow restrictor, two main steam isolation valves, a condenser bypass line, a turbine stop valve, and a turbine control valve. Flow exits the steam line via a negative fill which is administered by a control system.

3.1.5 Steam Bypass Lines

The bypass modeling consists of a bypass valve, line volumes on either side of the valve, and the condenser.

3.1.6 Safety/Relief Valves

All sixteen safety/relief valves are modeled as relief valves in five groups based on their setpoints. Some valves are modeled as low-low set valves. Low-low set valves include additional logic which serves to open and close the valves at lower pressures than the normal relief setpoints. This serves to limit Safety Relief Valve (SRV) cycling to the low-low set valves rather than all of the valves. Relief valves exhaust from the second steam line volume downstream from the vessel into a large volume representing containment.

3.2 HEAT DEPOSITION

The RETRAN options for heat deposition used in the RBS model are powered heat conductors, non-powered heat conductors, and non-conducting heat exchangers. This section describes these heat deposition options. Heat conductor data are shown in Table 3.3.

3.2.1 Powered Conductors

Powered heat conductors are used to represent the fuel rods. Fuel rod information included in the powered heat conductor input includes material and geometry data for the fuel pellet, diametral gap, and cladding. The flux solution from the neutronic model determines the power source in these conductors, which transmit heat to the fluid in the active core volumes. Material properties for the fuel and clad where obtained from standard reference sources. A specific gap heat transfer coefficient was developed using ESCORE as described in Section 5.

3.2.2 Non-Powered Conductors

Non-powered conductors are used for the core shroud, upper plenum, lower plenum, and standpipes. These structures allow storage of heat but contain no power source.

3.2.3 Non-Conducting Heat Exchangers

The non-conducting heat exchanger logic provides direct heat input to a region. This option simulates the power deposition in the bypass region, which is assumed to be 2% of the total core power.

3.3 POWER GENERATION

Transient power generation is calculated by space-time kinetics and the multi-state control rod model. The space-time kinetics option solves the time-dependent neutron diffusion equation in one (axial) dimension. The multi-state control rod model maintains the initial axial

control rod distribution during a scram, moving all of the control rods together until full insertion is reached. These RETRAN options provide the most mechanistic prediction of the axial power shape change during a BWR transient.

Data for the neutronic regions are shown in Table 3.4.

3.4 TRIP LOGIC

The RBS protective systems are characterized by 101 trips. These trips include reactor scram, turbine and feedwater trips, recirculation pump trip and transfer, and safety/relief valve logic. The RBS trips also include logic for event initiation and control system functions. RBS trips are shown in Table 3.5.

3.5 CONTROL SYSTEMS

The control systems used to simulate RBS include an instrumentation section (i.e. sensed process variable), water level measurement, recirculation flow control section, turbine control section, feedwater/level control system, and a miscellaneous edits section. The control schemes are shown in Figures 3.2 through 3.7.

Table 3.1 Control Volume Geometric Information

ID	BUB	IRD	VOL	ZVOL	ZM	FLOWL	FLOWA	DIAMV	ELEV	DESCRIPTION
100	0	0	48.953	0.911	0.911	0.911	65.709	0.366	16.469	CORE INLET SECTION
101	0	0	32.8547	0.500	0.500	0.500	65.7093	0.0428	17.380	CORE VOLUME 1
102	0	0	32.8547	0.500	0.500	0.500	65.7093	0.0428	17.880	CORE VOLUME 2
103	0	0	32.8547	0.500	0.500	0.500	65.7093	0.0428	18.380	CORE VOLUME 3
104	0	0	32.8547	0.500	0.500	0.500	65.7093	0.0428	18.880	CORE VOLUME 4
105	0	0	32.8547	0.500	0.500	0.500	65.7093	0.0428	19.380	CORE VOLUME 5
106	0	0	32.8547	0.500	0.500	0.500	65.7093	0.0428	19.880	CORE VOLUME 6
107	0	0	32.8547	0.500	0.500	0.500	65.7093	0.0428	20.380	CORE VOLUME 7
108	0	0	32.8547	0.500	0.500	0.500	65.7093	0.0428	20.880	CORE VOLUME 8
109	0	0	32.8547	0.500	0.500	0.500	65.7093	0.0428	21.380	CORE VOLUME 9
110	0	0	32.8547	0.500	0.500	0.500	65.7093	0.0428	21.880	CORE VOLUME 10
111	0	0	32.8547	0.500	0.500	0.500	65.7093	0.0428	22.380	CORE VOLUME 11
112	0	0	32.8547	0.500	0.500	0.500	65.7093	0.0428	22.880	CORE VOLUME 12
113	0	0	32.8547	0.500	0.500	0.500	65.7093	0.0428	23.380	CORE VOLUME 13
114	0	0	32.8547	0.500	0.500	0.500	65.7093	0.0428	23.880	CORE VOLUME 14
115	0	0	32.8547	0.500	0.500	0.500	65.7093	0.0428	24.380	CORE VOLUME 15
116	0	0	32.8547	0.500	0.500	0.500	65.7093	0.0428	24.880	CORE VOLUME 16
117	0	0	32.8547	0.500	0.500	0.500	65.7093	0.0428	25.380	CORE VOLUME 17
118	0	0	32.8547	0.500	0.500	0.500	65.7093	0.0428	25.880	CORE VOLUME 18
119	0	0	32.8547	0.500	0.500	0.500	65.7093	0.0428	26.380	CORE VOLUME 19
120	0	0	32.8547	0.500	0.500	0.500	65.7093	0.0428	26.880	CORE VOLUME 20
121	0	0	32.8547	0.500	0.500	0.500	65.7093	0.0428	27.380	CORE VOLUME 21
122	0	0	32.8547	0.500	0.500	0.500	65.7093	0.0428	27.880	CORE VOLUME 22
123	0	0	32.8547	0.500	0.500	0.500	65.7093	0.0428	28.380	CORE VOLUME 23
124	0	0	32.8547	0.500	0.500	0.500	65.7093	0.0428	28.880	CORE VOLUME 24
125	0	0	32.8547	0.500	0.500	0.500	65.7093	0.0428	29.380	CORE VOLUME 25
126	0	0	88.471	1.198	1.198	1.198	73.829	0.050	29.880	CORE OUTLET SECTION
141	0	0	47.8928	0.911	0.911	0.911	52.5712	0.1553	16.469	CORE BYPASS VOL. 1
142	0	0	657.1398	12.500	12.500	12.500	52.5712	0.1553	17.380	CORE BYPASS VOL. 2
144	0	0	62.9803	1.198	1.198	1.198	52.5712	0.1553	29.880	CORE BYPASS VOL. 3
200	0	0	3185.000	16.469	16.469	24.460	75.38	51.699	0.0	LOWER PLENUM

Table 3.1 Control Volume Geometric Information (Continued)

ID	BUB	IRD	VOL	ZVOL	ZM	FLOWL	FLOWA	DIAMV	ELEV	DESCRIPTION
210	0	0	938.000	5.100	5.100	5.100	183.922	1.303	31.078	UPPER PLENUM
220	0	0	274.620	5.905	5.905	5.905	46.507	0.5298	36.178	STANDPIPES
230	1	0	744.380	7.533	6.53187	7.533	102.790	0.2647	42.083	STEAM SEPARATORS
232	0	0	784.951	7.406	7.406	7.406	105.989	0.0833	52.021	STEAM DRYER
234	0	0	2861.900	17.292	17.292	29.240	97.876	6.4780	52.021	VESSEL DOME
240	2	0	1426.611	12.391	3.10524	2.405	232.578	0.7460	42.083	UPPER DOWNCOMER*
244	3	0	284.349	9.604	3.12889	9.604	29.607	1.0625	42.417	WATER ANNULUS
250	0	0	1335.570	7.275	7.275	7.542	177.079	1.9440	35.142	MIDDLE DOWNCOMER
256	0	0	1489.800	24.017	24.017	30.716	48.502	1.4550	11.125	LOWER DOWNCOMER
300	0	0	181.692	33.002	33.002	51.237	3.546	1.5025	-18.376	RECIRC SUCTION
305	0	0	64.100	2.418	2.418	9.015	3.546	0.7513	-15.958	RECIRC PUMP
311	0	0	157.210	20.736	20.736	44.333	3.546	1.5025	-15.043	RECIRC PUMP DISCHARGE
315	0	0	85.977	1.197	1.197	11.773	7.303	1.2116	5.693	RECIRC MANIFOLD
320	0	0	152.184	20.980	20.980	30.508	4.988	0.7953	6.890	RECIRC RISER
325	0	0	159.351	14.818	14.818	14.818	20.058	0.8772	10.938	JET PUMPS
500	0	0	336.290	26.336	26.336	33.155	10.143	1.797	27.500	STEAM LINE VOL. 1
501	0	0	204.787	1.797	1.797	20.190	10.143	1.797	26.391	STEAM LINE VOL. 2
502	0	0	126.706	1.797	1.797	12.492	10.143	1.797	26.164	STEAM LINE VOL. 3
504	0	0	510.526	2.318	2.318	50.333	10.143	1.797	25.643	STEAM LINE VOL. 4
506	0	0	438.028	5.521	5.521	43.185	10.143	1.797	21.919	STEAM LINE VOL. 5
508	0	0	438.028	5.521	5.521	43.185	10.143	1.797	18.195	STEAM LINE VOL. 6
510	0	0	438.028	5.521	5.521	43.185	10.143	1.797	14.471	STEAM LINE VOL. 7
511	0	0	438.028	5.521	5.521	43.185	10.143	1.797	10.747	STEAM LINE VOL. 8
512	0	0	229.787	3.257	3.257	3.257	16.663	3.257	10.017	TURBINE HEADER
513	0	0	280.164	2.443	2.443	27.622	10.143	1.797	10.102	STEAM LINE VOL. 9
514	0	0	101.610	7.982	7.982	10.017	10.143	1.797	3.917	STEAM LINE VOL. 10
600	0	0	113.356	3.948	3.948	78.364	1.446	0.227	12.151	STEAM BYPASS VOL 1
602	0	0	156.780	17.307	17.307	151.190	1.037	0.190	-5.156	STEAM BYPASS VOL 2
650	0	1	10000.0	20.000	20.000	20.000	500.000	14.300	-14.750	CONDENSER
900	0	2	1.43E+6	186.250	186.250	177.000	8080.000	101.000	-32.000	CONTAINMENT

*Indicates non-equilibrium volume option

Table 3.2 Junction Geometric Information

JUN	FROM	TO	AREA	JUNELEV	JUNINRT	KFLOSSC	HYDIA	DESCRIPTION
100	200	100	18.4140	16.469	0.00	-1.0000	0.1940	CORE INLET
101	100	101	65.7093	17.380	0.00	-1.0000	0.0428	CORE JUNCTION
102	101	102	65.7093	17.880	0.00	-1.0000	0.0428	CORE JUNCTION
103	102	103	65.7093	18.380	0.00	-1.0000	0.0428	CORE JUNCTION
104	103	104	65.7093	18.880	0.00	-1.0000	0.0428	CORE JUNCTION
105	104	105	65.7093	19.380	0.00	-1.0000	0.0428	CORE JUNCTION
106	105	106	65.7093	19.880	0.00	-1.0000	0.0428	CORE JUNCTION
107	106	107	65.7093	20.380	0.00	-1.0000	0.0428	CORE JUNCTION
108	107	108	65.7093	20.880	0.00	-1.0000	0.0428	CORE JUNCTION
109	108	109	65.7093	21.380	0.00	-1.0000	0.0428	CORE JUNCTION
110	109	110	65.7093	21.880	0.00	-1.0000	0.0428	CORE JUNCTION
111	110	111	65.7093	22.380	0.00	-1.0000	0.0428	CORE JUNCTION
112	111	112	65.7093	22.880	0.00	-1.0000	0.0428	CORE JUNCTION
113	112	113	65.7093	23.380	0.00	-1.0000	0.0428	CORE JUNCTION
114	113	114	65.7093	23.880	0.00	-1.0000	0.0428	CORE JUNCTION
115	114	115	65.7093	24.380	0.00	-1.0000	0.0428	CORE JUNCTION
116	115	116	65.7093	24.880	0.00	-1.0000	0.0428	CORE JUNCTION
117	116	117	65.7093	25.380	0.00	-1.0000	0.0428	CORE JUNCTION
118	117	118	65.7093	25.880	0.00	-1.0000	0.0428	CORE JUNCTION
119	118	119	65.7093	26.380	0.00	-1.0000	0.0428	CORE JUNCTION
120	119	120	65.7093	26.880	0.00	-1.0000	0.0428	CORE JUNCTION
121	120	121	65.7093	27.380	0.00	-1.0000	0.0428	CORE JUNCTION
122	121	122	65.7093	27.880	0.00	-1.0000	0.0428	CORE JUNCTION
123	122	123	65.7093	28.380	0.00	-1.0000	0.0428	CORE JUNCTION
124	123	124	65.7093	28.880	0.00	-1.0000	0.0428	CORE JUNCTION
125	124	125	65.7093	29.380	0.00	-1.0000	0.0428	CORE JUNCTION
126	125	126	65.7093	29.880	0.00	-1.0000	0.0428	CHIMNEY
139	100	141	2.5540	17.008	0.00	-1.0000	0.0030	LOWER TIE PLATE TO BYPASS
141	200	141	1.7930	16.469	0.00	37.6900	0.1553	LOWER PLENUM TO BYPASS
142	141	142	52.5712	17.380	0.00	0.0000	0.1553	BYPASS JUNCTION
144	142	144	52.5712	29.880	0.00	0.0000	0.1553	BYPASS JUNCTION
200	325	200	19.7330	10.938	0.00	-1.0000	1.1210	JET PUMPS TO LOWER PLENUM
210	126	210	54.2820	31.078	0.00	-1.0000	0.0270	CHIMNEY TO UPPER PLENUM

Table 3.2 Junction Geometric Information (Continued)

JUN	FROM	TO	AREA	JUNELEV	JUNINRT	KFLOSSC	HYDIA	DESCRIPTION
212	144	210	16.4150	31.078	0.00	-1.0000	0.0890	BYPASS TO UPPER PLENUM
220	210	220	46.5070	36.178	0.08	0.3780	0.5300	UPPER PLENUM TO STAND PIPES
230	220	230	46.5070	42.083	0.16	-1.0000	0.5300	STAND PIPES TO SEPARATORS
232	240	232	82.2470	52.021	0.04	0.3230	0.6630	STEAM DRYER INLET
233	230	240	72.9180	49.616	0.17	-1.0000	0.7310	SEPARATOR EXIT
234	232	234	82.2470	55.724	0.18	-1.0000	2.2320	STEAM DRYER TO DOME
235	244	234	15.3150	52.021	0.00	0.5000	0.5420	WATER ANNULUS TO DOME
240	230	240	16.7580	42.104	0.00	-1.0000	0.0630	SEPARATOR TO UPPER DOWNCOMER
244	250	244	29.6070	42.417	0.00	0.0000	1.0620	MIDDLE DC - WATER ANNULUS
250	0	250	10.0000	40.287	0.00	0.0000	0.9770	FEEDWATER
252	240	250	112.8450	42.083	0.00	-1.0000	0.7310	UPPER DC TO MIDDLE DC
256	250	256	58.5170	35.142	0.00	-1.0000	2.1670	MIDDLE DC TO LOWER DC
300	256	300	3.5460	13.875	0.00	0.5896	1.5020	LOWER DC TO RECIRC SUCTION
315	300	305	3.5460	-15.958	0.00	-1.0000	1.5020	RECIRC SUCTION TO PUMP
311	305	311	3.5460	-14.292	7.52	-370.0000	1.5020	RECIRC FLOW CONTROL VALVE
315	311	315	3.5460	5.693	0.00	0.9050	1.5020	RECIRC DISCHARGE TO MANIFOLD
320	315	320	4.9680	6.890	0.00	0.8940	0.7950	MANIFOLD TO RISER
325	320	325	0.6960	25.756	0.00	-1.0000	0.0940	RISER TO JP (DRIVE FLOW)
327	256	325	3.2300	25.756	0.00	0.0640	0.2120	LOWER DC TO JET PUMP
500	234	500	10.1430	52.938	0.00	0.2385	1.7970	DOME TO STEAM LINE
501	500	501	10.1430	27.884	0.00	0.4160	1.7970	STEAM LINE
502	501	502	2.6590	27.289	0.00	0.1193	0.9200	FLOW RESTRICTOR
504	502	504	10.1430	27.062	0.00	1.1897	1.7970	INBOARD MSIV
506	504	506	10.1430	26.541	0.00	1.0207	1.7970	OUTBOARD MSIV
508	506	508	10.1430	22.817	0.00	0.4479	1.7970	STEAM LINE
510	508	510	10.1430	19.093	0.00	0.4094	1.7970	STEAM LINE
511	510	511	10.1430	15.369	0.00	0.4207	1.7970	STEAM LINE
512	511	512	10.1430	11.645	0.00	-1.0000	1.7970	TURBINE HEADER
513	512	513	10.1430	11.645	0.00	0.2319	1.7970	STEAM LINE
514	513	514	10.1430	11.000	0.00	0.8263	1.5210	TSV
516	0	514	10.0000	3.917	0.00	2.5128	1.4580	TCV
600	512	600	1.4110	12.398	0.00	0.7900	0.9480	BYPASS LINE
602	600	602	0.2510	12.151	100.67	-275.0000	0.2950	BYPASS VALVE

Table 3.2 Junction Geometric Information (Continued)

JUN	FROM	TO	AREA	JUNELEV	JUNINRT	KFLOSSC	HYDIA	DESCRIPTION
650	602	650	1.0370	-4.750	0.00	99.1670	0.8120	INLET TO CONDENSER
910	501	900	0.1144	27.951	0.00	0.6400	0.3820	GROUP 1 S/RV
912	501	900	0.1144	27.951	0.00	0.6400	0.3820	GROUP 2 S/RV
914	501	900	0.3432	27.951	0.00	0.6400	0.3820	GROUP 3 S/RV
916	501	900	0.4576	27.951	0.00	0.6400	0.3820	GROUP 4 S/RV
918	501	900	0.8009	27.951	0.00	0.6400	0.3820	GROUP 5 S/RV

Table 3.3 Heat Conductor Information

ID	ISL	ISR	ASUL	ASUR	VOLS	HDML	HDMR	DHEL	DHER	CHNL	CHNR		
101	0		101	0	2417.71	24.3282	0	0	0	0.0544	0	0.5	
102	0		102	0	2417.71	24.3282	0	0	0	0.0544	0	0.5	
103	0		103	0	2417.71	24.3282	0	0	0	0.0544	0	0.5	
104	0		104	0	2417.71	24.3282	0	0	0	0.0544	0	0.5	
105	0		105	0	2417.71	24.3282	0	0	0	0.0544	0	0.5	
106	0		106	0	2417.71	24.3282	0	0	0	0.0544	0	0.5	
107	0		107	0	2417.71	24.3282	0	0	0	0.0544	0	0.5	
108	0		108	0	2417.71	24.3282	0	0	0	0.0544	0	0.5	
109	0		109	0	2417.71	24.3282	0	0	0	0.0544	0	0.5	
110	0		110	0	2417.71	24.3282	0	0	0	0.0544	0	0.5	
111	0		111	0	2417.71	24.3282	0	0	0	0.0544	0	0.5	
112	0		112	0	2417.71	24.3282	0	0	0	0.0544	0	0.5	
113	0		113	0	2417.71	24.3282	0	0	0	0.0544	0	0.5	
114	0		114	0	2417.71	24.3282	0	0	0	0.0544	0	0.5	
115	0		115	0	2417.71	24.3282	0	0	0	0.0544	0	0.5	
116	0		116	0	2417.71	24.3282	0	0	0	0.0544	0	0.5	
117	0		117	0	2417.71	24.3282	0	0	0	0.0544	0	0.5	
118	0		118	0	2417.71	24.3282	0	0	0	0.0544	0	0.5	
119	0		119	0	2417.71	24.3282	0	0	0	0.0544	0	0.5	
120	0		120	0	2417.71	24.3282	0	0	0	0.0544	0	0.5	
121	0		121	0	2417.71	24.3282	0	0	0	0.0544	0	0.5	
122	0		122	0	2417.71	24.3282	0	0	0	0.0544	0	0.5	
123	0		123	0	2417.71	24.3282	0	0	0	0.0544	0	0.5	
124	0		124	0	2417.71	24.3282	0	0	0	0.0544	0	0.5	
125	0		125	0	2417.71	24.3282	0	0	0	0.0544	0	0.5	
241	141		256	43.225	44.18	7.291	0.17	1.464	4.675	4.001	0.911	0.911	
242	142		256	593.093	606.196	100.039	0.17	1.464	4.675	4.001	12.5	12.5	
244	144		256	56.842	58.098	9.588	0.17	1.464	4.675	4.001	1.198	1.198	

Table 3.4 RETRAN Core Neutronic Region Information

REGION ID	MESH INTERVAL	CORE VOLUME	CORE CONDUCTOR	REGION ELEVATION	REGION HEIGHT
1	24	100	0	0.911	0.911
2	12	101	1	1.411	0.500
3	12	102	2	1.911	0.500
4	12	103	3	2.411	0.500
5	12	104	4	2.911	0.500
6	12	105	5	3.411	0.500
7	12	106	6	3.911	0.500
8	12	107	7	4.411	0.500
9	12	108	8	4.911	0.500
10	12	109	9	5.411	0.500
11	12	110	10	5.911	0.500
12	12	111	11	6.411	0.500
13	12	112	12	6.911	0.500
14	12	113	13	7.411	0.500
15	12	114	14	7.911	0.500
16	12	115	15	8.411	0.500
17	12	116	16	8.911	0.500
18	12	117	17	9.411	0.500
19	12	118	18	9.911	0.500
20	12	119	19	10.411	0.500
21	12	120	20	10.911	0.500
22	12	121	21	11.411	0.500
23	12	122	22	11.911	0.500
24	12	123	23	12.411	0.500
25	12	124	24	12.911	0.500
26	12	125	25	13.411	0.500
27	36	126	0	14.609	1.198

Table 3.5 RBS Trip Control Data

CARD #	IDTRP	IDSIG	IX1	IX2	SETPT	DELAY	DESCRIPTION
040010	1	1	0	0	0.0	0.0	*PROBLEM END TIME *
040020	2	-14	10	0	450.0	0.0	*HFMG TO LFMG PERMISSVE*
040030	3	1	0	0	0.0	0.0	*1/3 ELEMENT SELECT *
040040	5	1	0	0	0.0	0.0	*FW MATS VLV DEMAND *
040050	6	1	0	0	0.0	0.0	*BPV INHIBITOR SWITCH *
040060	7	1	0	0	1.E+7	0.0	*MSTR CNTRLR MATS *
040070	8	14	-310	0	110.0	0.0	*SPAN ANTIWINDUP *
040080	-8	-14	-310	0	110.0	0.0	*SPAN ANTIWINDUP RESET *
040090	9	14	-328	0	102.5	0.0	*FLX CNTRLR HI ANTI *
040100	-9	-14	-328	0	102.5	0.0	*FLX CNTR HI ANTI RESET*
040110	10	-14	-328	0	48.0	0.0	*FLX CNTRLR LO ANTI *
040120	-10	14	-328	0	48.0	0.0	*FLX CNTR LO ANTI RESET*
040130	11	1	0	0	1.E+7	0.0	*FLUX CNTRLR MATS *
040140	12	1	0	0	1.E+7	0.0	*LOOP CNTRLR MATS *
040150	13	1	0	0	1.E+7	0.0	*FW LOSS OF HEATING *
040160	50	1	0	0	1.E+7	0.0	*MANUAL 1-FWP TRIP *
040170	51	1	0	0	1.E+7	0.0	*MANUAL 3-FWP TRIP *
040180	52	1	0	0	1.E+7	0.0	*MANUAL TSV CLOSURE *
040190	53	1	0	0	1.E+7	0.0	*MANUAL MSIV CLOSURE *
040200	54	1	0	0	0.0	0.0	*MSIV SCRAM PERMISSIVE *
040210	55	1	0	0	1.E+7	0.0	*MANUAL REACTOR SCRAM *
040220	56	14	-140	0	51.0	0.0	*HIGH LEVEL-8 *
040230	57	-14	-140	0	31.8	0.0	*LOW LEVEL-4 *
040240	58	-14	-140	0	9.7	0.0	*LOW LEVEL-3 *
040250	59	-14	-146	0	-43.0	0.0	*LOW LEVEL-2 *
040260	60	-14	-146	0	-143.0	0.0	*LOW LEVEL-1 *
040270	61	14	-6	0	0.0	0.0	*HIGH REACTOR FLUX *
040280	62	14	-5	0	0.0	0.0	*HIGH SIM THERM POWER *
040290	63	14	-7	0	1079.4	0.0	*HIGH DOME PRES SCRAM *
040300	64	-14	-10	0	20.0	0.0	*LOW FEED WATER FLOW *
040310	65	-14	-368	0	26.0	0.0	*MINIMUM FCV POSITION *
040320	66	14	-3	0	40.0	0.0	*TURB PRES PERMISSIVE *
040330	-66	-14	-3	0	40.0	0.0	*TURB PRES PERMISSIVE *

Table 3.5 RBS Trip Control Data (Continued)

CARD #	IDTRP	IDSIG	IX1	IX2	SETPT	DELAY	DESCRIPTION
040340	67	14	-19	0	140.0	0.0	*HIGH STEAMLINE FLOW *
040350	68	-14	-9	0	863.7	0.0	*LOW STEAMLINE PRESSURE*
040360	71	1	0	0	1.E+7	0.0	*MANUAL 2 OF 2 RPT TRIP*
040370	72	1	0	0	1.E+7	0.0	*MANUAL 1 OF 2 RPT TRIP*
040380	73	14	-7	0	1141.7	0.0	*HI DOME PRES ATWS RPT *
040390	74	1	0	0	1.E+7	0.0	*MAN TCV FAST CLOSURE *
040400	75	-14	-100	3	0.0	0.0	*LOW FW FLOW (HF-LF MG)*
040410	105	12	52	0	0.0	0.0	*TSV CLOSURE SIGNAL *
040420	105	12	56	0	0.0	0.0	*TSV CLOSURE SIGNAL *
040430	105	12	69	0	0.0	0.0	*TSV CLOSURE SIGNAL *
040440	106	12	105	0	0.0	0.1	*LIMITER SET TO ZERO *
040450	107	12	105	0	0.0	0.05	*TCV FAST CLOSURE *
040460	107	12	70	0	0.0	0.0	*TCV FAST CLOSE SIGNAL *
040470	107	12	74	0	0.0	0.0	*TCV FAST CLOSE SIGNAL *
040486	108	12	107	0	0.0	0.1	*LOAD REFERENCE TO ZERO*
040490	109	12	105	0	0.0	0.1	*BPV FAST OPEN SIGNAL *
040500	109	12	107	0	0.0	0.1	*BPV FAST OPEN SIGNAL *
040510	110	12	53	0	0.0	0.5	*MSIV CLOSURE SIGNAL *
040520	110	12	60	0	0.0	0.5	*MSIV CLOSURE SIGNAL *
040530	110	12	67	0	0.0	0.5	*MSIV CLOSURE SIGNAL *
040540	110	12	68	0	0.0	0.5	*MSIV CLOSURE SIGNAL *
040550	111	12	105	107	0.0	0.0	*EOC-RPT LOGIC *
040560	112	13	66	111	0.0	0.0	*EOC-RPT LOGIC *
040570	116	13	65	75	0.0	15.0	*HFMG TO LFMG LOGIC *
040580	117	12	58	0	0.0	0.14	*HFMG TO LFMG LOGIC *
040590	117	12	1**	-	0.0	0.14	*HFMG TO LFMG LOGIC *
040600	117	12	116	0	0.0	0.0	*HFMG TO LFMG LOGIC *
040610	118	13	2	117	0.0	0.0	*HFMG TO LFMG LOGIC *
040620	120	12	50	0	0.0	0.0	*FCV RUNBACK LOGIC *
040630	120	12	51	0	0.0	0.0	*FCV RUNBACK LOGIC *
040640	120	12	64	0	0.0	0.0	*FCV RUNBACK LOGIC *
040650	121	13	57	120	0.0	0.1	*FCV RUNBACK SIGNAL *

Table 3.5 RBS Trip Control Data (Continued)

CARD #	IDTRP	IDSIG	IX1	IX2	SETPT	DELAY	DESCRIPTION
040660	122	12	59	73	0.0	0.1	*ATWS-RPT SIGNAL *
040670	122	12	71	0	0.0	0.0	*ATWS-RPT SIGNAL *
040680	123	12	51	56	0.0	0.01	*FW PUMP TRIP *
040690	124	12	117	121	0.0	0.0	*LOOP CNTRLR TO MANUAL *
040700	130	12	55	0	0.0	0.05	*SCRAM SIGNAL *
040710	130	12	56	0	0.0	0.05	*SCRAM SIGNAL *
040720	130	12	58	0	0.0	0.05	*SCRAM SIGNAL *
040730	130	12	61	0	0.0	0.05	*SCRAM SIGNAL *
040740	130	12	62	0	0.0	0.05	*SCRAM SIGNAL *
040750	130	12	63	0	0.0	0.05	*SCRAM SIGNAL *
040760	130	13	54	110	0.0	0.41	*SCRAM SIGNAL *
040770	130	13	66	105	0.0	0.068	*SCRAM SIGNAL *
040780	130	13	66	107	0.0	0.07	*SCRAM SIGNAL *
040790	135	12	59	0	0.0	0.0	*RCIC ON/OFF SIGNAL *
040800	-135	14	-140	0	51.0	0.0	*RCIC ON/OFF SIGNAL *
040810	136	12	59	0	0.0	0.0	*HPCS ON/OFF SIGNAL *
040820	-136	14	-140	0	51.0	0.0	*HPCS ON/OFF SIGNAL *
040830	137	12	60	0	0.0	0.0	*LPCS START SIGNAL *
040840	180	4	234	0	1117.7	0.4	*LOW-LOW SET PERMISSIVE*
040850	181	4	234	0	1047.7	0.4	*GR-1 SRV LSS OPEN PRES*
040860	182	13	180	181	0.0	0.0	*GR-1 SRV OPEN *
040870	-181	-4	234	0	940.7	1.2	*GR-1 SRV LSS CLSE PRES*
040880	-182	-4	234	0	940.7	1.2	*GR-1 SRV CLOSE *
040890	183	4	234	0	1087.7	0.4	*GR-2 SRV LSS OPEN PRES*
040900	184	13	180	183	0.0	0.0	*GR-2 SRV OPEN *
040910	-183	-4	234	0	950.7	1.2	*GR-2 SRV LSS CLSE PRES*
040920	-184	-4	234	0	950.7	1.2	*GR-2 SRV CLOSE *
040930	185	4	234	0	1127.7	0.4	*GR-3 SRV LSS OPEN PRES*
040940	186	13	180	185	0.0	0.0	*GR-3 SRV OPEN *
040950	-185	-4	234	0	960.7	1.2	*GR-3 SRV LSS CLSE PRES*
040960	-186	-4	234	0	960.7	1.2	*GR-3 SRV CLOSE *

Table 3.5 RBS Trip Control Data (Continued)

CARD #	IDTRP	IDSIG	IX1	IX2	SETPT	DELAY	DESCRIPTION	
040970	187	4	234	0	1127.7	0.4	*GR-4 SRV OPEN	*
040980	-187	-4	234	0	1027.7	1.2	*GR-4 SRV CLOSE	*
040990	188	4	234	0	1137.7	0.4	*GR-5 SRV OPEN	*
041000	-188	-4	234	0	1037.7	1.2	*GR-5 SRV CLOSE	*
049990	99	1	0	0	-1.0	0.0	*START MCHX	*

Figure 3.1 RBS System Nodalization

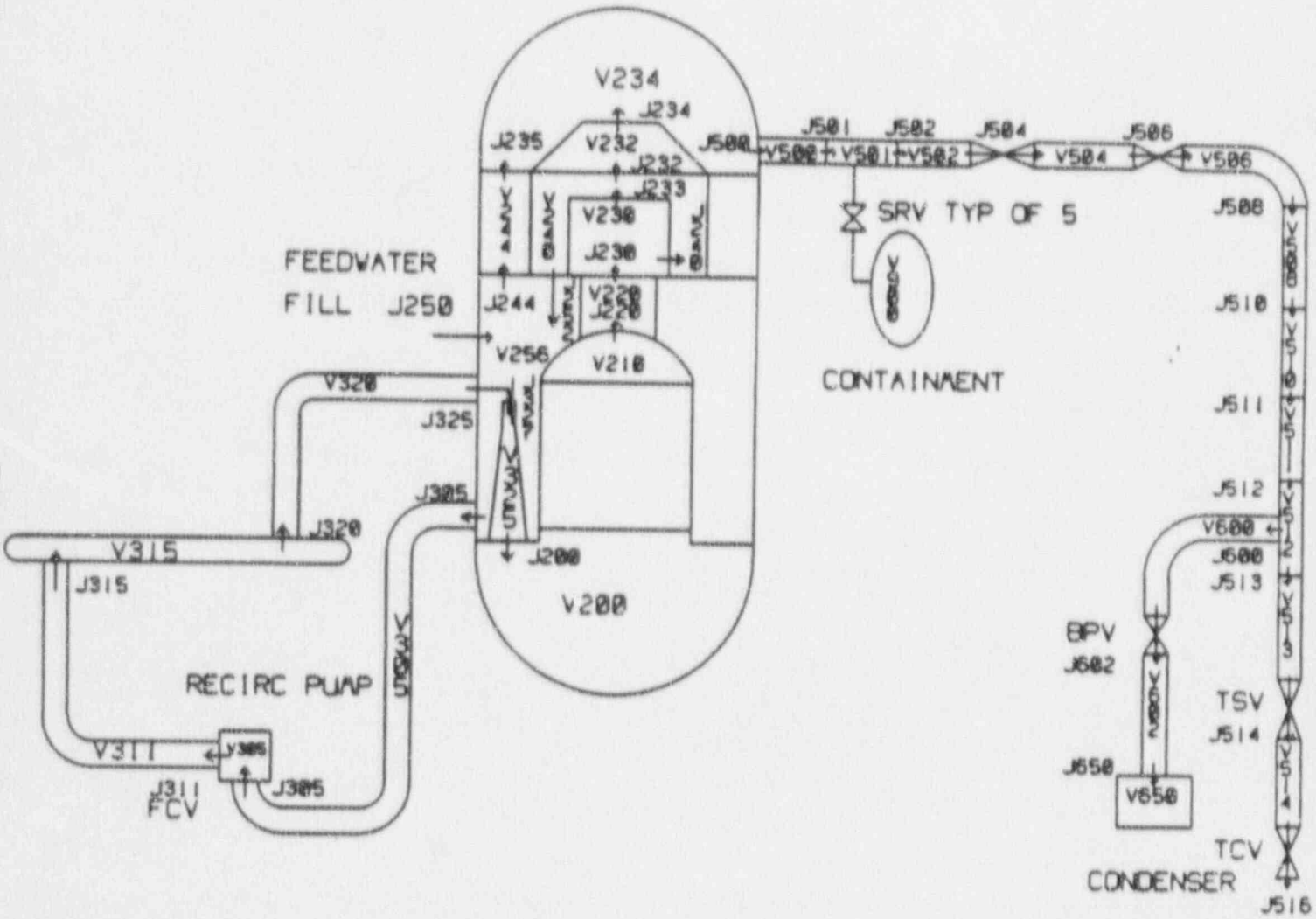

Figure 3.2 RBS Instrumentation Control System

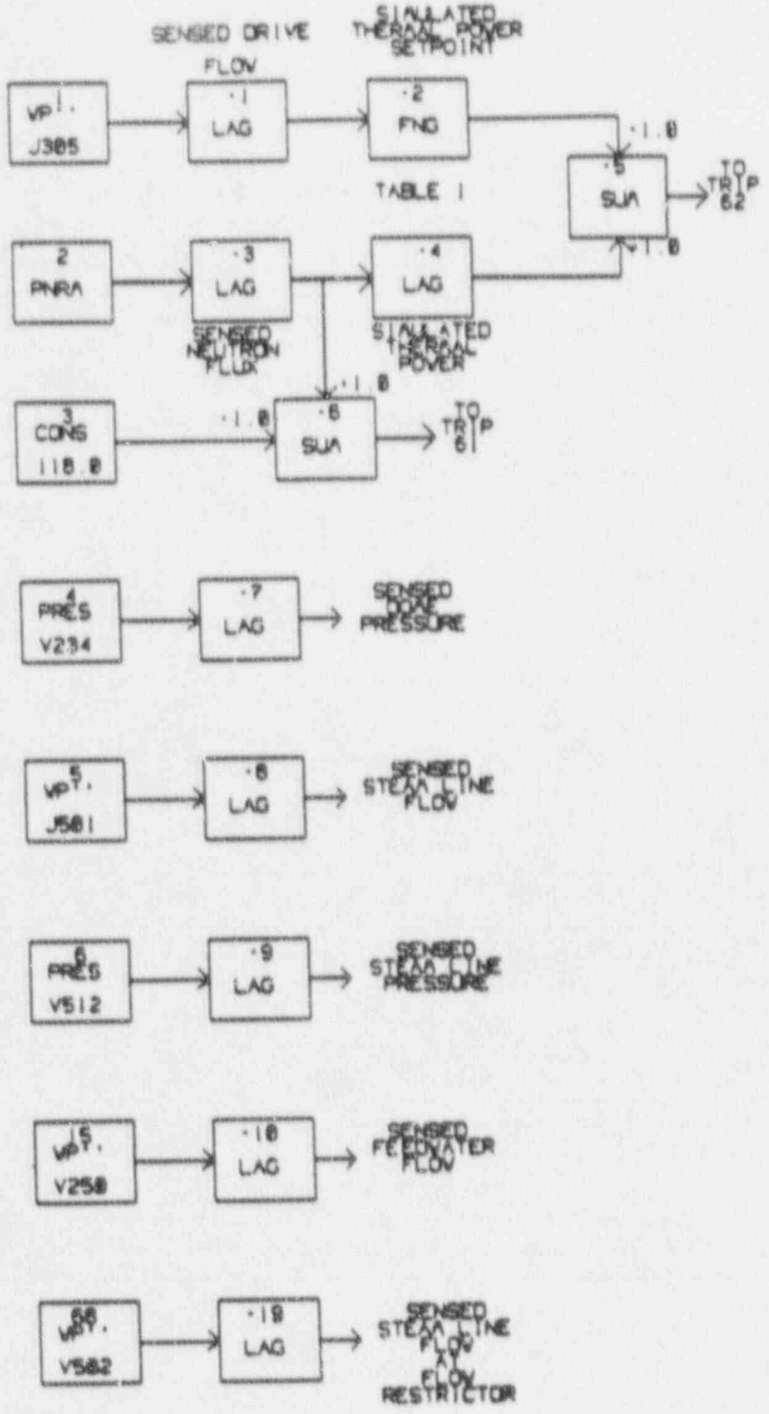

Figure 3.3 RBS Water Level Control System

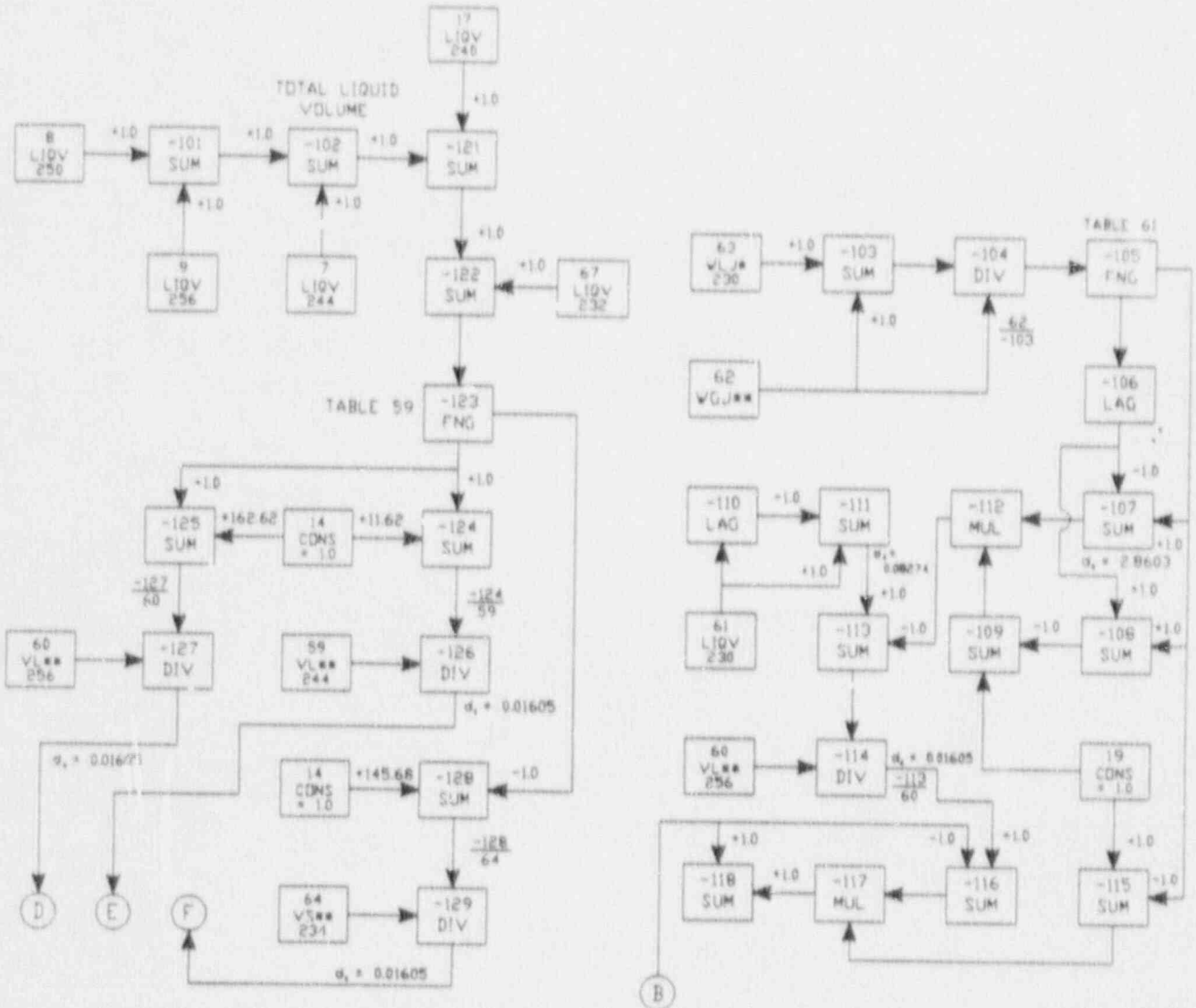

Figure 3.3 RBS Water Level Control System (Continued)

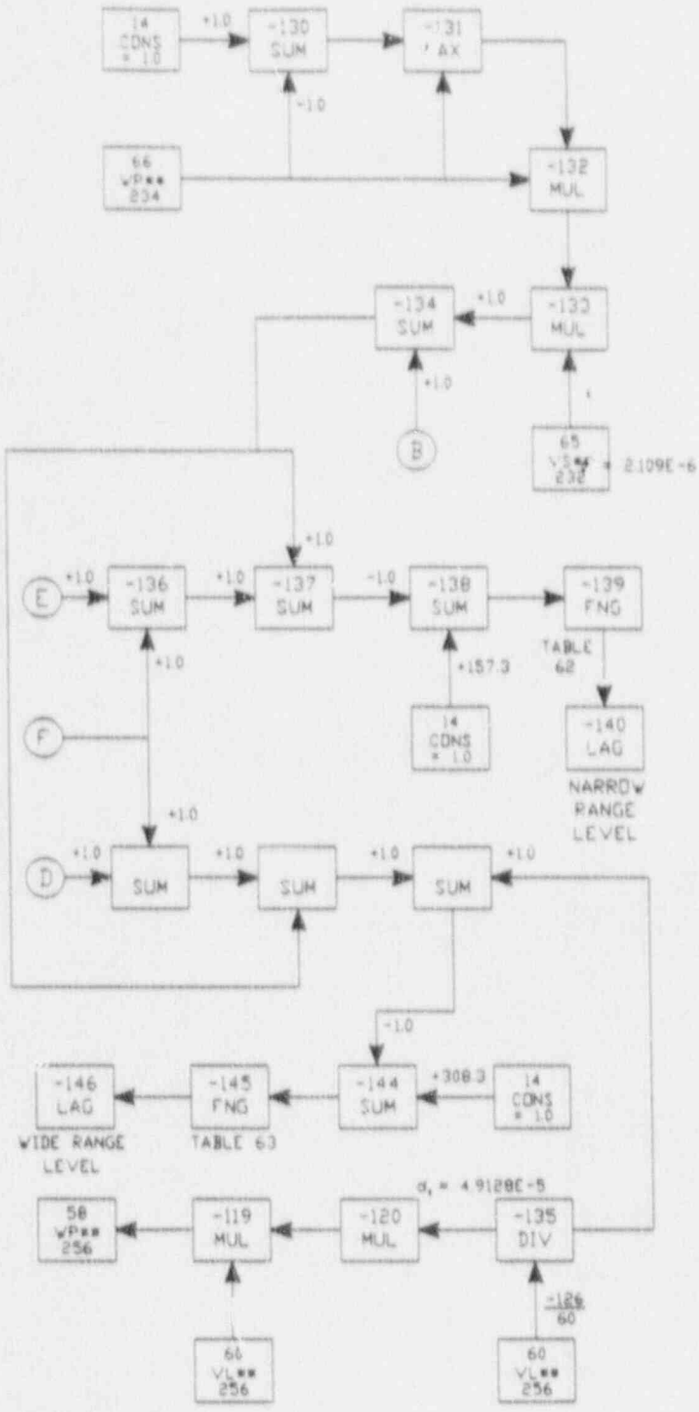

Figure 3.4 RBS Recirculation Flow Control System

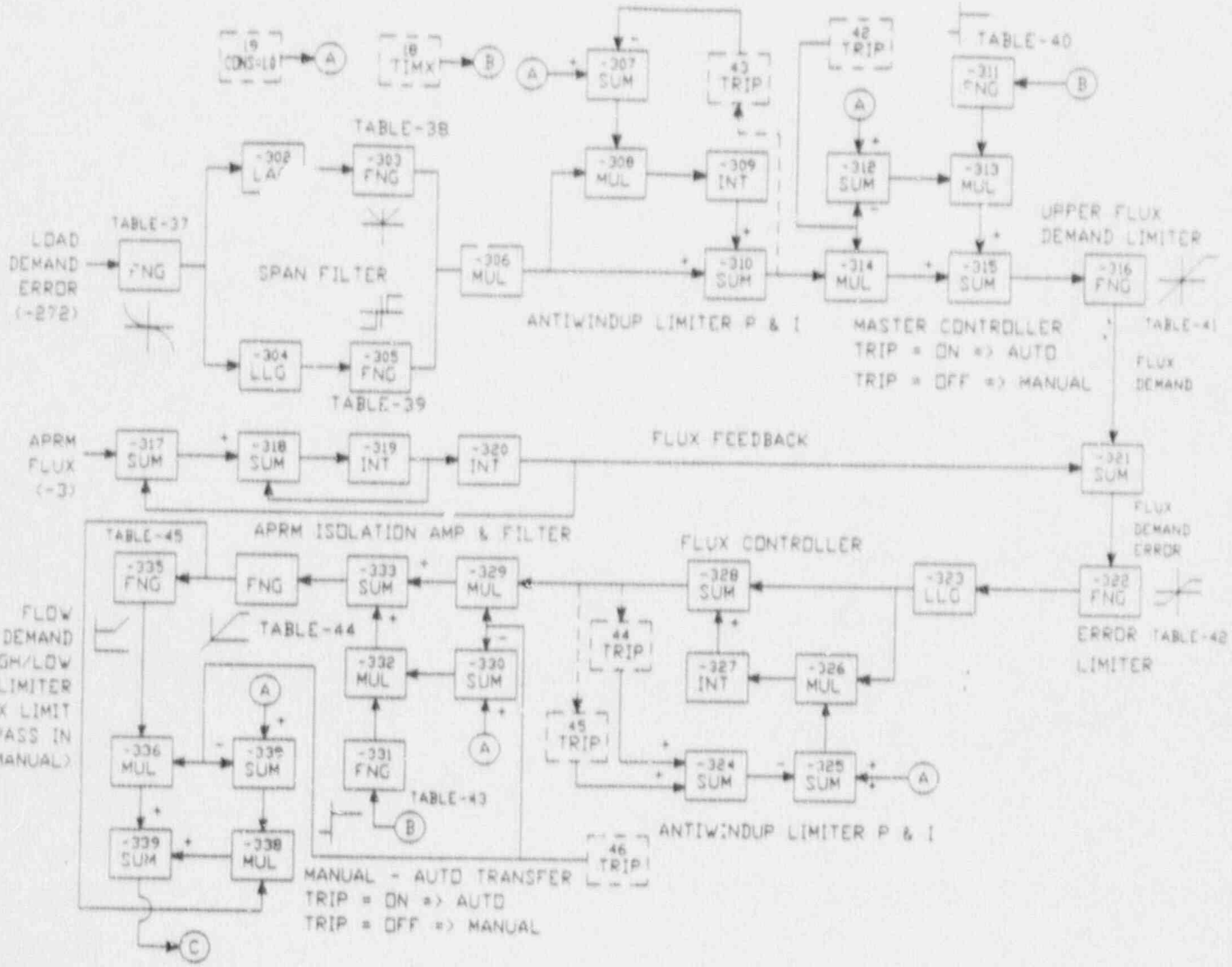

Figure 3.4 RBS Recirculation Flow Control System (Continued)

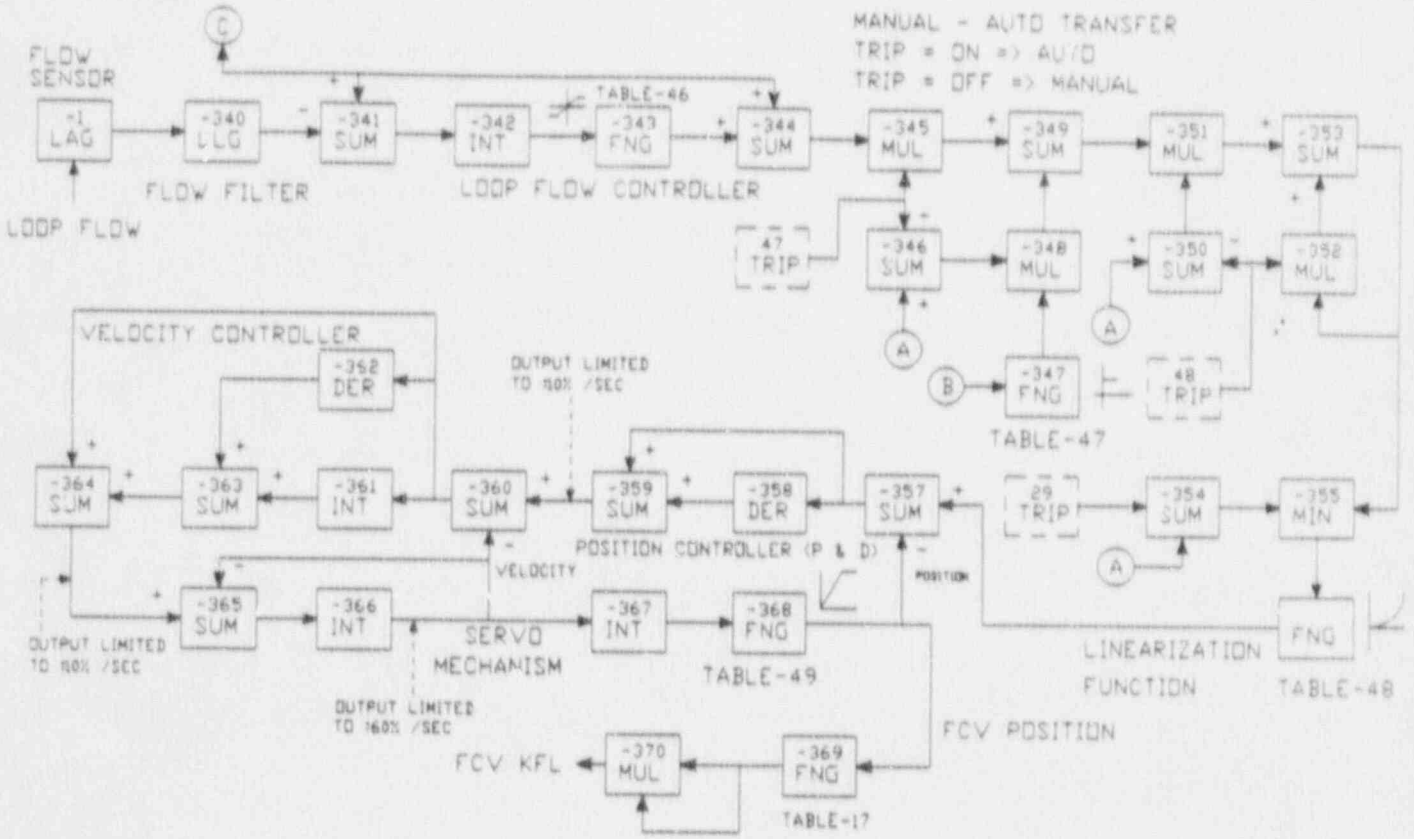

Figure 3.5 RBS Turbine Control System

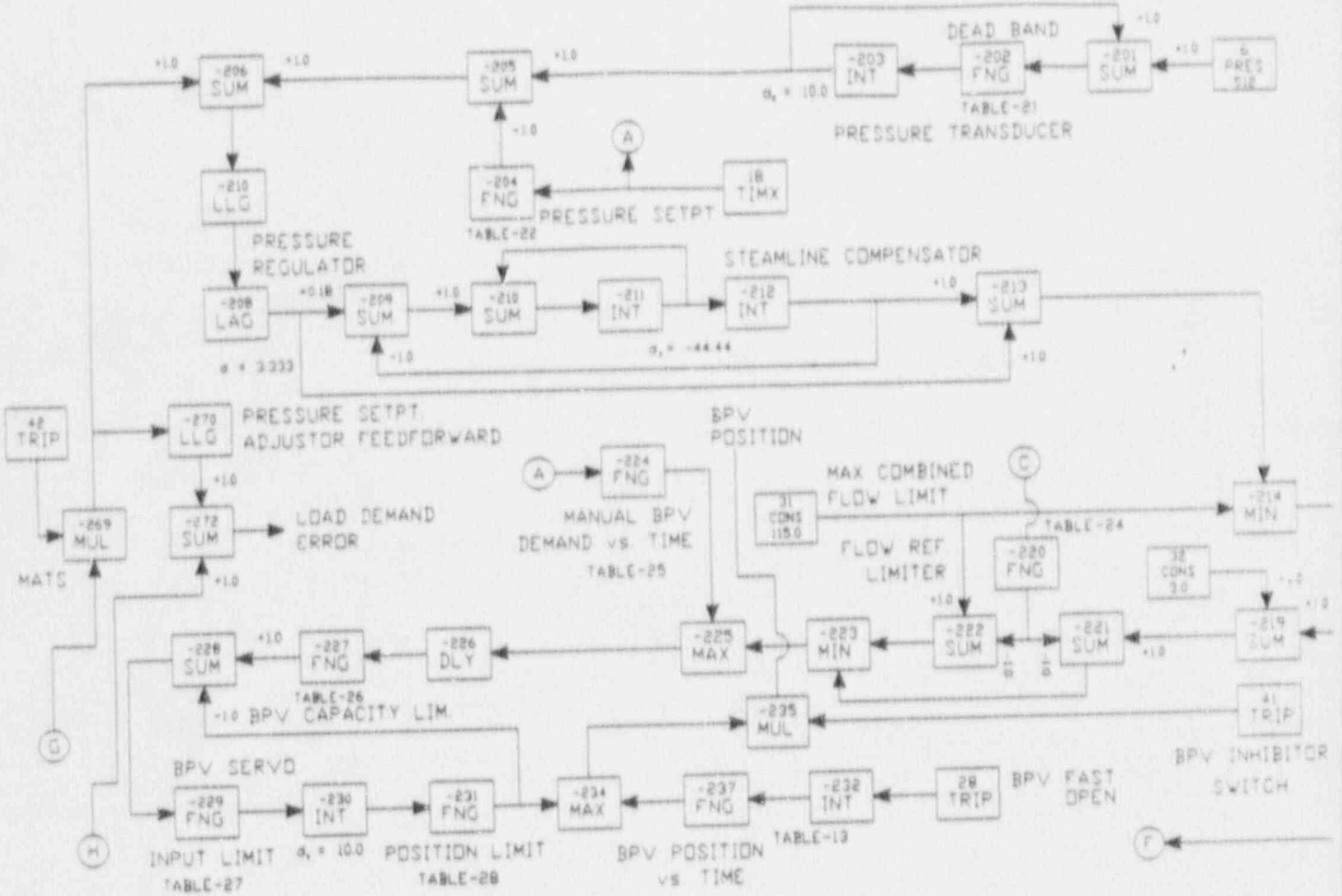

Figure 3.5 RBS Turbine Control System (Continued)

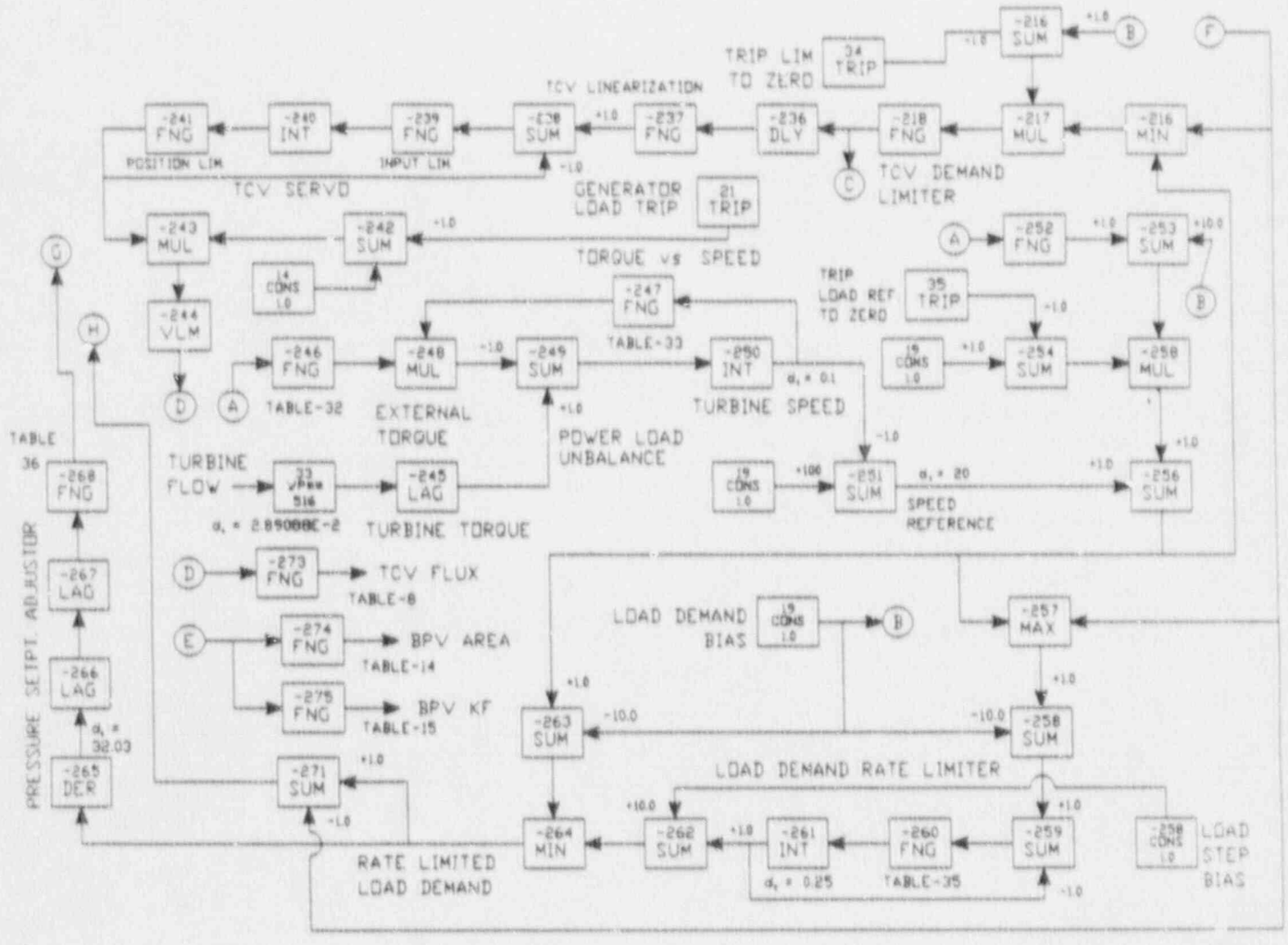

Figure 3.6 RBS Feedwater Control System

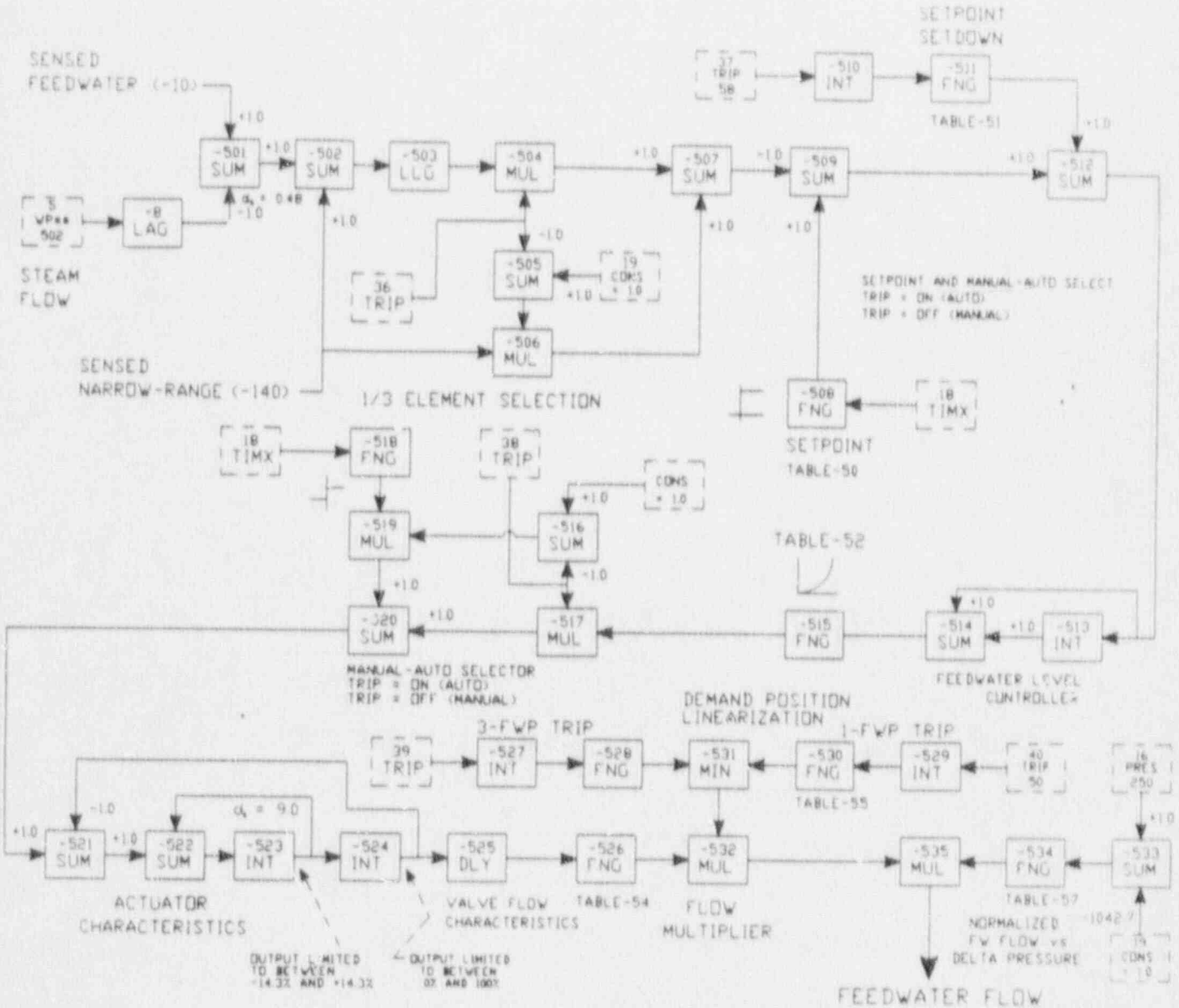

Figure 3.7 RBS Miscellaneous Edits Control System

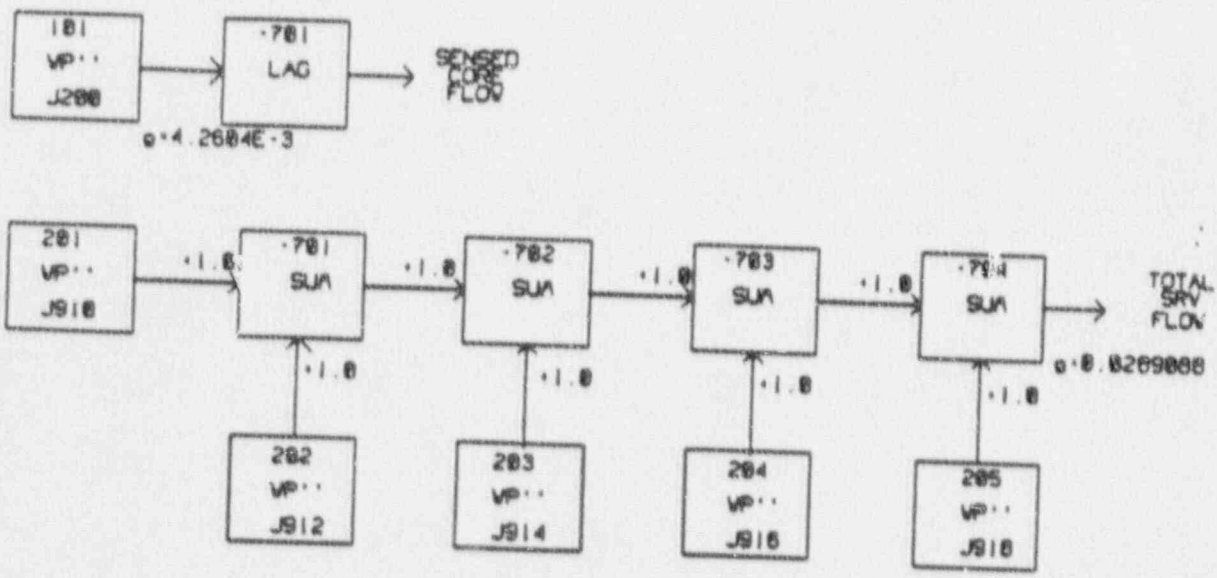

Figure 3.7 RBS Miscellaneous Edits Control System (Continued)

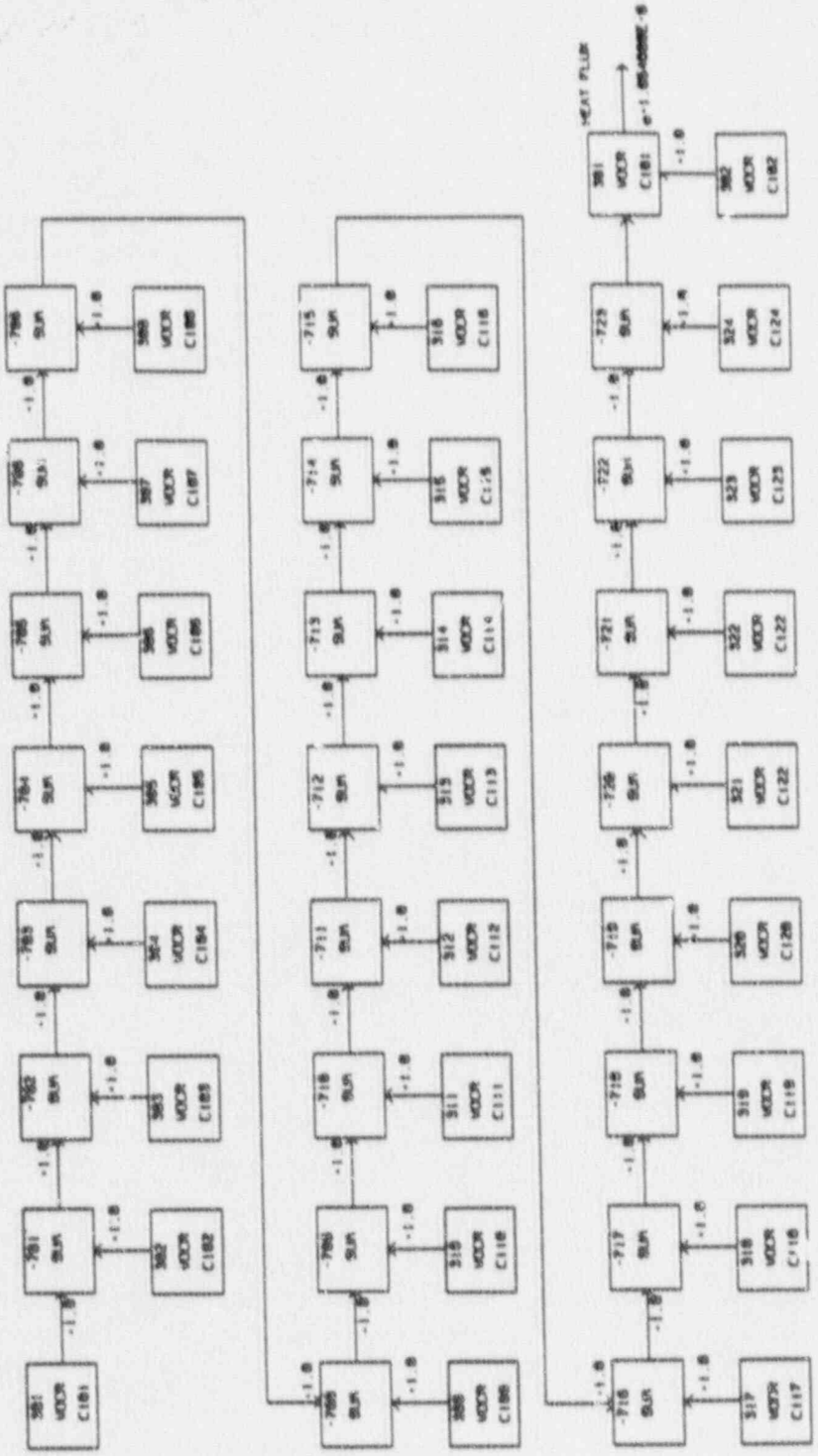

4.0 CROSS SECTION GENERATION

This section describes the procedure used to obtain the cross section information used in the RETRAN core model. Polynomial expressions for the cross sections required by the diffusion equation are prepared by SIMTRAN from SIMULATE-E restart files. The SIMULATE-E cross section data contains delayed neutron fractions and energy group inverse velocities calculated by lattice physics codes contributing to the SIMULATE-E analysis. The SIMTRAN calculation is described in Section 2.2.

Consistent with the RBS RETRAN model, the SIMTRAN model includes 25 active core neutronic regions and two reflector regions. THE RBS SIMULATE-E modeling also contains 25 active core regions, eliminating the need for axial collapsing or expansion of the core analysis data.

For transient analyses involving control rod scram, three separate SIMTRAN calculations are performed. As noted in Section 2.2, the base case uses core and system conditions consistent with the initial conditions to be modeled in the transient analysis. Secondary cases provide data for partial and full insertion of the control rods.

SIMTRAN includes several additional weighting features to allow flexibility in obtaining the spatially averaged nodal temperatures and densities. The code also contains provisions to adjust reflector cross sections so that boundary conditions between SIMULATE-E and RETRAN-02 will agree.

A sensitivity study was performed to identify the optimum temperature and density weighting options, as well as the reflector cross section adjustment option. These sensitivities were performed using the model for the Peach Bottom Atomic Power Station, and the data for the three turbine trip tests conducted. The power distribution and the neutron flux response were used as the figure of merit. The result of this study indicated that the best results achieved were with the reflector group 2 absorption cross section adjusted to match nodal power, the power distribution is used as the density weighting function, and an inverse distribution is used as the temperature weighting function.

Previous utility experience with RETRAN using SIMTRAN-collapsed cross sections has shown overprediction of transient power peaks relative to the Peach Bottom test data. In the GSU modeling, however, analyses with

unmodified SIMTRAN cross sections predict the power peaks accurately. This agreement is due in part to the use of delayed neutron information from the ENDF/B-V library rather than the ENDF/B-III data coded in the original CASMO[1] and in part to EPRI-developed improvements in the multi-state control rod model. Analyses reported in this document are based on cross section information extracted directly from SIMTRAN output without further normalization.

5.0 CALCULATION OF FUEL ROD GAP CONDUCTANCE

Gap conductance directly affects how rapidly a change in rod power will produce an associated change in rod surface heat flux. RETRAN requires hot channel and core average gap conductances to perform transient analyses.

RETRAN treats the gap as a material through which heat is conducted. The RBS RETRAN model implements the transient gap conductance using cold gap width and fill gas conductivity as a function of temperature. The methodology used by GSU to determine gap conductance values for safety analysis is described in greater detail in Appendix A.

The gap conductance values used in the RETRAN analysis have two conflicting effects on the consequences of the transient. Low values are more conservative for system or core average effects and high values are more conservative for hot channel effects. Gap conductance values are calculated separately for these applications.

The core average gap conductance affects the reactivity feedback due to a change in moderator density and void fraction. During a rapid power increase

transient, heat transferred to the coolant causes coolant voiding, which has a negative reactivity effect. Faster heat deposition in the water produces more negative void reactivity feedback, which mitigates the power increase. Lower gap conductance values in the RETRAN system model delays the onset of corewide coolant voiding, resulting in a larger power increase. In slow events, the gap conductance has a negligible effect because the heat flux remains approximately equal to the neutron flux throughout the transient.

The power response of the hot channel analysis is driven by boundary conditions from the core average system analysis. The gap conductance determines the heat flux response in the hot channel analysis.

For pressurization transients and other events which include rapid power increases, a larger value of hot channel gap conductance results in a larger prompt increase in heat flux. Higher values of heat flux result in more severe thermal margin decrease during transients, as indicated by a larger value of Change in Critical Power Ratio (ΔCPR).

The methodology described in Appendix A was used to produce sample gap conductances for RBS Cycle 3. The

core average gap conductance was calculated to be 1218 BTU/hr-ft^2-°F and the hot channel gap conductance was calculated to be 2315 BTU/hr-ft^2-°F.

6.0 COMPARISON TO RIVER BEND STATION TRANSIENTS

The RBS RETRAN model is qualified by comparison of calculated results to measured data from operational events and startup tests at the plant. As part of the Emergency Response Information System (ERIS), RBS is equipped with a transient data recorder which can digitally store many plant variables continuously during plant operation.

6.1 GENERATOR LOAD REJECTION

RBS experienced a generator load rejection transient on December 1, 1989. The scram resulting from this event was termed Scram 89-04. The initial conditions for this transient are shown in Table 6.1. The timing of major events during the transient is shown in Table 6.2. RETRAN predictions are compared with ERIS data in Figures 6.1 through 6.8.

With the reactor operating at 96% power, a turbine-generator trip resulted in an automatic reactor scram on Turbine Control Valve (TCV) fast closure. Concurrent

with the turbine trip, the recirculation pumps automatically transferred to the LFMG sets. Immediately following the scram, reactor pressure rose rapidly to approximately 1120 psig, causing the four groups of safety relief valves, including the five low-low set SRVs, to cycle open. The turbine bypass valves also opened.

Water level initially decreased due to collapse of steam voids resulting from the rapid pressure increase and reactor scram. The narrow range level dropped to as low as 10" above instrument zero from an initial level of 37". Feedwater flow remained relatively high since the water level was well below the normal water level setpoint. When water level is below this setpoint, feedwater regulator valves are opened to increase feedwater flow. Water level then recovered, reaching the level 8 high water level trip at around 50 seconds. This resulted in a feedwater pump trip.

Figure 6.1 shows the Average Power Range Monitor (APRM) flux response. Since the bypass valves opened and the reactor scrammed, neither the predictions nor the data show any increase in flux above the initial value. Flux decreases rapidly following scram. Figure 6.2 shows the predicted reactor pressure response compared to data

from two channels. RETRAN predictions are in good agreement with the peak pressure. The predictions are in agreement with the data regarding the number of SRVs which opened in the relief mode (nine). However, analysis of tailpipe temperature responses indicates that several of the remaining seven valves opened briefly in the safety mode at pressures somewhat below the normal relief or safety valve setpoints. To accommodate these open safety valves, the opening of two valves in the safety mode is included in the RETRAN modeling.

Reactor pressure decreases rapidly following opening of the SRVs, which close in sequence as the pressure decreases. The pressure decrease is terminated when the bypass closes at around 21 seconds. These valves reopen for a brief period at around 33 seconds to relieve the subsequent pressure increase.

Total steam flow as measured by the elbow flow meters upstream of the SRVs is shown in Figure 6.3. Predicted and measured steam flow both drop rapidly following fast closing of the TCVs. The subsequent increase is due to opening of the SRVs and the bypass. The steam flow decreases as relief valves close during the pressure decrease period. Step changes in flow

indicate the times when groups of valves closed. The flow measurement at low flow is inaccurate due to the type of instruments used and the calibration range. The prediction provides a more realistic representation beyond 20 seconds, when the steam flow is low. The predicted increase of flow at around 40 seconds occurred when the bypass reopened.

Figure 6.4 shows the measured and predicted core flow response. Both show a rapid decrease in core flow following transfer to the LFMGs. The prediction is in excellent agreement from above 30% of rated flow. The flow measuring instruments are less accurate at low flow.

Feedwater flow response is shown in Figure 6.5. Both measurements and predictions show a general decrease in feedwater flow and then a rapid decrease following feedwater pump trip on a high level 8 at around 50 seconds. Differences between the predictions and plant data are due to the differences in predicted narrow range water level shown in Figure 6.6. Water level, with steam/feed flow mismatch, is the main determinant of feed flow magnitude. Water level is one of the more difficult variables to predict accurately.

In addition, the feedwater control system had two trains in auto and one in manual at the time this event occurred. The RETRAN base model is set up for three trains in auto mode, with an approximation used for the 2 auto/1 manual mode. An earlier benchmark[11] for a similar event, which also occurred while the feedwater system was in the 2 auto/1 manual mode, the feedwater flow was forced to model measured data. More accurate predictions of water level were obtained in that case. For this benchmark, feedwater flow response is included in the prediction to provide a more general simulation of the plant response. The overall water level response trend is predicted well. However, the prediction does not drop as low as the plant data and recovers somewhat more slowly. The first water level recovery is over-predicted by the code.

Figure 6.7 shows excellent agreement in recirculation pump speed including speed following pickup of the LFMGs. This shows that the RETRAN recirculation pump model is a very good representation of the actual component.

Figure 6.8 shows predicted and measured bypass valve position. The RETRAN prediction shows a shorter period of valve reopening.

Simulation of this load rejection transient shows that RETRAN can predict plant performance during this type of event with good accuracy. Predictions are especially good during the first second or so following initiation of the event. This is the time period during which Maximum Average Planar Linear Heat Generation Rate (MCPR) will occur for similar but more severe events such as those analyzed for the thermal limits determination.

6.2 WATER LEVEL INCREASE EVENT

RBS experienced a water level increase transient on June 18, 1987. The reactor was operating at approximately 70 percent power and 54.5 percent core flow when a battery inverter failed. Initial conditions for this transient are shown in Table 6.3.

The inverter failure interrupted power to panel 1VBN-PNL01B1, which in turn locked the feedwater regulating valves in position. In addition to the loss of power

to the feedwater controller, a recirculation flow control valve (FCV) runback signal was generated causing both valves to begin to close. FCV "A" completed the runback; however, the hydraulic power unit serving FCV "B" failed, causing the valve to stop short of the full runback. Recirculation Pump "B" attempted to transfer to slow speed immediately; however, the LFMG for the pump did not engage and the pump coasted down to zero speed. This concurrent core flow reduction caused a reduction in power and steam flow, which was not offset by a decrease in feedwater flow because the feedwater regulating valves were locked in position. Water level rose to near the Level 8 setpoint, where the reactor protection system generated a scram signal. The indicated level did not exceed Level 8 on all water level instrumentation, so the turbines and feedwater pumps did not trip initially. The turbine and one feedwater pump were manually tripped following the reactor scram.

Following the reactor scram, water level decreased and rose again, eventually exceeding the Level 8 trip setpoint and tripping the feedwater pumps. The timing of major events during the transient is shown in Table 6.4.

Predicted plant performance is compared with ERIS data in Figures 6.9 through 6.14.

The RETRAN results agree with measured plant data available for the event. RETRAN predicts a slightly slower level recovery than the data; this difference is probably caused by modeling asymmetric recirculation loop conditions with a single, composite recirculation loop. Instruments recording narrow range water level and core flow draw power from the failed bus, so these indications are unreliable during the first 21 seconds of the transient. When power was restored, the instrumentation resumed functioning.

Figure 6.9 shows the neutron flux during the transient. The predicted flux follows a similar trend as that exhibited by the data, except that the flux level is higher before scram occurs. This is most likely due to uncertainties in the core flow measurement when one pump is running and the other pump is idle.

Figures 6.10 and 6.11 show the water level response as determined from the narrow range and wide range instrumentation. The rise in level following the recirculation flow decrease matches the observed level very well. The subsequent drop in level following

reactor scram also matches the observed data. The level recovery following the scram is somewhat delayed in the RETRAN calculation. As discussed above, this is felt to be due to the limitations in modeling asymmetric loop behavior with a single composite loop model.

Figure 6.12 shows the core flow response during the transient. The initial portion of the transient agrees with data, however, the flow at this point was forced to agree with the measured flow. The flow coastdown following the trip of the remaining pump differs from the data by approximately 7% of rated flow. This is likely due to the imitations in modeling asymmetric loop behavior with a single composite loop model.

Figures 6.13 and 6.14 show the feedwater and turbine steam flows during the transient. The responses obtained agree very well with the measured data. Feedwater remains constant due to the feedwater regulating valves locking in position. Eventually one of the pumps is tripped, and feedwater flow decreases to very nearly the same value as calculated by RETRAN. Steam flow initially drops in response to the power decrease associated with the recirculation flow decrease. Following the scram,

the calculated flow decreases in a manner similar to that observed.

6.3 WATER LEVEL SETPOINT STEP CHANGES

RBS Startup Test 1-ST-23A, which was performed on May 24, 1986, included step changes in the reactor water level setpoint. The RETRAN model was benchmarked to the feedwater flow and reactor narrow range water level response to these changes. The unit was operating at near rated conditions for the test.

RETRAN predictions are compared with ERIS data in Figures 6.15 through 6.18 for the +6" and -6" level setpoint tests. For the +6" level setpoint change, both the feedwater flow and water level response agree closely with plant data. For the -6" test, it appears that a slightly larger step change than intended was initiated (approximately 7.8"). The plant feedwater response is much slower for the negative change. RETRAN predicts that changes in feedwater flow will take place at the same rate as for a positive step. However, the overall water level response is comparable.

Table 6.1 Initial Conditions, RBS Load Rejection Transient (Scram 8904)

	Plant Data	RETRAN
Power	96.8%	96.8%
Core Flow	96.6% (81.6 MLB/HR)	96.6%
Steam Flow	96.1% (12.0 MLB/HR)	96.8%
Feedwater Flow	96.1% (12.0 MLB/HR)	96.1%
Dome Pressure	1032.0	1032.0
Water Level	37.0"	37.0"
Recirculation Control	2 in Manual	2 in Manual
Pressure Regulator	Full Arc	Full Arc
Feedwater Control	3 Element 2 Auto, 1 Manual	3 Element 2 Auto, 1 Manual

Table 6.2 Sequence of Events, RBS Load Rejection Transient (Scram 8904)

	Plant Data	RETRAN TIME
Load Rejection	0.00	0.000
TCV Fast Closure	0.10	0.107
Scram	0.12	0.177
EOC HFMG Trip	0.14	0.247
BPV Fast Open	0.10 (0%)	0.207 (0%)
	0.8 (100%)	0.482 (100%)
SRV-1 Open (1)	1.4	1.78
SRV-2 Open (1)	1.5	1.78
SRV-3 Open (3)	1.5	1.92
SRV-4 Open (4)	1.5	1.92
Peak Pressure	2.0	2.2
SRV-4 Closed	4.5	5.97
SRV-3 Closed	11.8	9.38
SRV-2 Closed	14.7	10.05
SRV-1 Closed	20.8	10.76

Table 6.3 Initial Conditions, RBS Water Level Increase Event

	Plant Data	RETRAN
Power (%NBR)	70.0	70.0
Core Flow (%NBR)	54.5	54.5
Steam Flow (%NBR)	86.2	67.2[1]
Feedwater Flow (%NBR)	67.2	67.2
Narrow Range Water Level (in)	35.7	35.7
Recirculation Flow Control	2 loops in MANUAL	
Pressure Regulator	full arc	
Feedwater Controller	Three-Element	

[1]Non-condensible gas build-up in condensing chambers of steam flow instrumentation for feedwater control resulted in an error in the indicated steam flow.

Table 6.4 Sequence of Events, RBS Water Level Increase Event

	TIME (sec)	
Battery Inverter Failure	0.0	
FCV Runback Initiated	0.0	
Recirculation Pump B Tripped	0.0	
Reactor Scram on High Level	37.0	
Recirculation Pump A Tripped	43.0	
Feedwater Pump A Tripped	54.0	
Manual Turbine Trip	84.0	(Not Simulated)
Feedwater Pumps B & C Tripped	86.0	(Not Simulated)

Figure 6.1 Predicted vs Measured Neutron Flux, RBS Scram 89-04

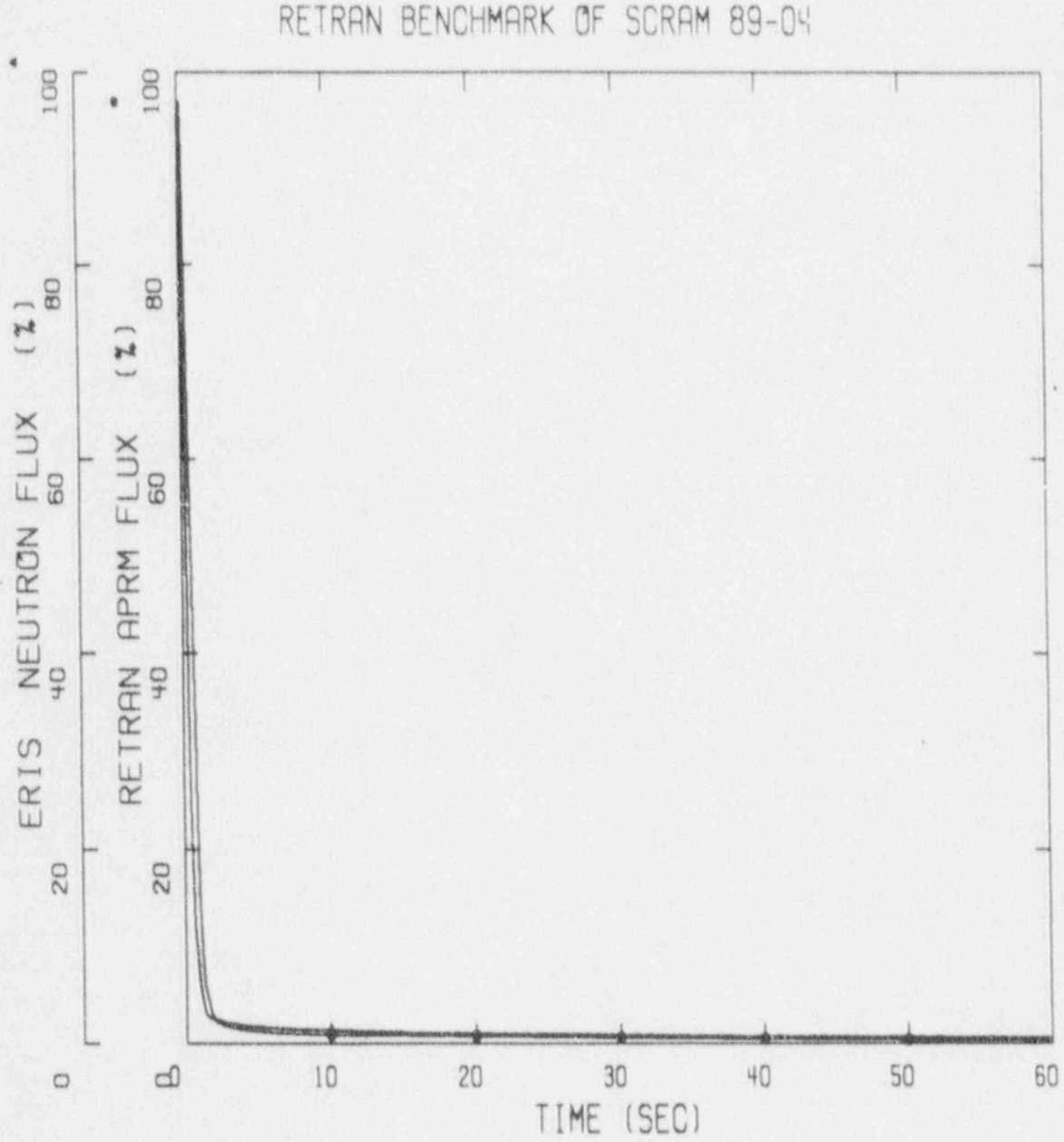

Figure 6.2 Predicted vs Measured Reactor Pressure, RBS Scram 89-04

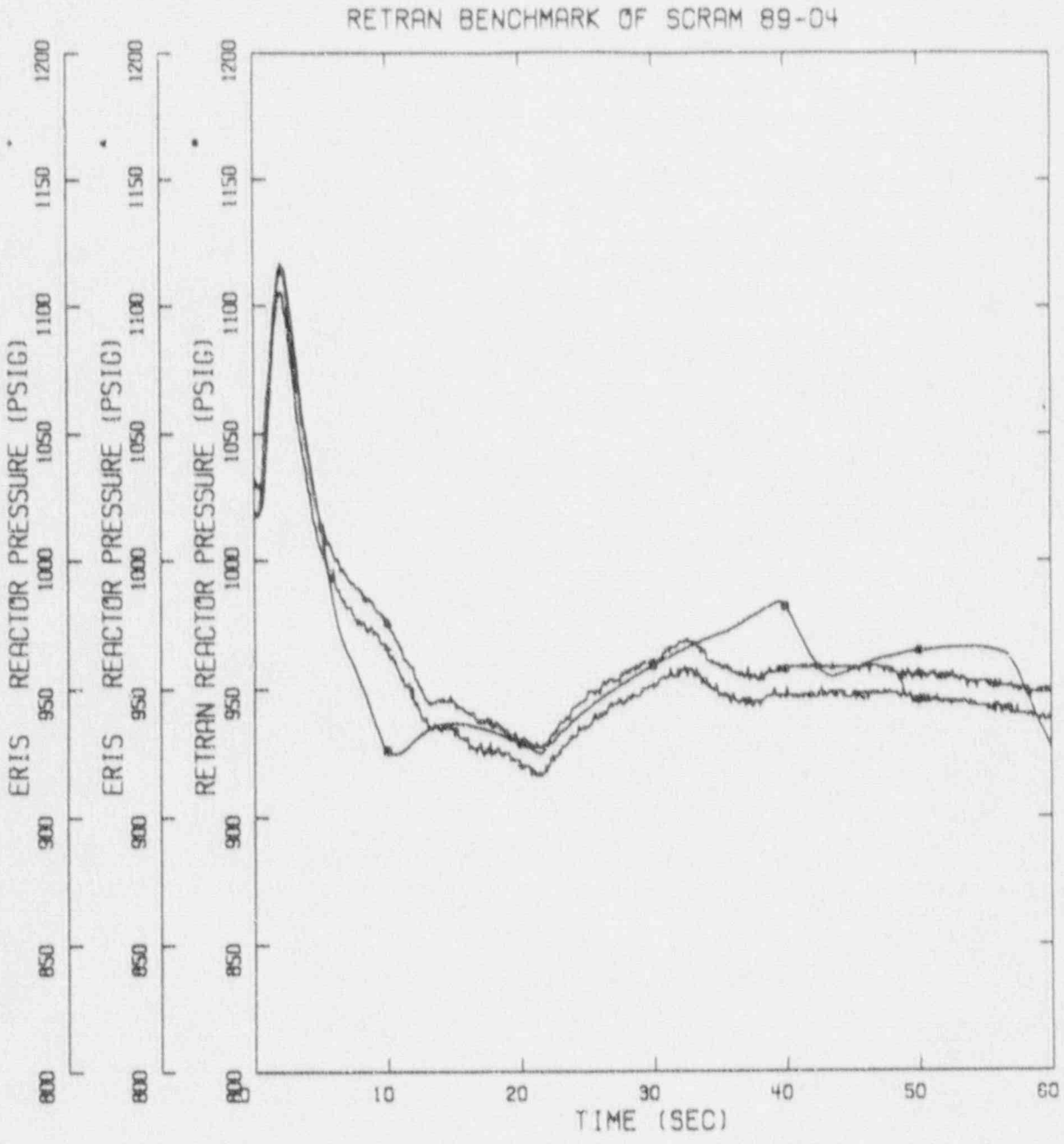

Figure 6.3 Predicted vs Measured Total Steam Flow, RBS Scram 89-04

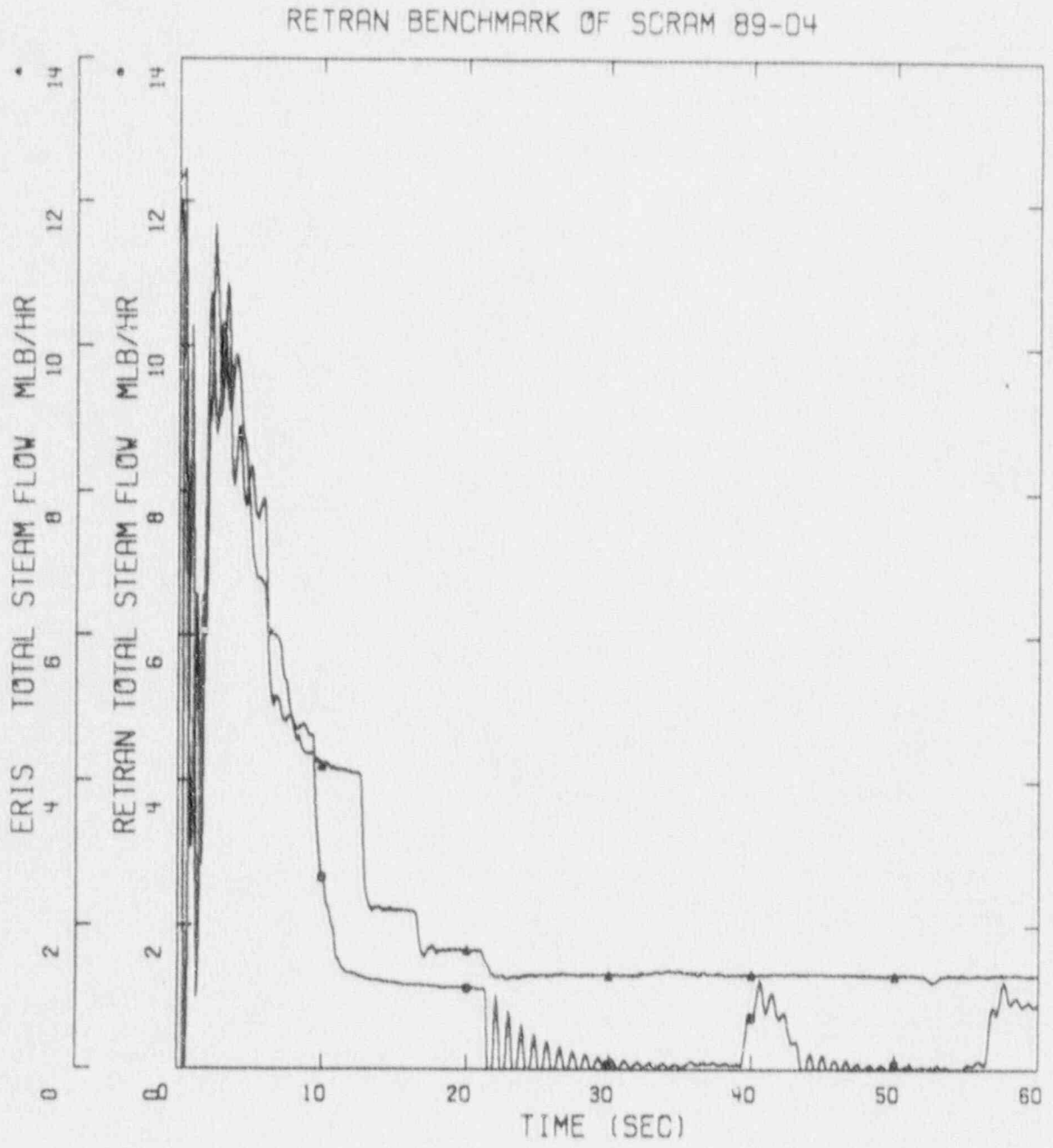

Figure 6.4 Predicted vs Measured Total Core Flow, RBS Scram 89-04

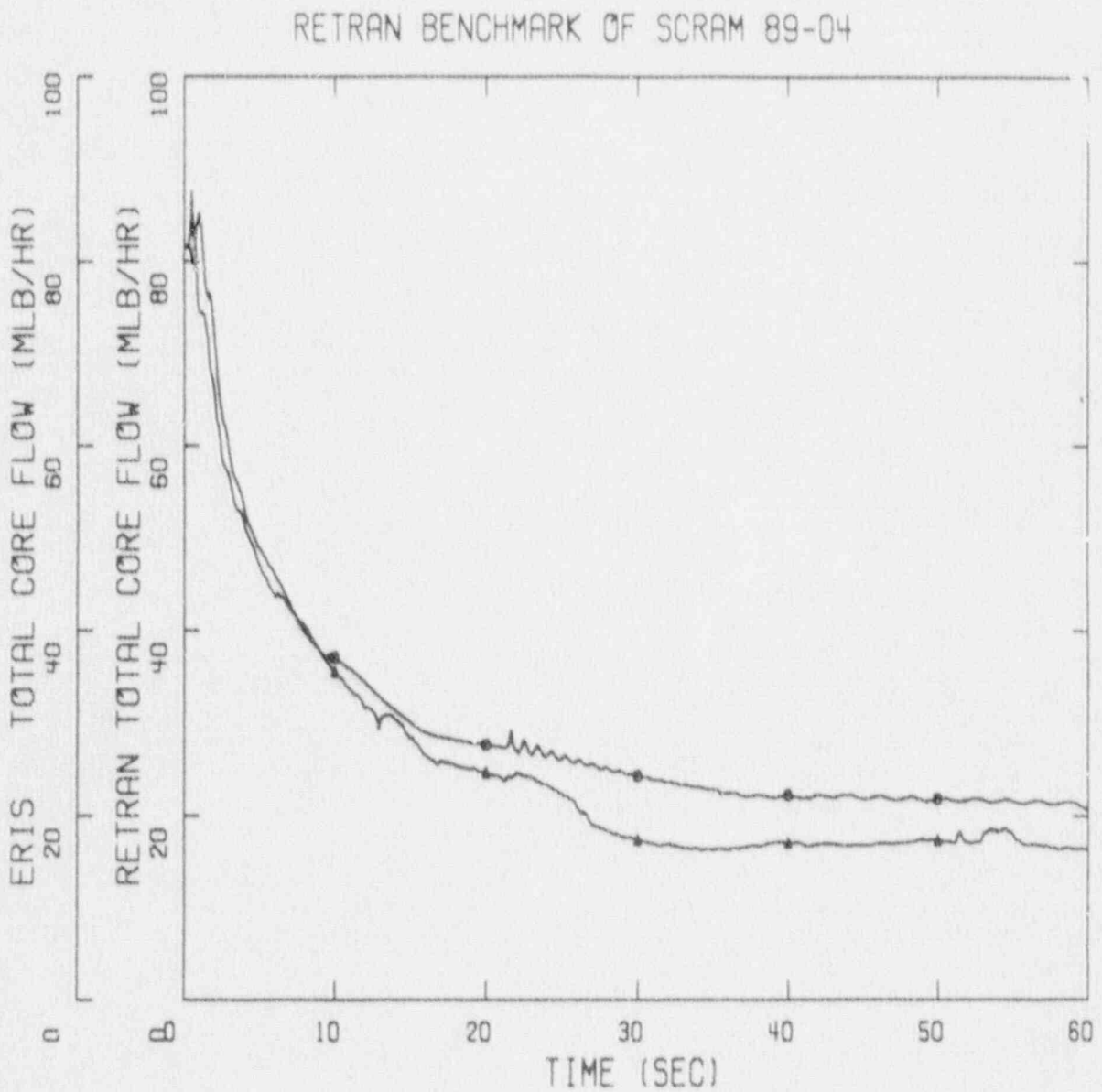

Figure 6.5 Predicted vs Measured Feedwater Flow, RBS Scram 89-04

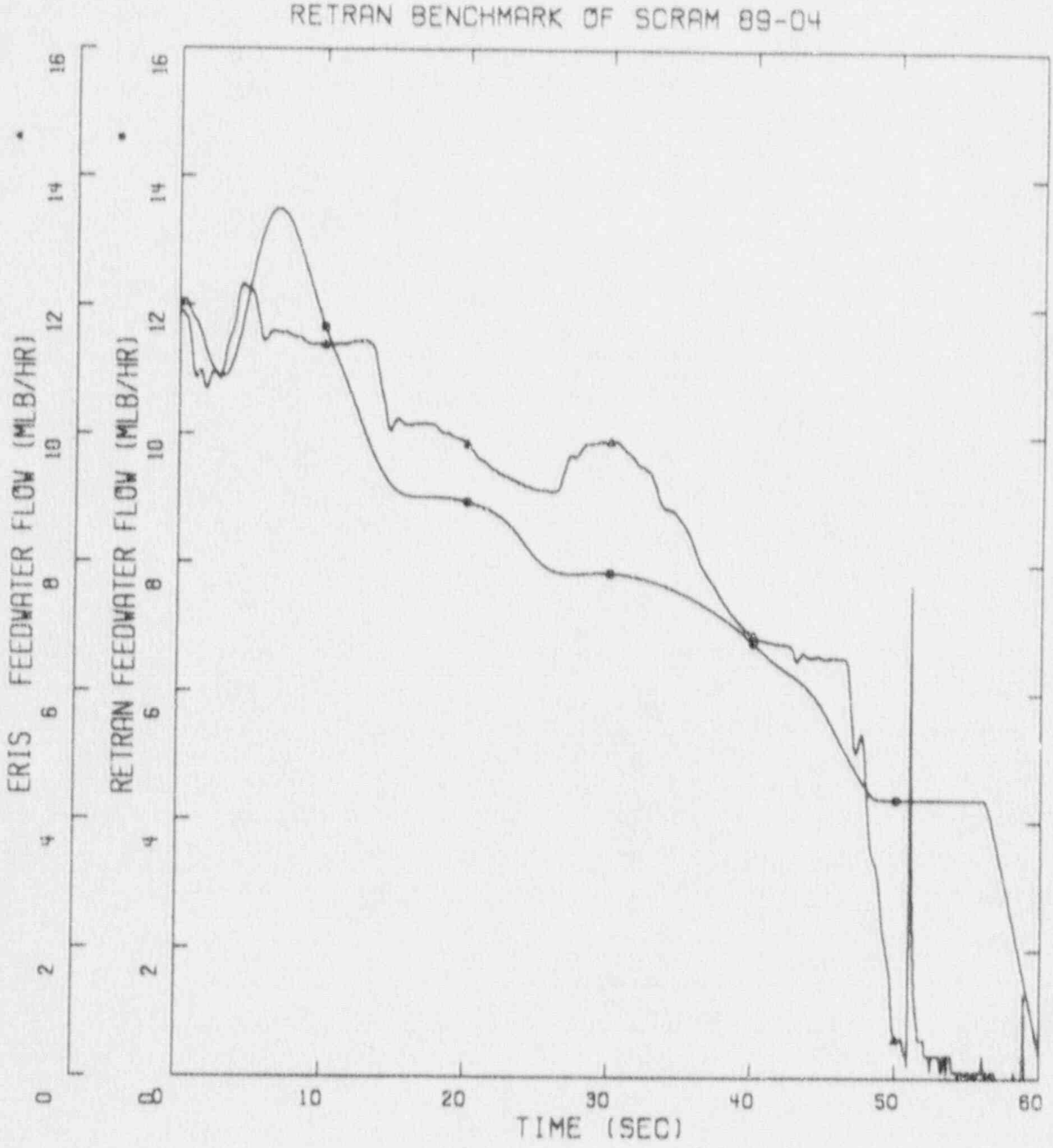

Figure 6.6 Predicted vs Measured Vessel Water Level, RBS Scram 89-04

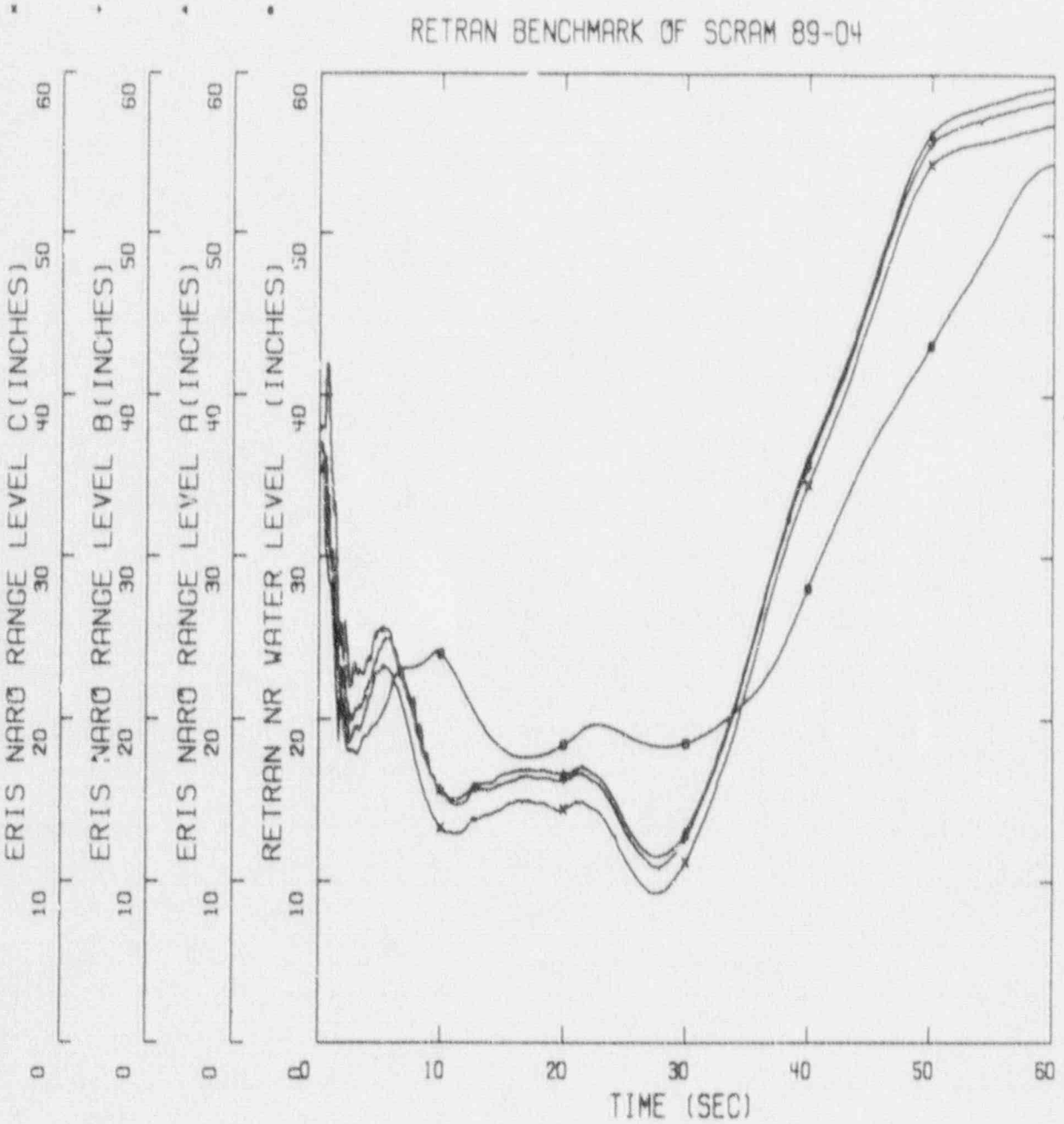

Figure 6.7 Predicted vs Measured Recirculation Pump Speed, RBS Scram 89-04

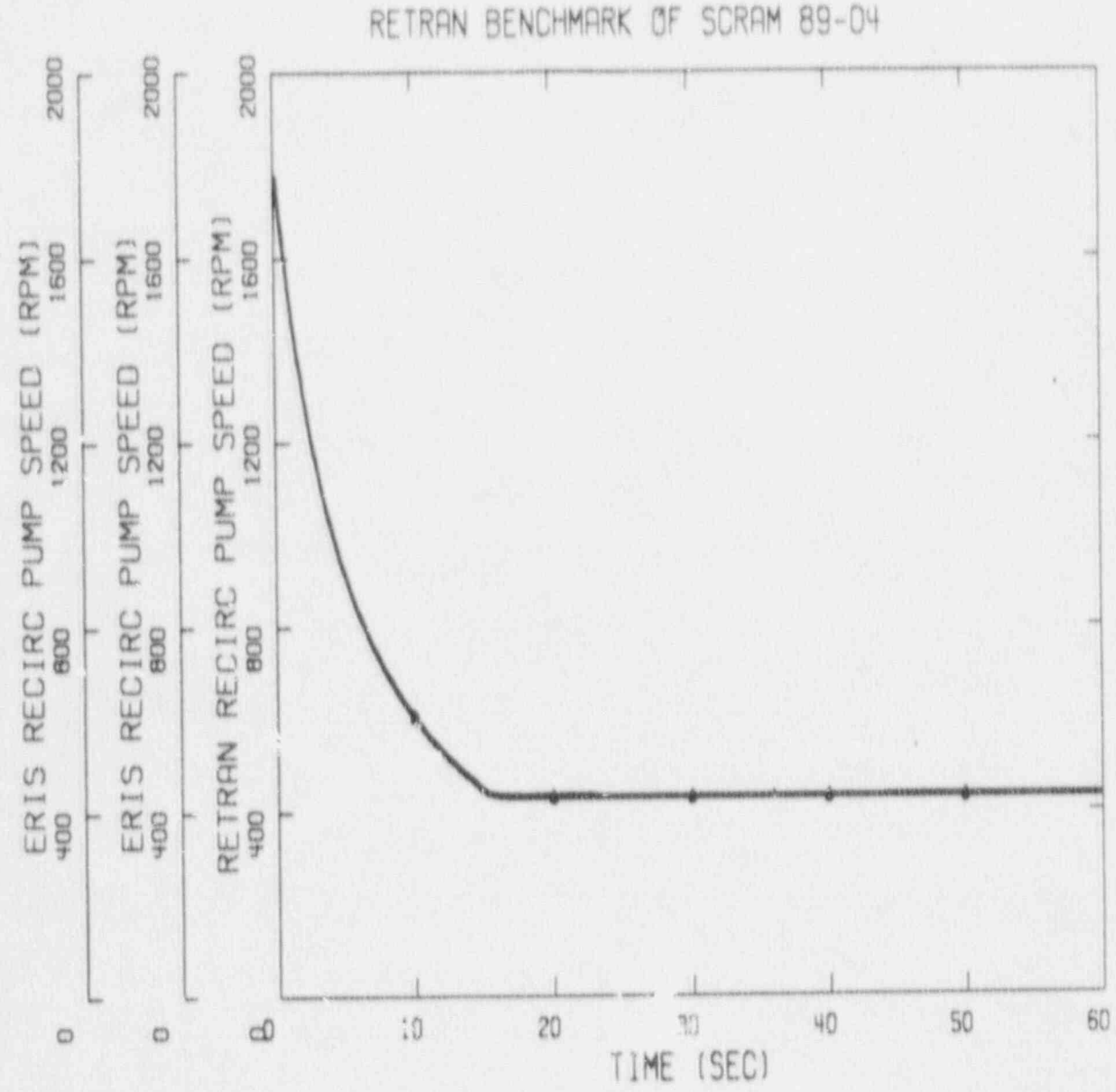

Figure 6.8 Predicted vs Measured Bypass Valve Position, RBS Scram 89-04

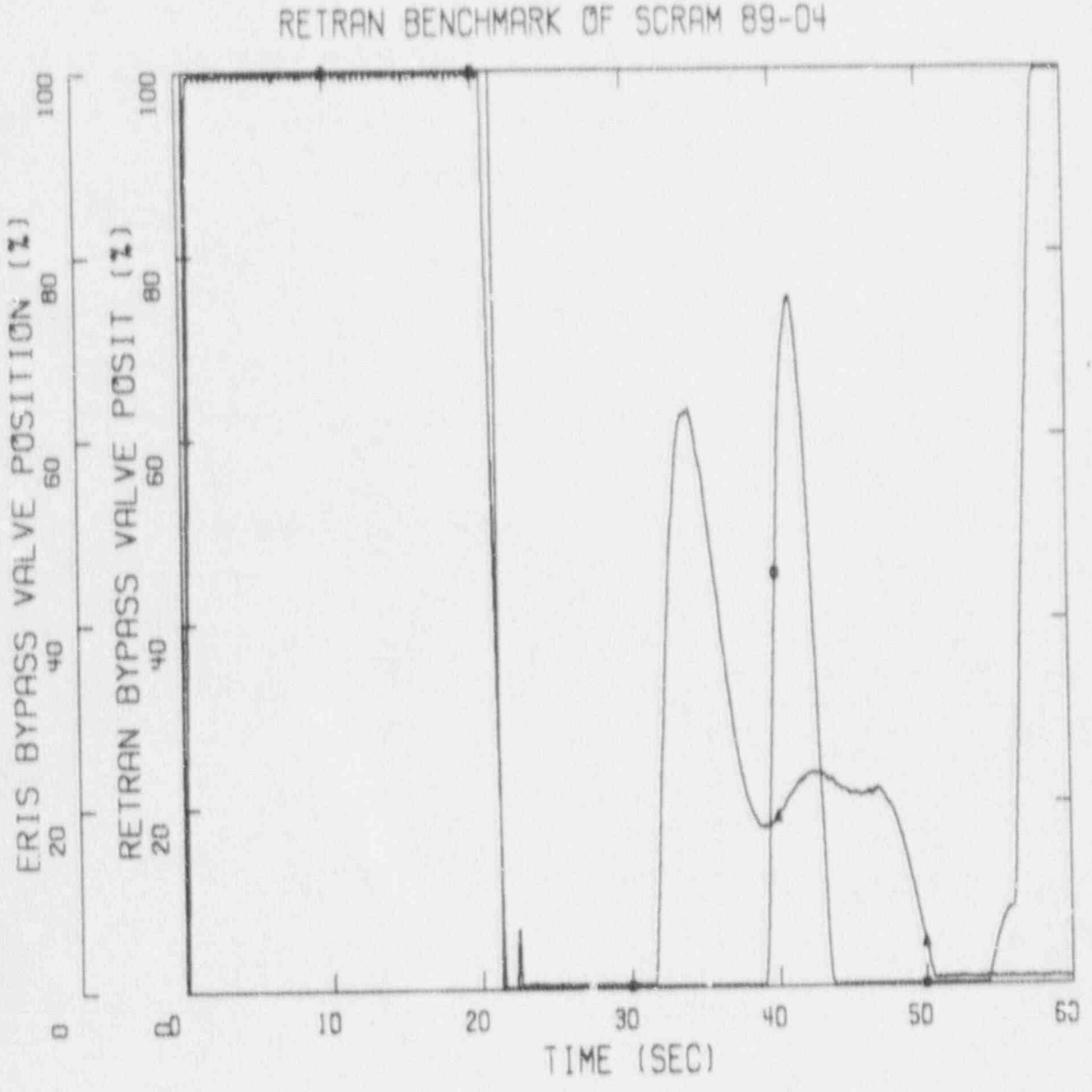

Figure 6.9 Predicted vs Measured Neutron Flux, RBS Water Level Increase Transient

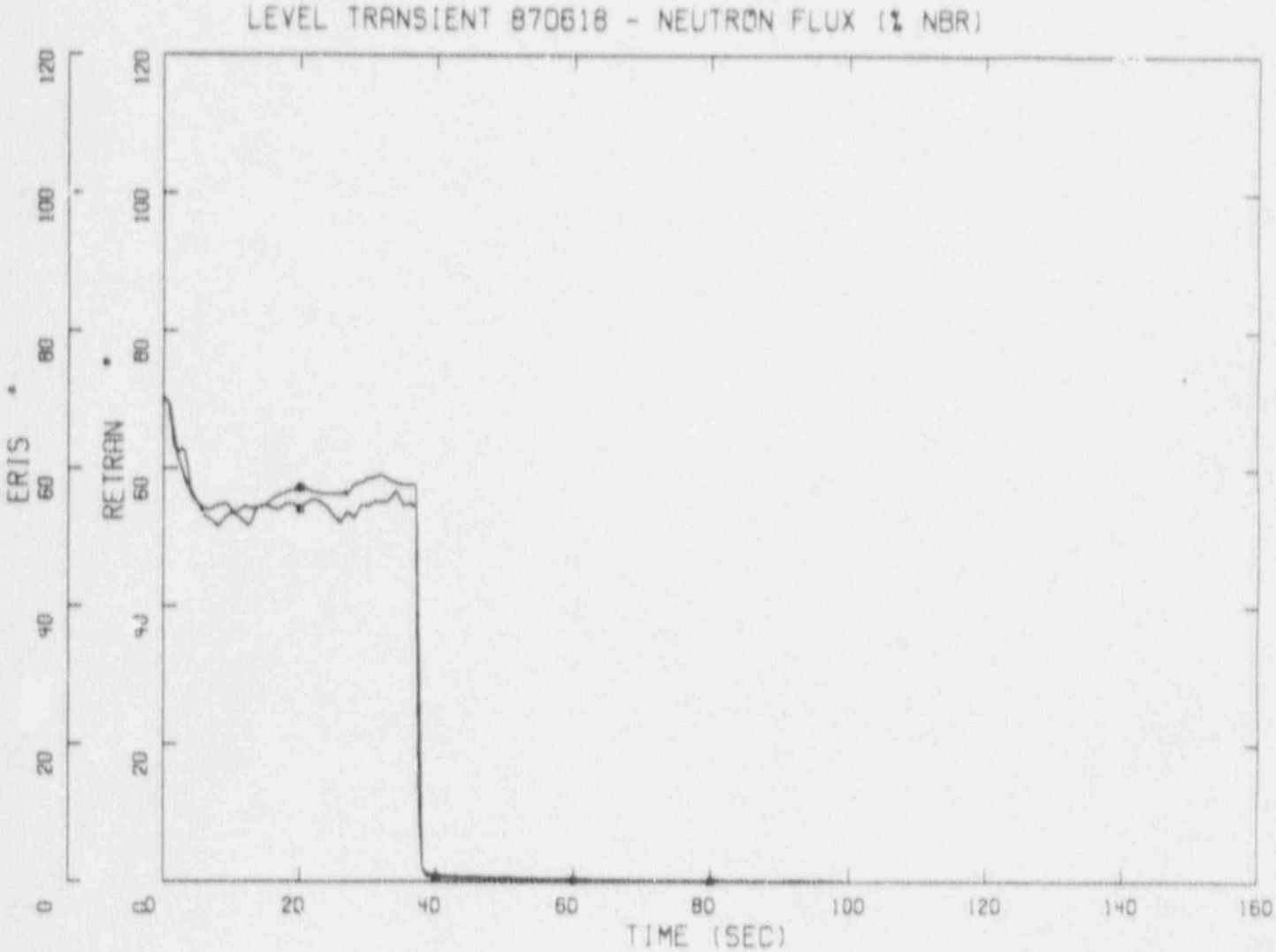

Figure 6.10 Predicted vs Measured Narrow Range Water Level, RBS Water Level Increase Transient

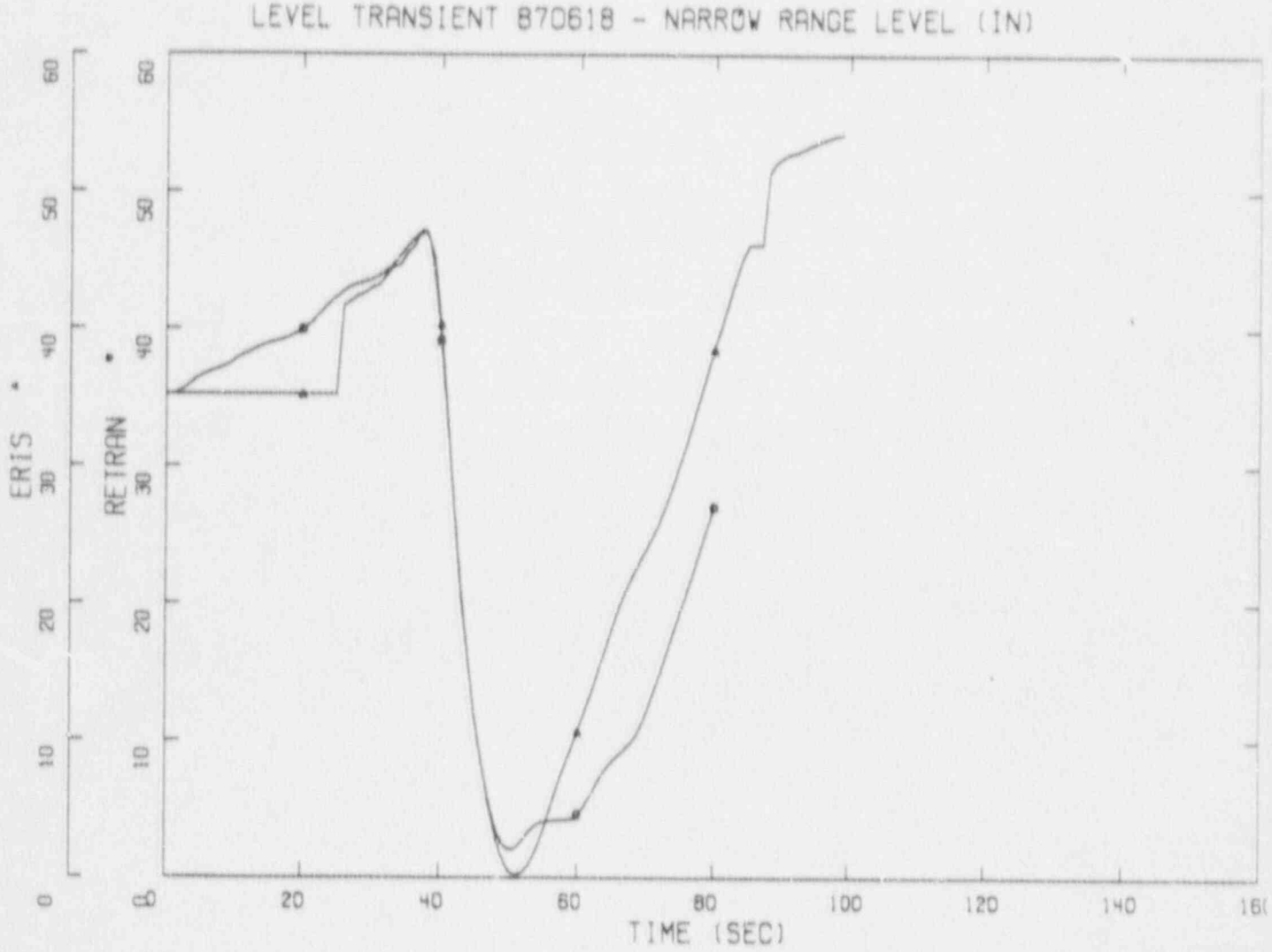

Figure 6.11 Predicted vs Measured Wide Range Water Level, RBS Water Level Increase Transient

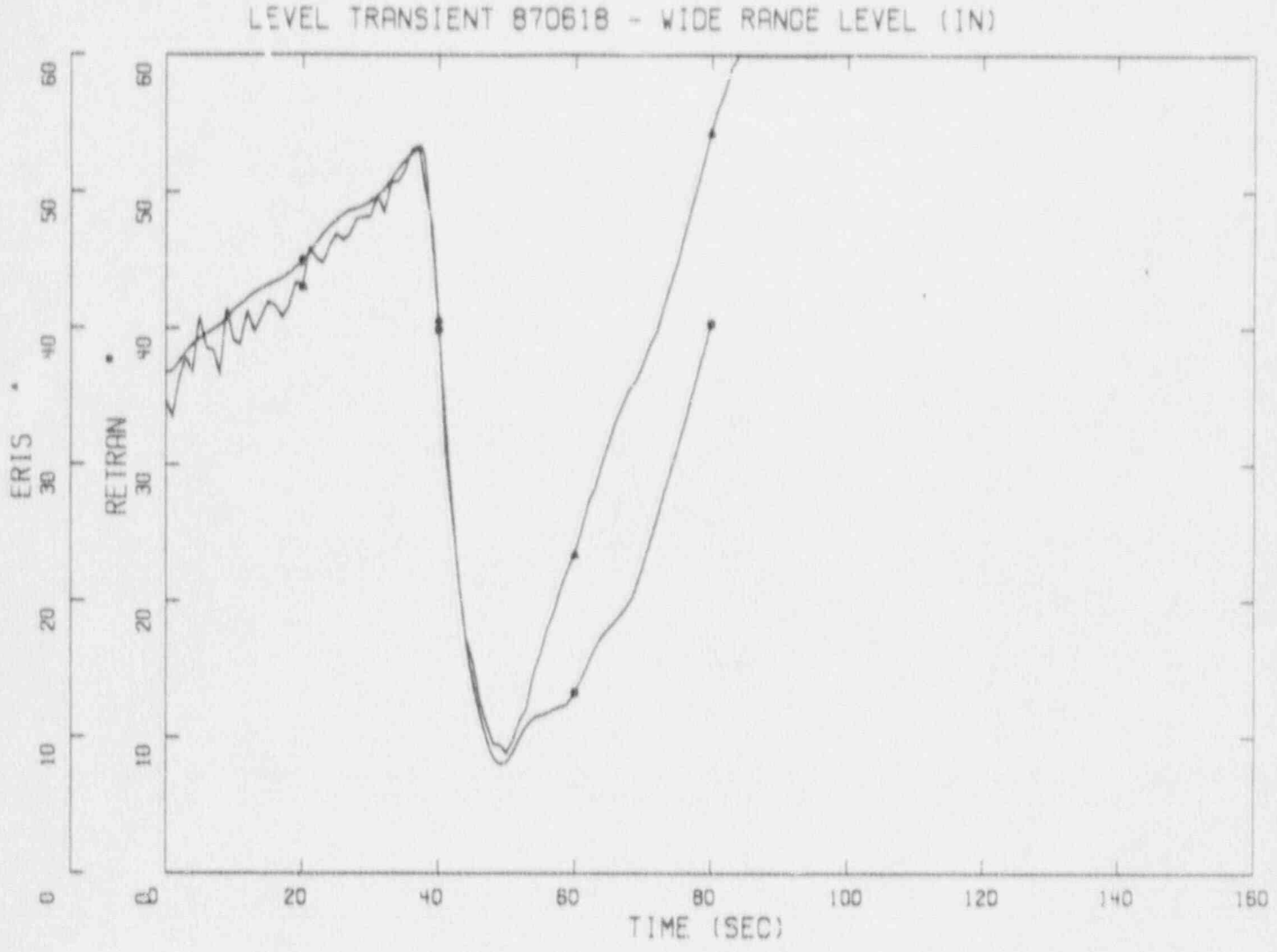

Figure 6.12 Predicted vs Measured Core Flow, RBS Water Level Increase Transient

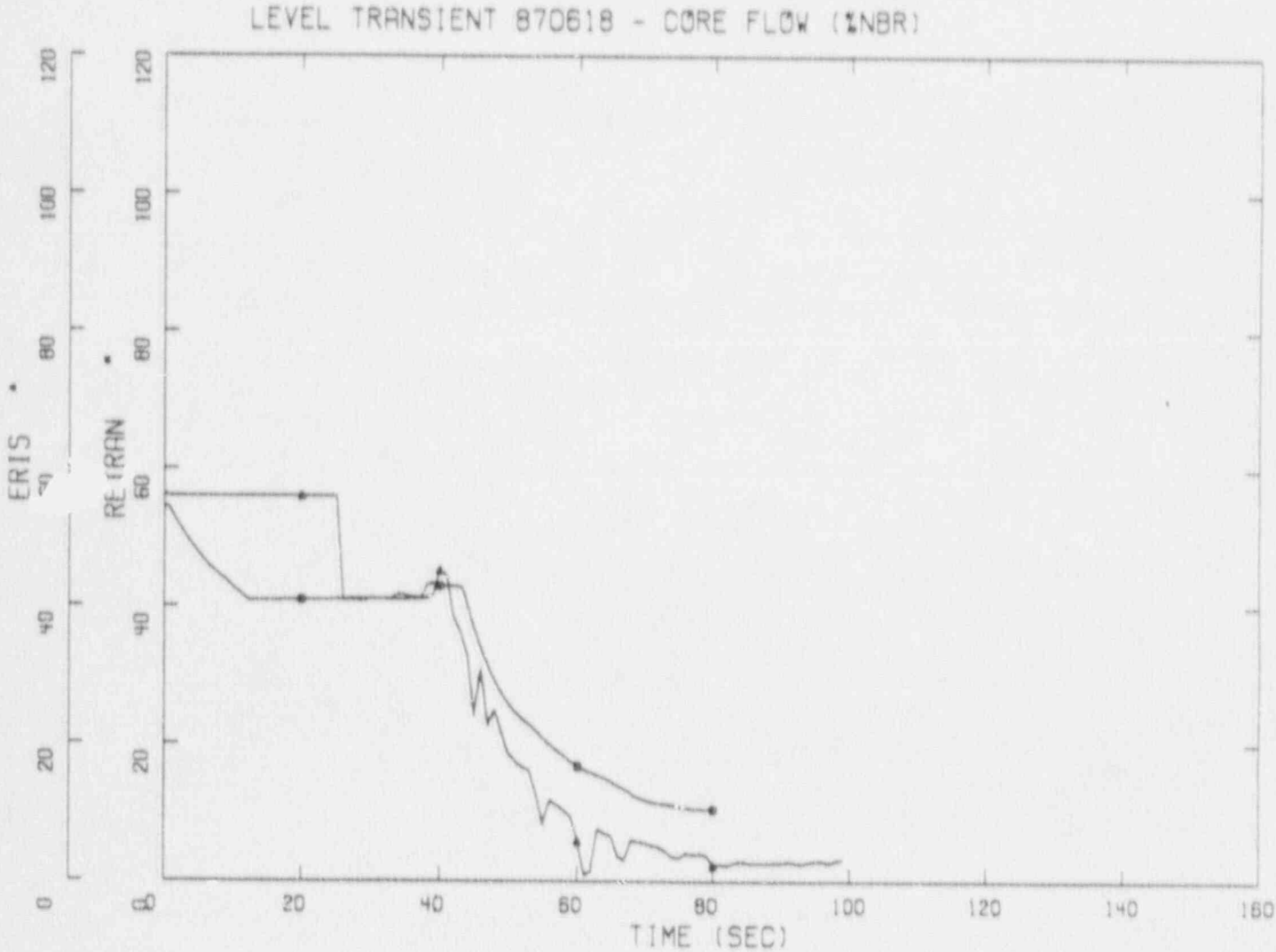

Figure 6.13 Predicted vs Measured Feedwater Flow, RBS Water Level Increase Transient

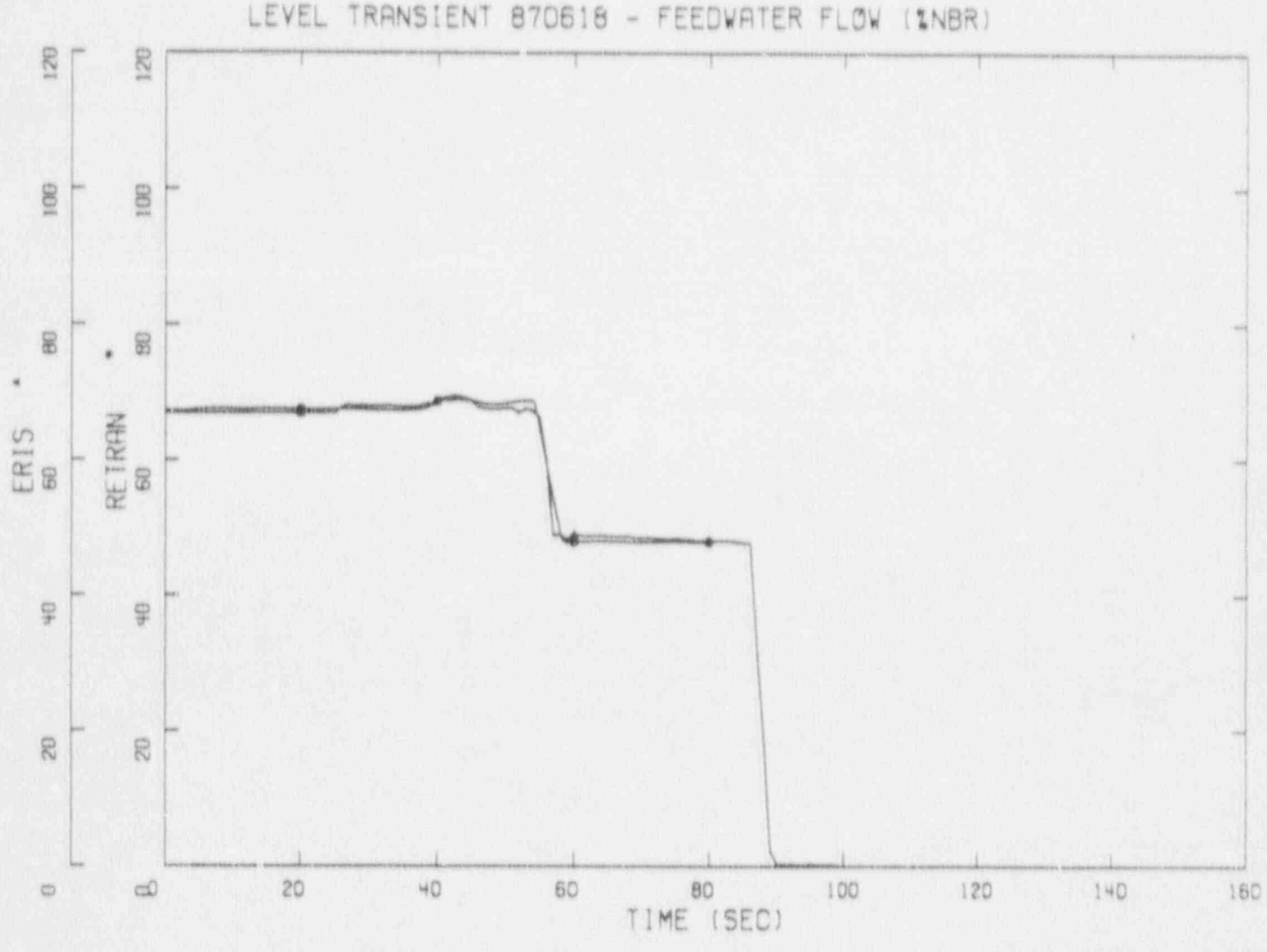

Figure 6.14 Predicted vs Measured Turbine Steam Flow, RBS Water Level Increase Transient

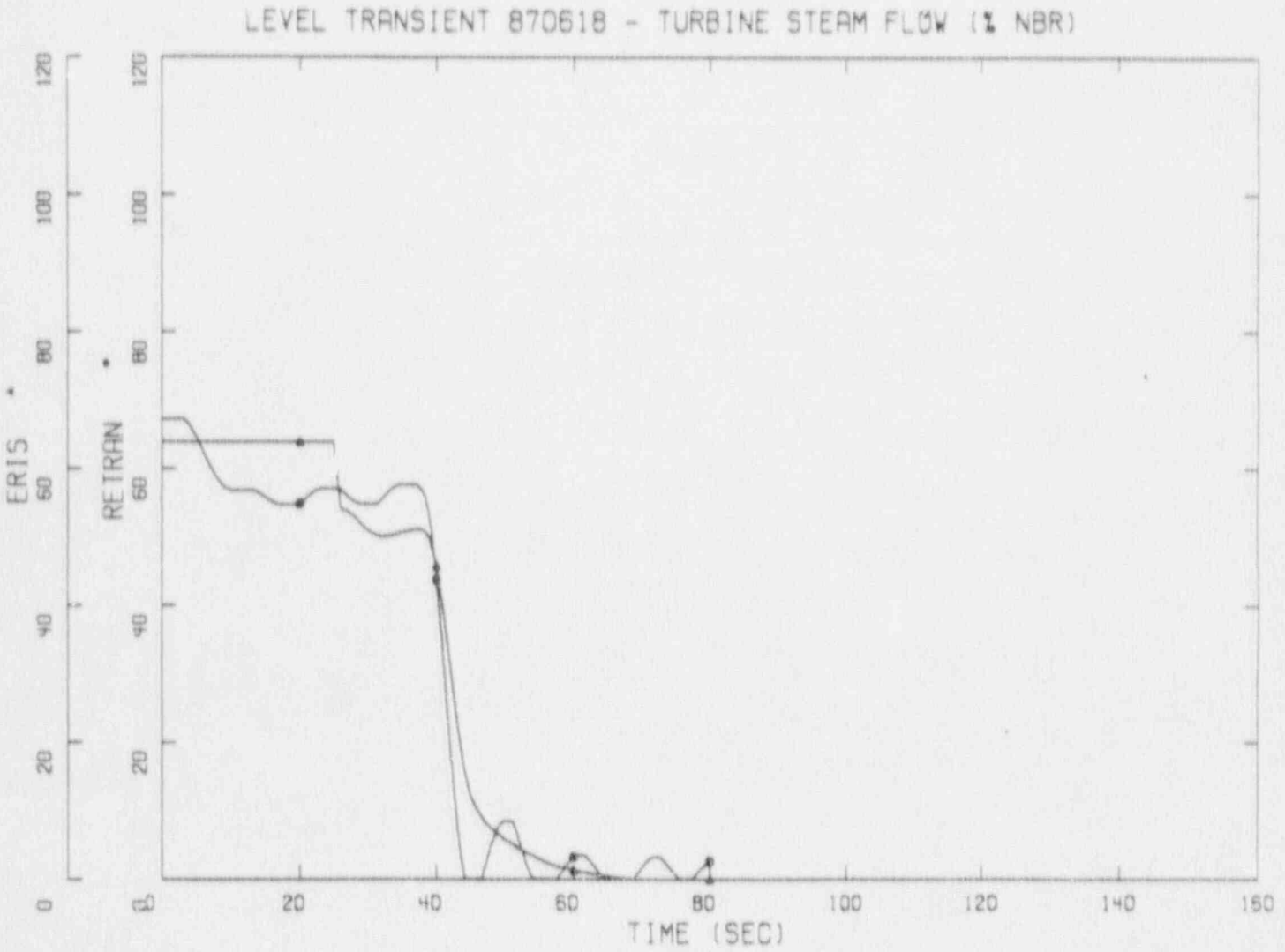

Figure 6.15 Predicted vs Measured Water Level, RBS Water Level Setpoint Change (+6")

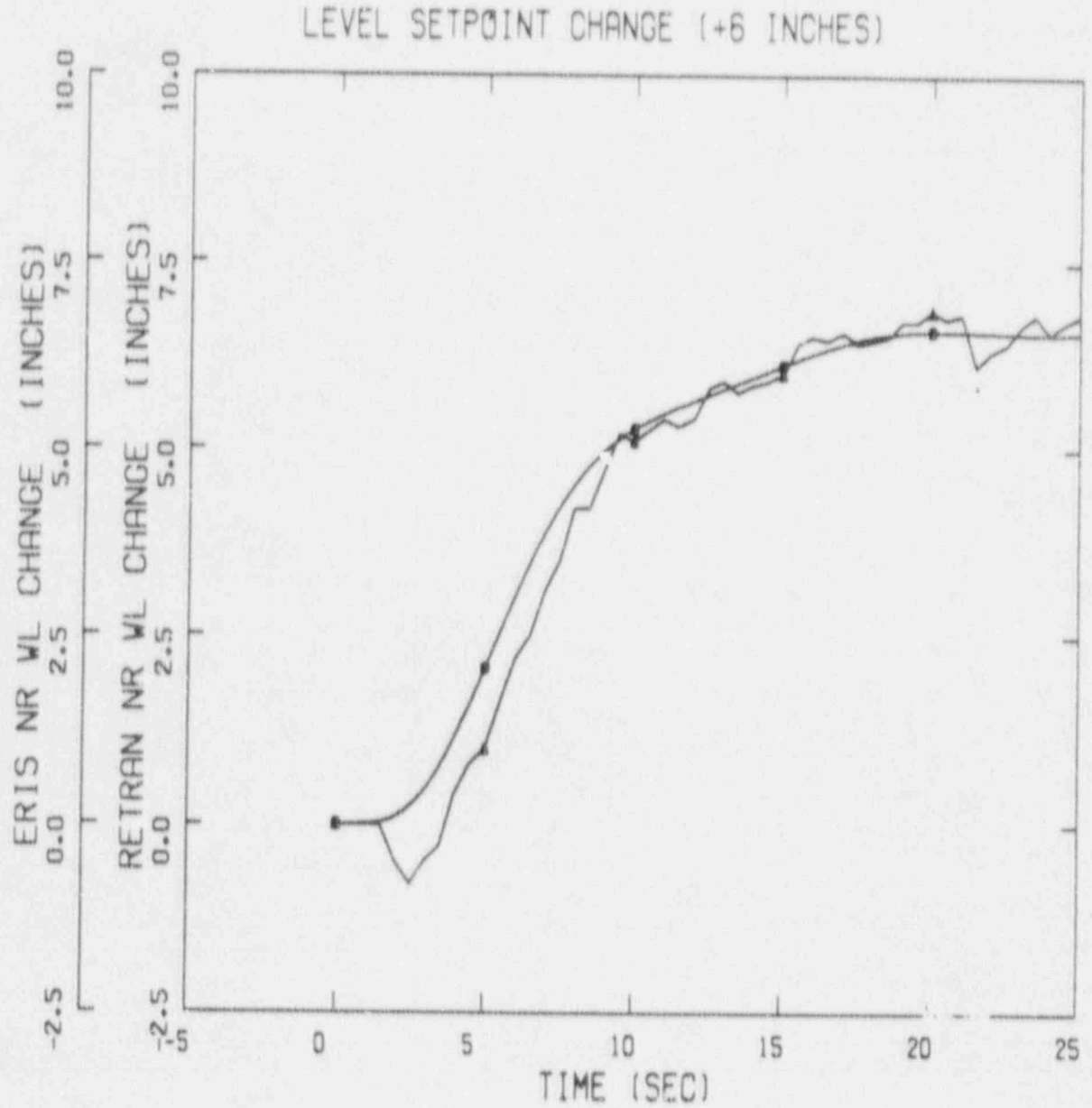

Figure 6.16 Predicted vs Measured Feedwater Flow, RBS Water Level Setpoint Change (+6")

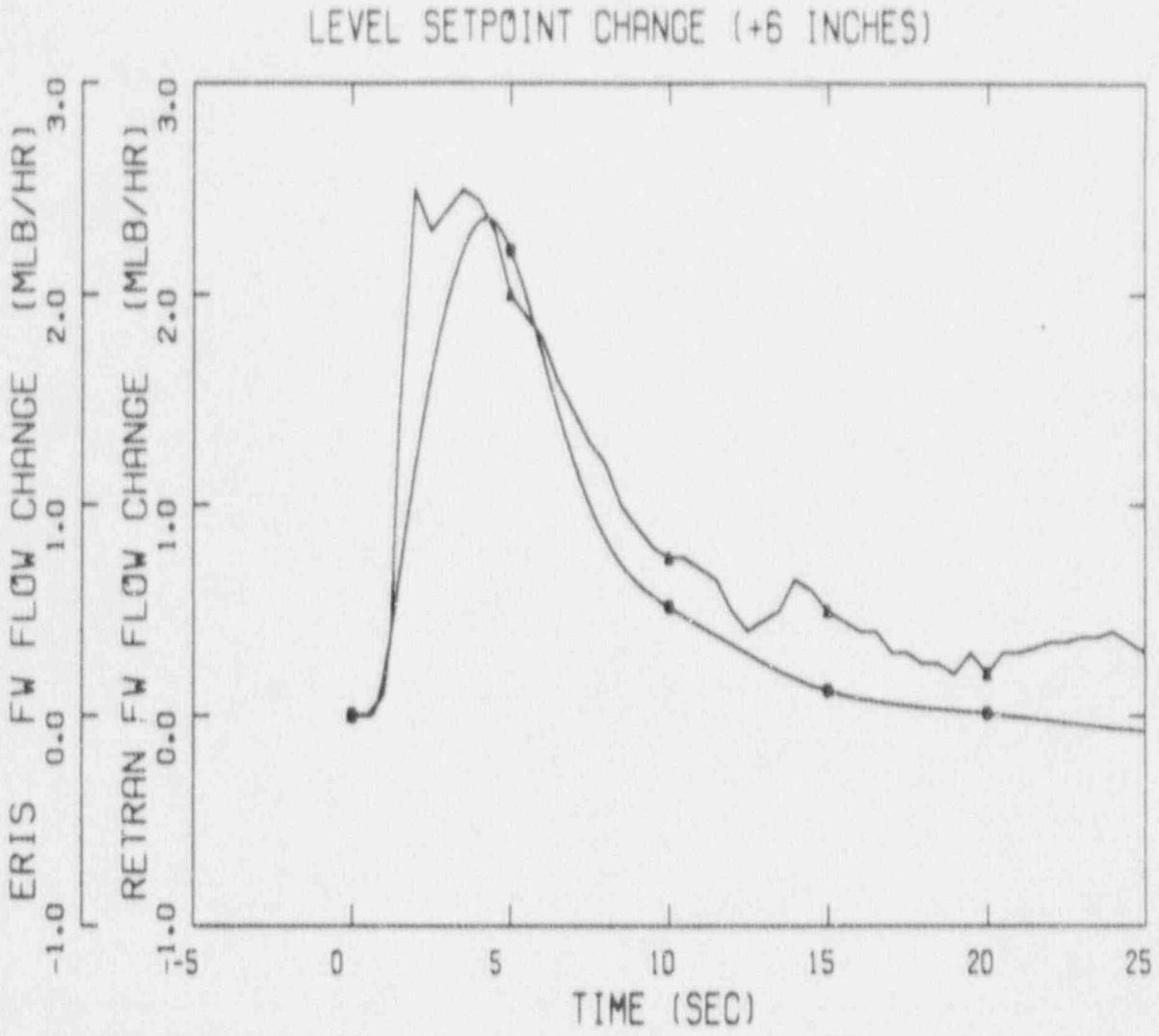

Figure 6.17 Predicted vs Measured Water Level, RBS Water Level Setpoint Change (-6")

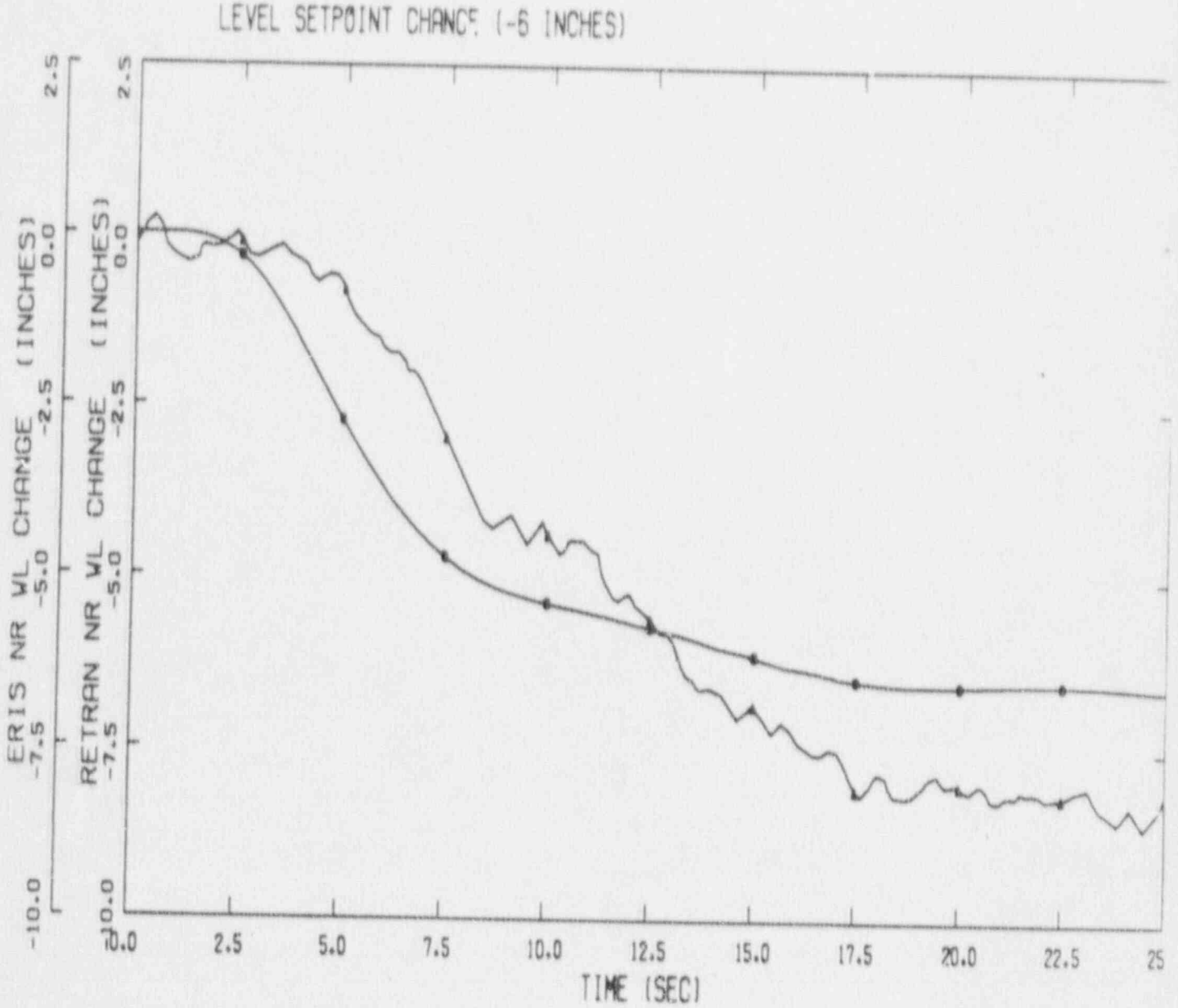

Figure 6.18 Predicted vs Measured Feedwater Flow, RBS Water Level Setpoint Change (-6")

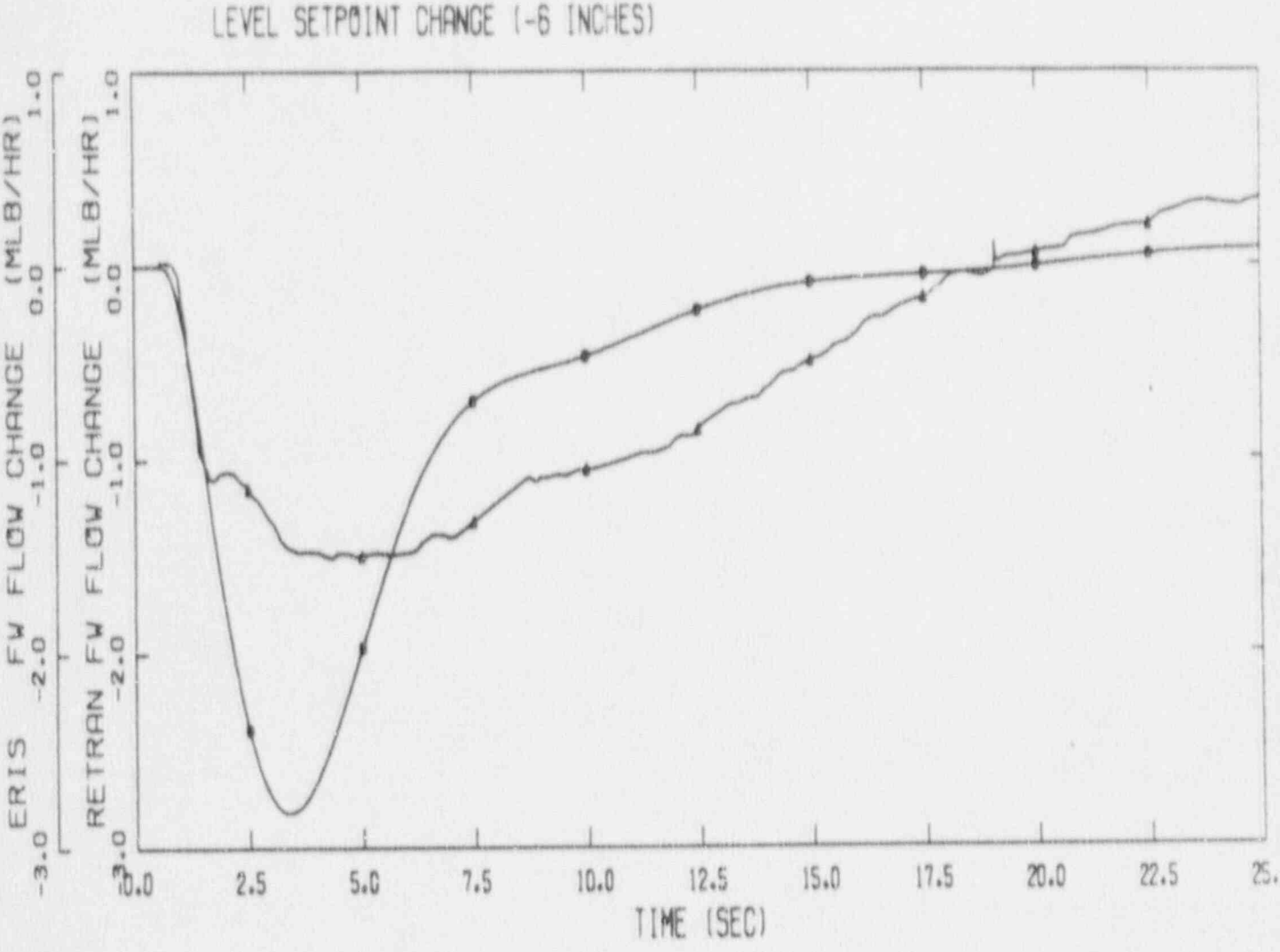

7.0 COMPARISON TO PEACH BOTTOM UNIT 2 TRANSIENTS

As a part of the methods qualification, GSU calculational results were compared with experimental data from Peach Bottom Atomic Power Station, Unit 2 ("Peach Bottom"). These comparisons demonstrate the validity of GSU methods for analysis of fast pressurization transients.

7.1 BENCHMARK DESCRIPTION

Three turbine trip transient experiments were performed at Peach Bottom in April 1977 at the end of Cycle 2[12]. The purpose of these tests was to investigate the effect on neutron flux of a pressure transient in the reactor core following a turbine trip. The three tests were identified as Tests TT1, TT2, and TT3; four stability tests were also performed during this period. Additional instrumentation was installed to gather more detailed information than is normally available and some normal protective features were disabled to allow a more severe transient than would normally be expected. The

results of these three tests are useful for reload analysis methods qualification.

The tests were each initiated by manual turbine trip. The normal reactor scram on turbine stop valve position was disabled, allowing a higher power spike consistent with design basis analyses. Reactor scram was initiated by high neutron flux at a reduced setpoint. Condenser bypass was allowed to initiate normally on turbine stop valve position.

In addition to the EPRI-sponsored tests, the Peach Bottom benchmark analyses also co.ered a License Basis Transient (LBT) problem developed by Brookhaven National Laboratory[13] to test the capabilities of transient computer codes to evaluate conditions more severe than those observed in the tests. Because the postulated LBT transient required assumptions outside the normal GSU methodology, the LBT benchmark is included as a demonstration of capabilities rather than methods.

7.2 PEACH BOTTOM RETRAN MODEL

The RETRAN model of Peach Bottom was developed with the same techniques as were used for River Bend. A nodalization diagram for the Peach Bottom system model is shown in Figure 7.1. Geometry and configuration were obtained primarily from the EPRI report[12] as supplemented by other sources[14,15].

Since the Peach Bottom benchmarks only cover a limited range of fast pressurization events, the control systems are much simpler than those in the River Bend model, which cover all anticipated operating modes. The Peach Bottom model includes simple controls to close the turbine stop valves, to initiate scram on either time or high power, to open the bypass valves, to adjust bypass valve and turbine stop valve loss coefficients as a function of position, and to set feedwater flow and enthalpy.

7.3 TURBINE TRIP TEST SIMULATION

This section describes the analysis of the test data obtained during the three turbine trip tests.

7.3.1 Initial Conditions

Initial statepoint conditions are determined from published data. RETRAN initialization requires additional data, sufficient to calculate initial conditions everywhere within the system. RETRAN initial conditions for Tests TT1, TT2, and TT3 are summarized in Table 7.1.

Plant Data. Actual plant data available includes core power and flow, dome pressure, steam flow, water level, recirculation flows and recirculation and jet pump specifications. This information was obtained from the literature[12, 14, 15] or from test data available on floppy disk through EPRI. A steam flow-feedwater temperature relationship and a core flow-recirculation flow relationship were determined from the available plant data.

Calculated Data. Core bypass flow and loss c[illegible] i-cients were calculated by FIBWR. REBAL was u[illegible] to determine the remaining necessary initial conditions.

Core neutronics data for each case was calculated by SIMULATE-E and processed for input to RETRAN by SIMTRAN. The methodology used for this data transfer is described in Section 4.0 and in Reference 1.

Initial values for the control system were calculated for each case and 10 second null-transient runs were made to verify that the system was initialized to a self-consistent steady state.

7.3.2 Transient Modeling

Several parameters are case dependent. These are generally items that control event timing, specify trip setpoints, or control boundary conditions. They are items that were set by the plant operators for the tests, or that were measured during the tests. However, separator inertia is condition dependent, specifically of separator inlet quality. Thus it varies with each case to the extent that quality varies.

The high flux scram setpoint was set at the plant differently for each test. Alternatively, the actual scram time as recorded can be input. Rod position as a function of time, and hence, speed, was also recorded. Turbine Stop Valve (TSV) and Bypass Valve (BPV) positions were recorded during each test.

Changes in feedwater flow and recirculation pump speed were not considered significant during the period modeled. These were assumed constant.

Separator inertia is determined independently for each case from General Electric ODYN Qualification Report[16]. The inertia is a function of inlet quality and does not effect the initialization of RETRAN. Best results were obtained by applying half the total inertia at the separator inlet, half of that part attributed to the standpipes at the standpipe inlet, and the remainder to the separator liquid return junction. The inertia of the steam outlet of the separators was based on the geometry of the steam region in the separators. The area of the steam region is calculated from the geometry of the separators and the water layer thickness obtained from General Electric ODYN Qualification.

7.3.3 Simulation Results

The results of the Test TT1 benchmark are shown in Figures 7.2 through 7.6. The results of the Test TT2 benchmark are shown in Figures 7.7 through 7.11. The results of the Test TT3 benchmark are shown in Figures 7.12 through 7.16. Each set of figures provides prediction versus measurement comparisons of core average power, upper plenum pressure, dome pressure, TSV "A" pressure, and core inlet flow, calculated at the jet pump exit.

The power comparisons show general agreement with the published data in both timing and magnitude. The Test TT1 simulation (Figure 7.2) shows an overprediction of the magnitude of the power peak, but the timing of the peak and the initial power rise are predicted very closely. The Test TT2 power spike (Figure 7.7) is in very close agreement with the data. Although the power trace follows the data closely, the predicted Test TT3 power peak (Figure 7.12) is later and slightly lower than the data. The greater width of the predicted impulse indicates it is conservative relative to the data.

The measured data for upper plenum pressure exhibits some fluctuation. The Test TT1 simulation (Figure 7.3) overpredicts the upper plenum pressure after the initial pressure surge is stopped. The Test TT2 (Figure 7.8) and TT3 (Figure 7.13) predictions follow the data trends closely.

The dome pressure data were also smoothed for comparison with predictions. The TT1 analysis (Figure 7.4) overpredicts the data after the initial pressure surge. As with the upper plenum pressure, the Test TT2 (Figure 7.9) and TT3 (Figure 7.14) follow the data trends closely.

As was the case with the other pressure data, some scatter in the TSV pressure data made smoothing necessary before reasonable graphic comparisons could be made. The predictions for Test TT1 (Figure 7.5), TT2 (Figure 7.10), and TT3 (Figure 7.15) all track the smoothed data.

The "measured" core flow data for the three tests were calculated from recorded jet pump differential pressures. The recorded signals show a large amount of noise, which was first filtered. The average of the four filtered signals was then used in the solution of the fundamental differential equation relating flow to

differential pressure and inertia. The resulting flows were plotted with an additional time adjustment of 0.25 s. to account for the process instrumentation delay discussed in Section 9, Reference 12. The predictions for Test TT1 (Figure 7.6), TT2 (Figure 7.11), and TT3 (Figure 7.16) show similarity of timing of the initial rise and of peaks and valleys, though the magnitudes of the changes are different. However in no case does the mismatch exceed 8% of the initial value of flow. The predicted behavior of the core inlet flow is consistent with the phenomenology.

7.4 LICENSE BASIS TRANSIENT MODELING

This section describes the demonstration analysis covering the Peach Bottom License Basis Transient.

7.4.1 Initial Conditions

Initial conditions for the LBT analysis were generated to be consistent with the Brookhaven analysis. Cross sections for this analysis were generated from a

two-cycle Haling depletion rather than the stepwise depletion used for the turbine trip test benchmarks. The original Haling distribution was not nearly as bottom peaked as that used by Brookhaven. To obtain better agreement with this power shape, the Haling depletions were re-run using a lower value of subcooling and a larger albedo value for the lower reflector. RETRAN initialization was accomplished consistently with the turbine trip test analyses. Initial conditions for the LBT analysis are summarized in Table 7.2.

7.4.2 Analytical Results

The analytical results of the License Basis Transient benchmark are shown in Figures 7.17 through 7.25. Comparisons are made to GE and BNL initial conditions of axial power shape, fuel temperature, void distribution, and clad surface heat flux. Transient comparisons to GE and BNL results included power, core pressure, core flow, and axial clad surface heat flux.

The calculated axial power distribution (Figure 7.17) is in good agreement with both the GE and the BNL

curves. The calculated initial fuel temperatures (Figure 7.18) agree well with the GE data. The initial heat flux (Figure 7.19) is a little lower than both the GE and the BNL data. Since the power and the power distribution are the same, this difference can probably be attributed to a difference in the type of fuel modeled which would lead to a difference in heat transfer area. The calculated initial void distribution (Figure 7.20) is higher than both the GE and the BNL curves. This may be due to differences in void models or in core bypass flow.

The calculated transient power (Figure 7.21) curve is higher and narrower than the GE curve, and both higher and wider than the BNL curve. The area under the calculated curve appears to be similar to that under the GE curve, indicating a similar total energy release. Since CPR calculations are more sensitive to the total energy of an impulse than to the height of the impulse, the calculated results are not unconservative.

The transient pressure calculation (Figure 7.22) shows good agreement to both the GE and the BNL curves. The calculated core inlet flow (Figure 7.23) shows an initial rise which appears to be due to the initial scram induced power decrease. This flow surge is turned around

in both the calculated and the GE curves by the power impulse due to void collapse. Since the GE impulse occurs first, the GE flow decreases first. By about 1 second, the calculated flow appears to be following a similar trend to the GE data, about 5% lower.

The clad surface heat flux at 0.8 and 1.2 seconds (Figures 7.24 and 7.25) is similar in shape to both the GE and BNL curves, reflecting the changes during the transient due to scram and void collapse.

Table 7.1 Peach Bottom Turbine Trip Test Initial Conditions

	TT1	TT2	TT3
Power, MW_{th}	1562	2030	2275
Core flow, lbm/s	28139	23028	28306
Dome pressure, psia	991.6	976.1	986.6
Core inlet enthalpy, Btu/lbm	528.0	518.3	522.7
Water level, inches	23.0	29.2	29.8
Steam flow, lbm/s	1638	2171	2470
Recirculation flow, lbm/s	9090	7652	9378
APRM high power trip, % rated	85	95	77

Table 7.2 Peach Bottom License Basis Transient Initial Conditions

Power, MW_t	3441.2
Core flow, lbm/s	28472.2
Dome pressure, psia	1034.
Core inlet enthalpy, Btu/lbm	522.7
Water level, inches	28.0
Steam flow, lbm/s	3900
Recirculation flow, lbm/s	9500

Figure 7.1 Peach Bottom RETRAN Model Nodalization

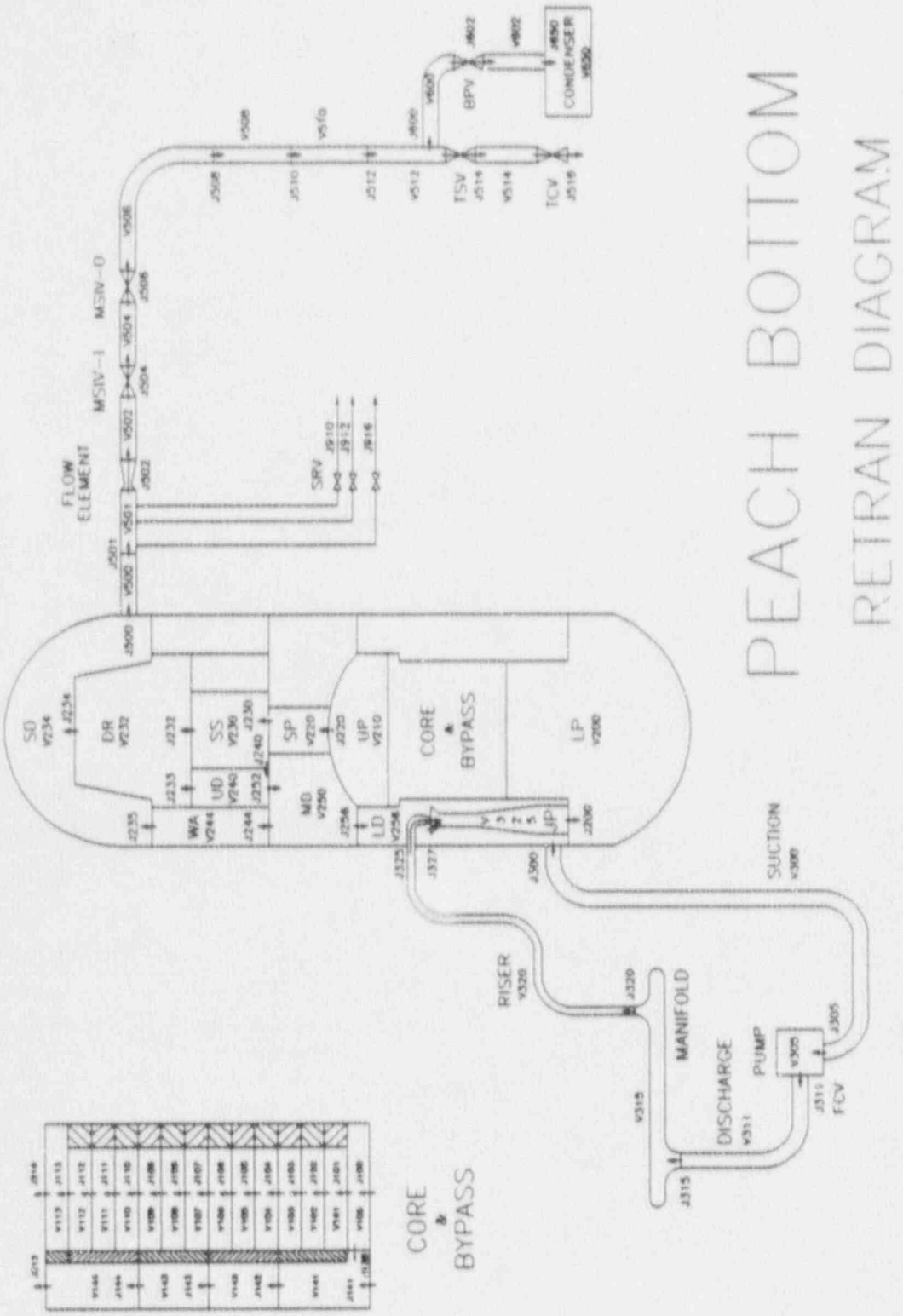

Figure 7.2 Predicted vs Measured Core Power, Peach Bottom Test TT1

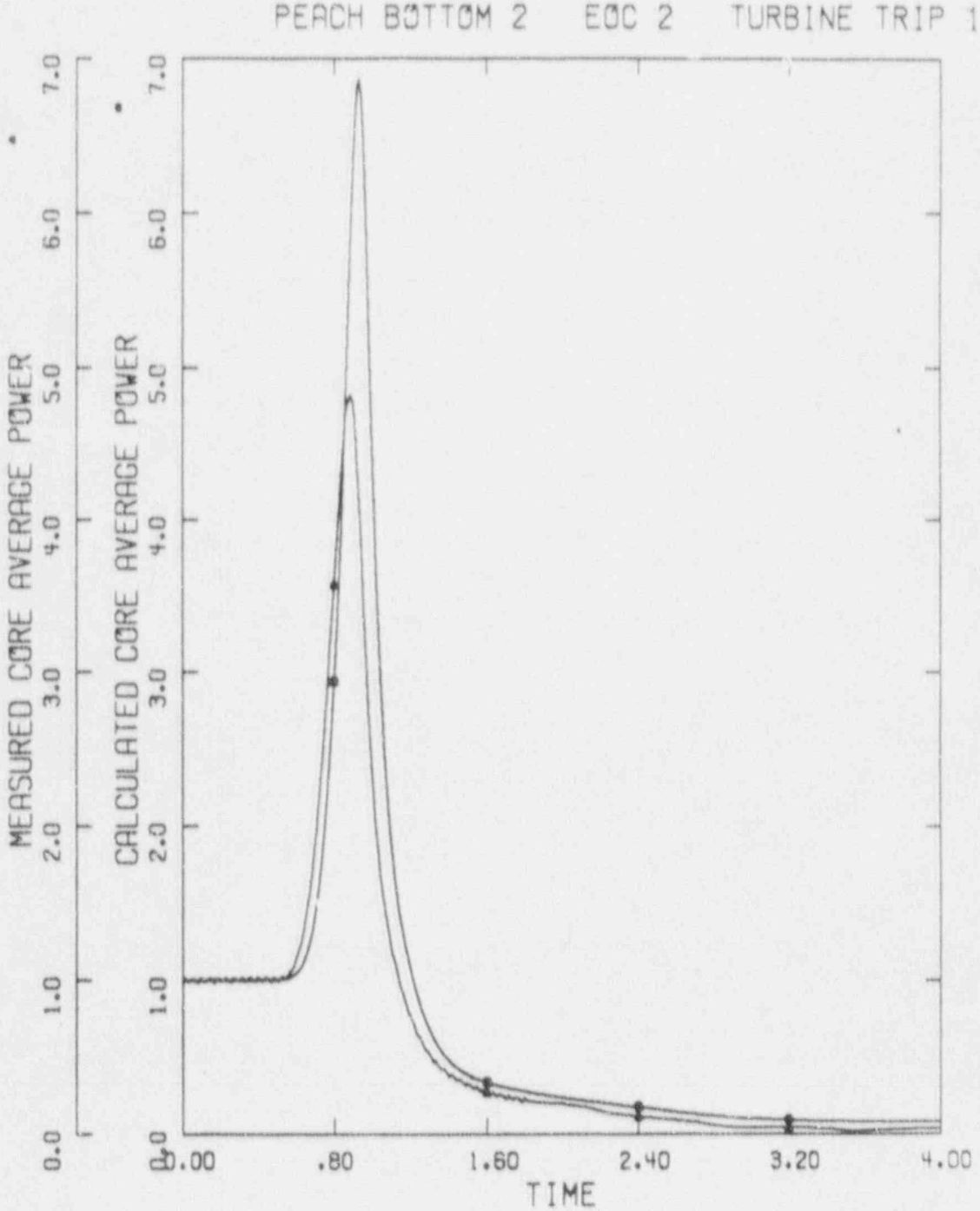

Figure 7.3 Predicted vs Measured Upper Plenum Pressure, Peach Bottom Test TT1

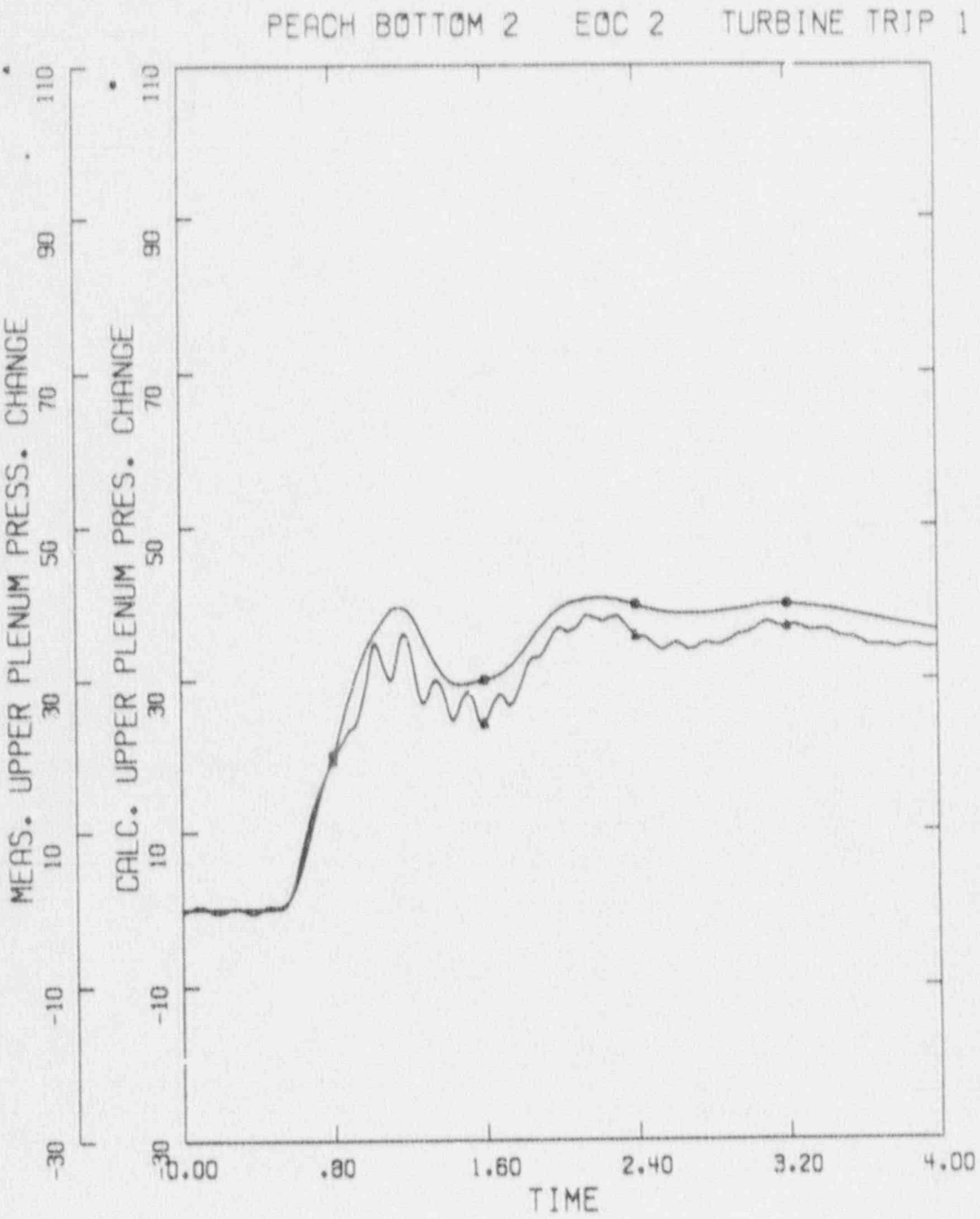

Figure 7.3 Predicted vs Measured Upper Plenum Pressure, Peach Bottom Test TT1

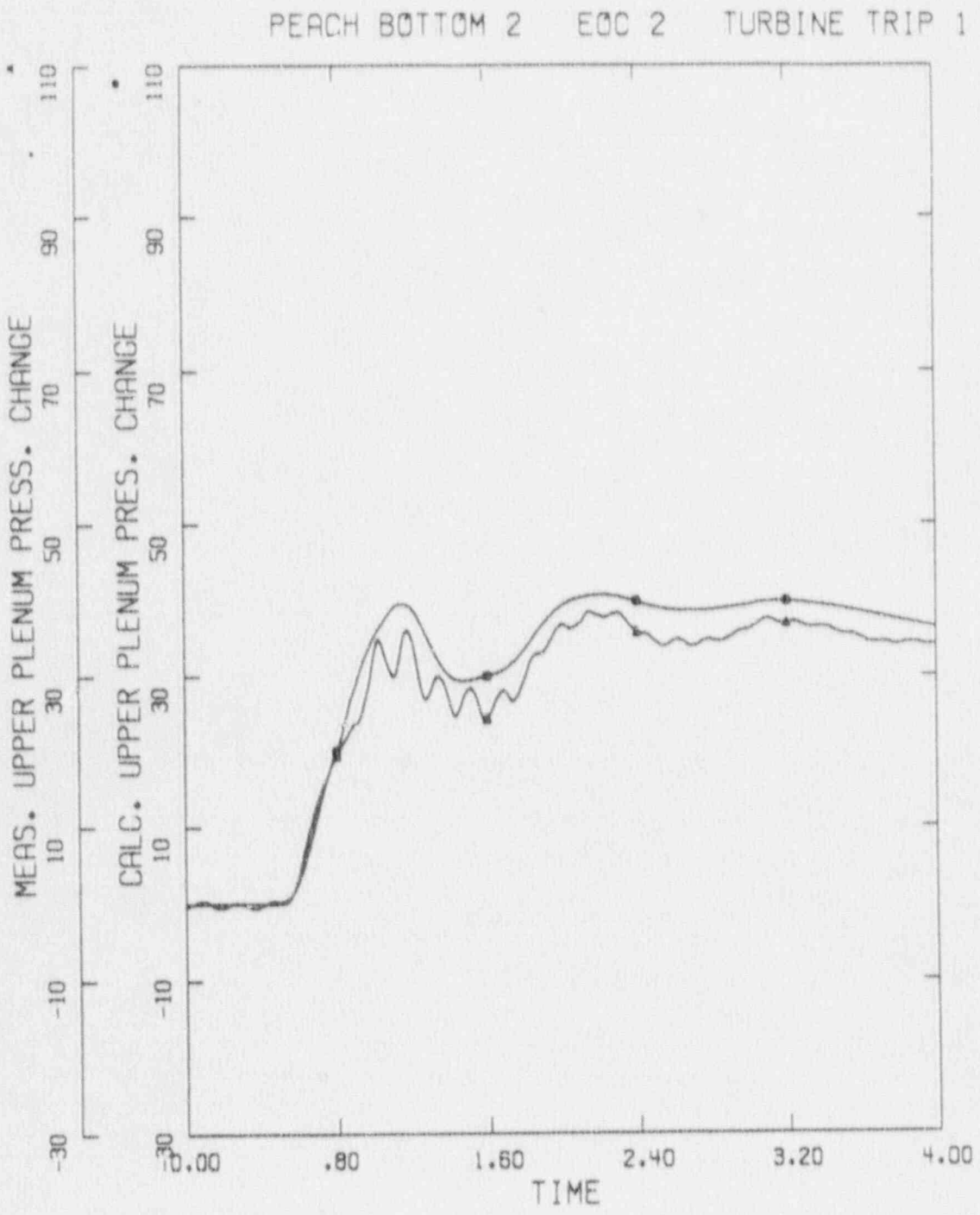

Figure 7.4 Predicted vs Measured Dome Pressure, Peach Bottom Test TT1

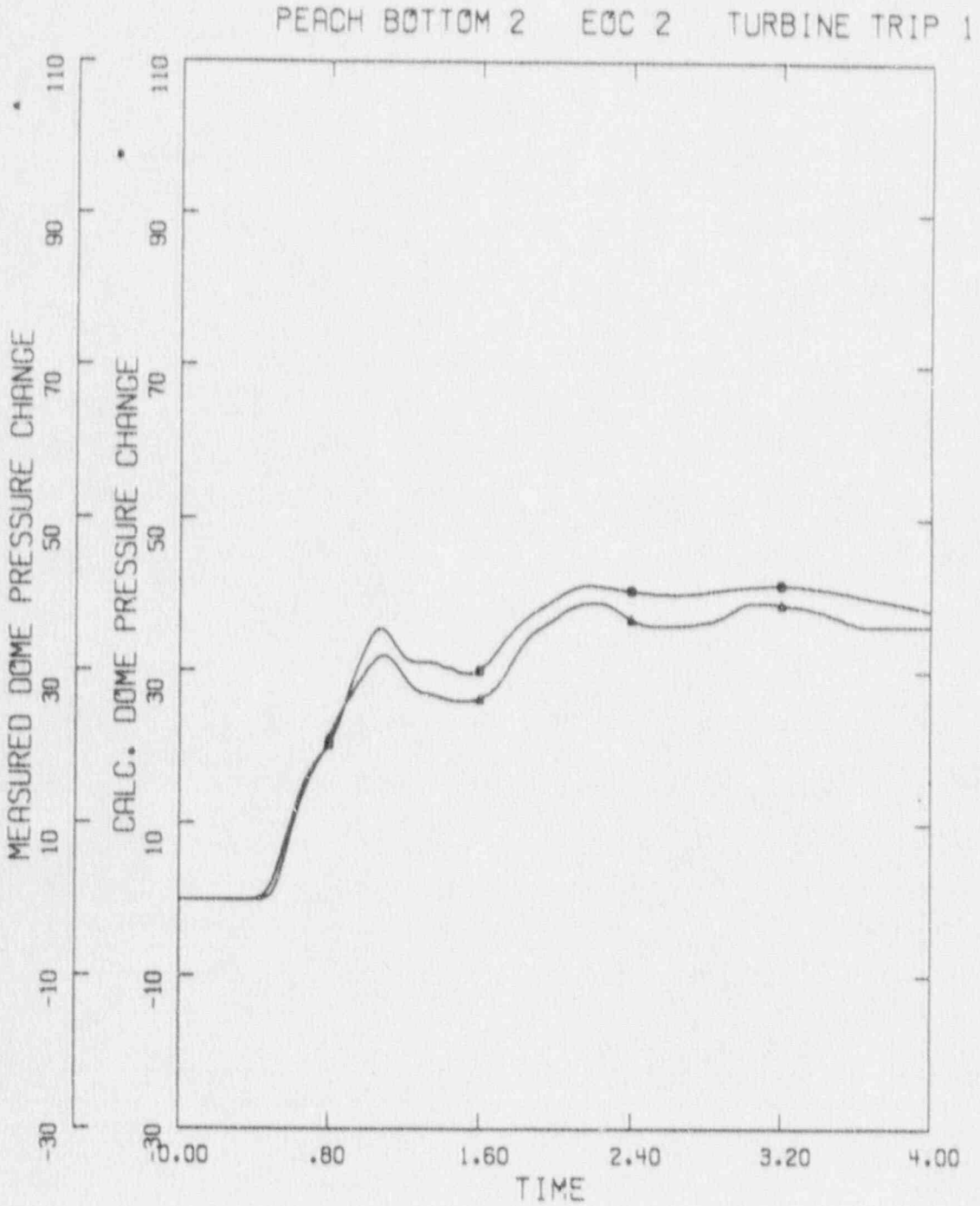

Figure 7.5 Predicted vs Measured TSV Pressure, Peach Bottom Test TT1

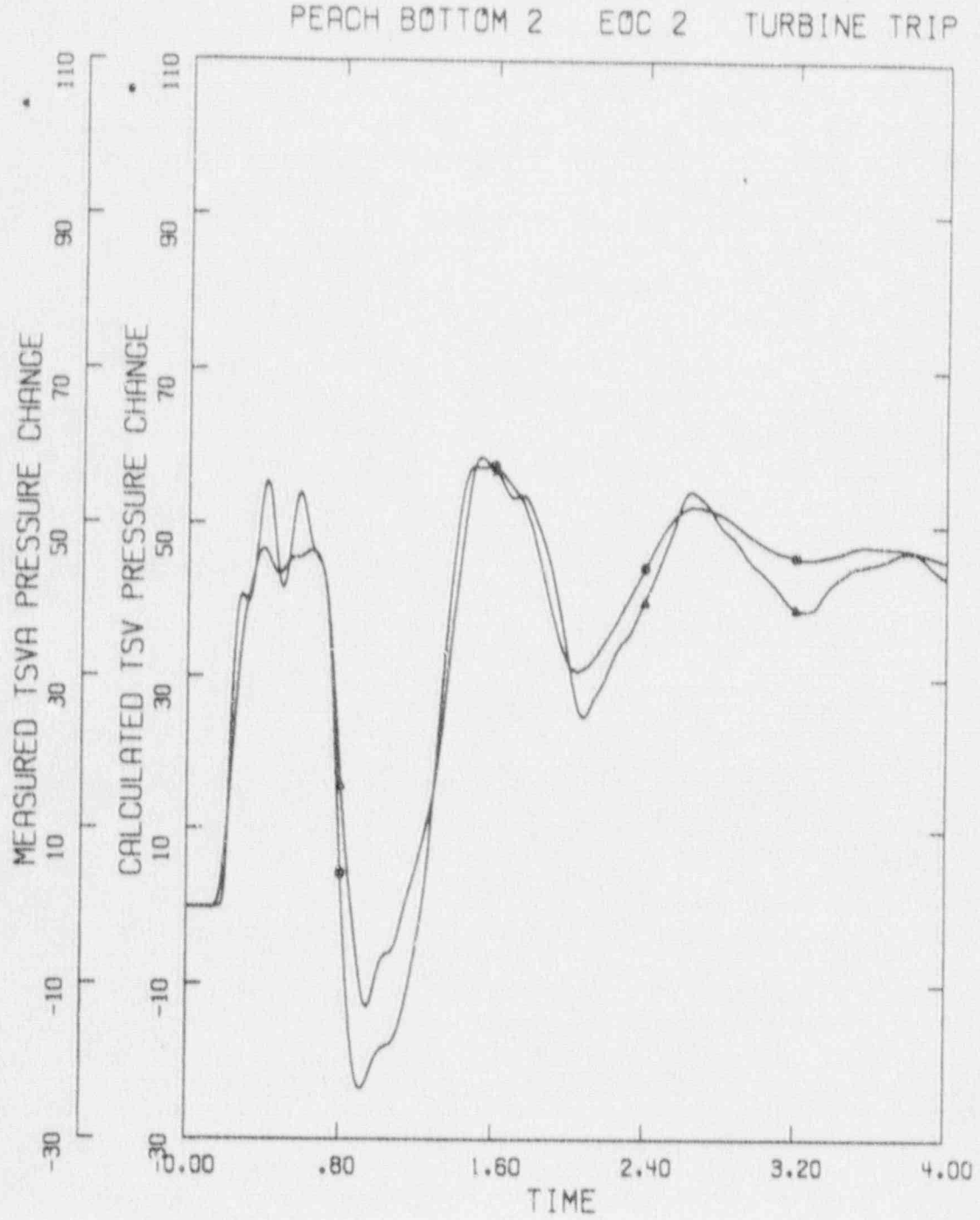

Figure 7.6 Predicted vs Measured Core Inlet Flow, Peach Bottom Test TT1

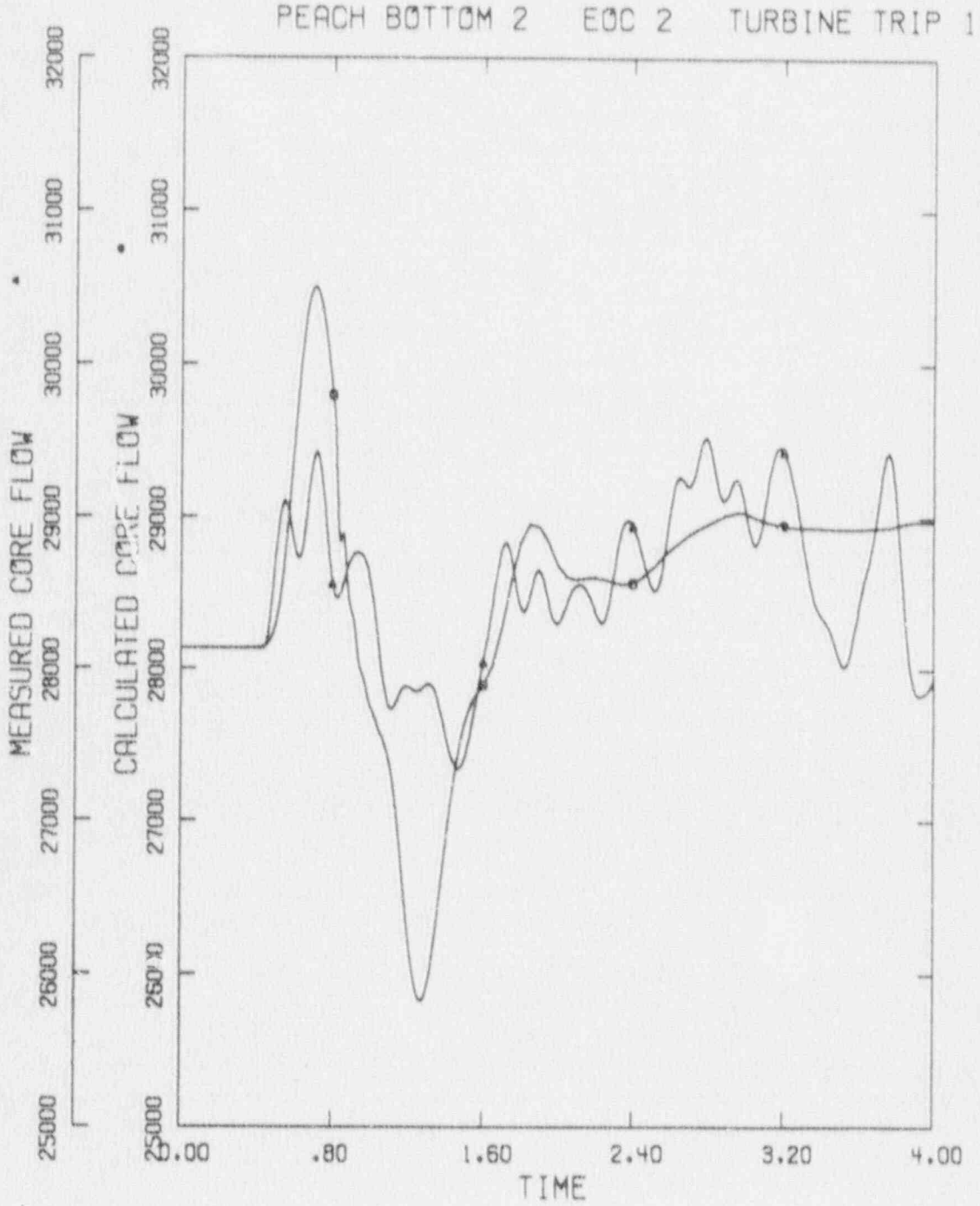

Figure 7.7 Predicted vs Measured Core Average Power, Peach Bottom Test TT2

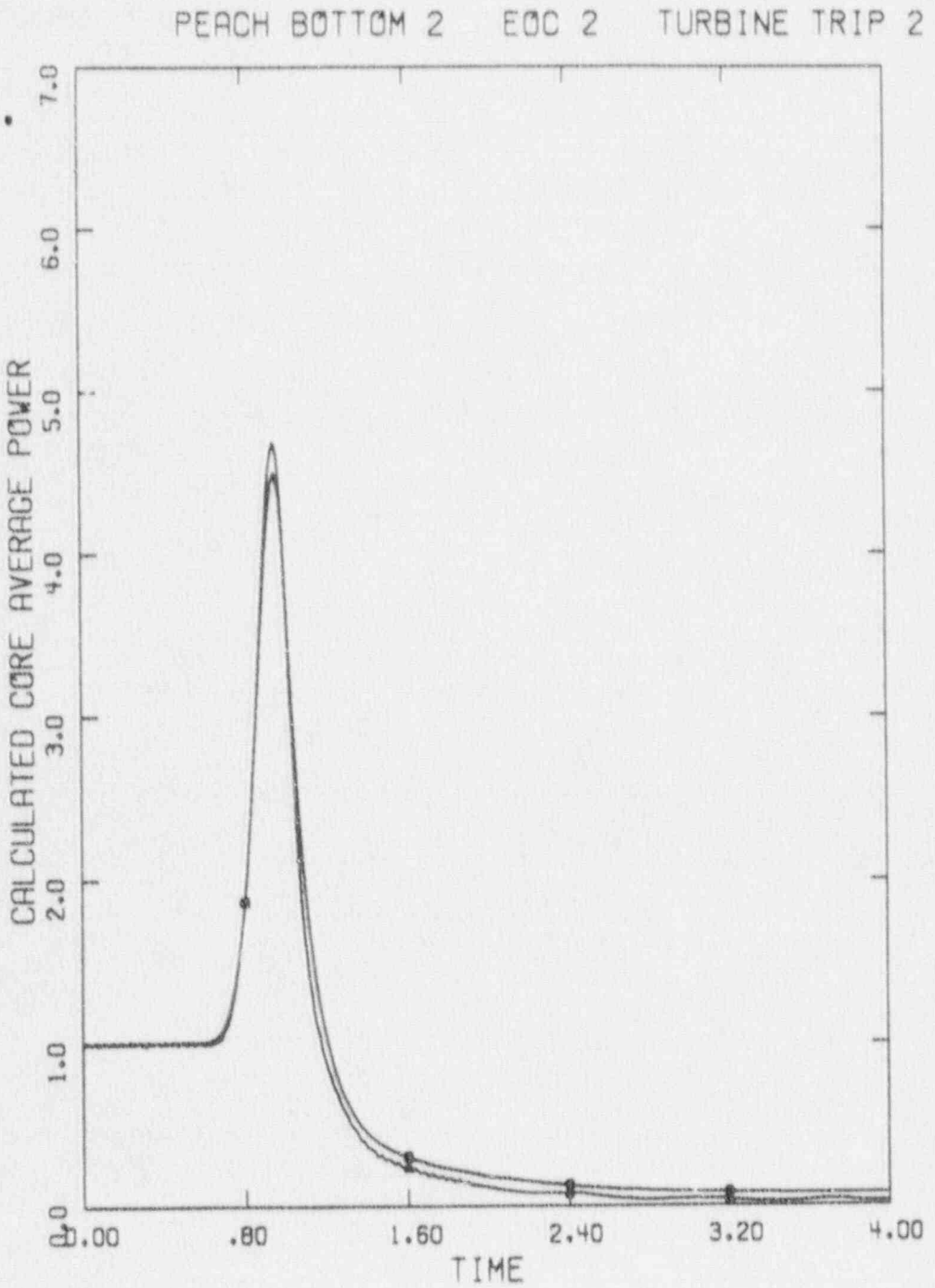

Figure 7.8 Predicted vs Measured Upper Plenum Pressure, Peach Bottom Test TT2

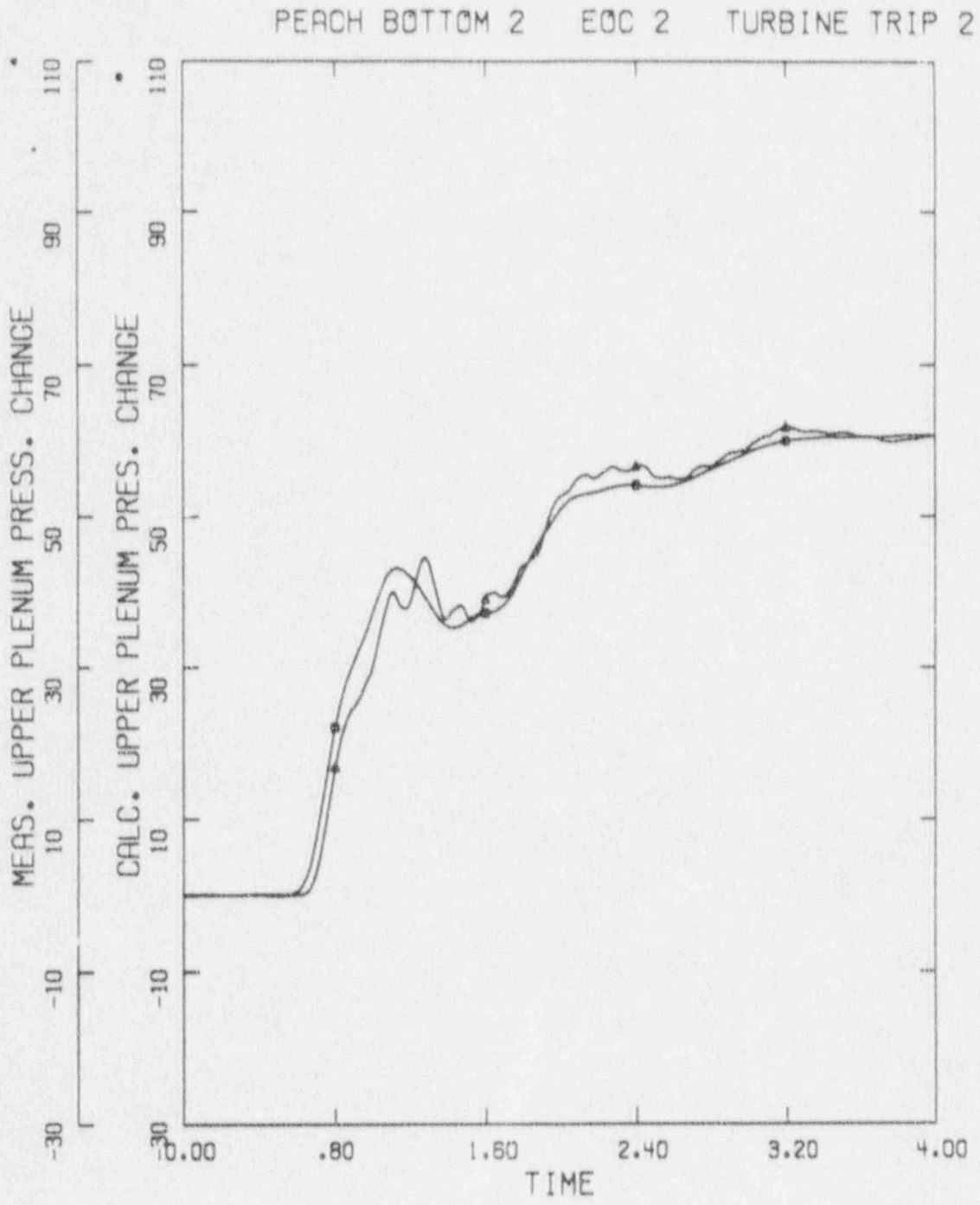

Figure 7.9 Predicted vs Measured Dome Pressure, Peach Bottom Test TT2

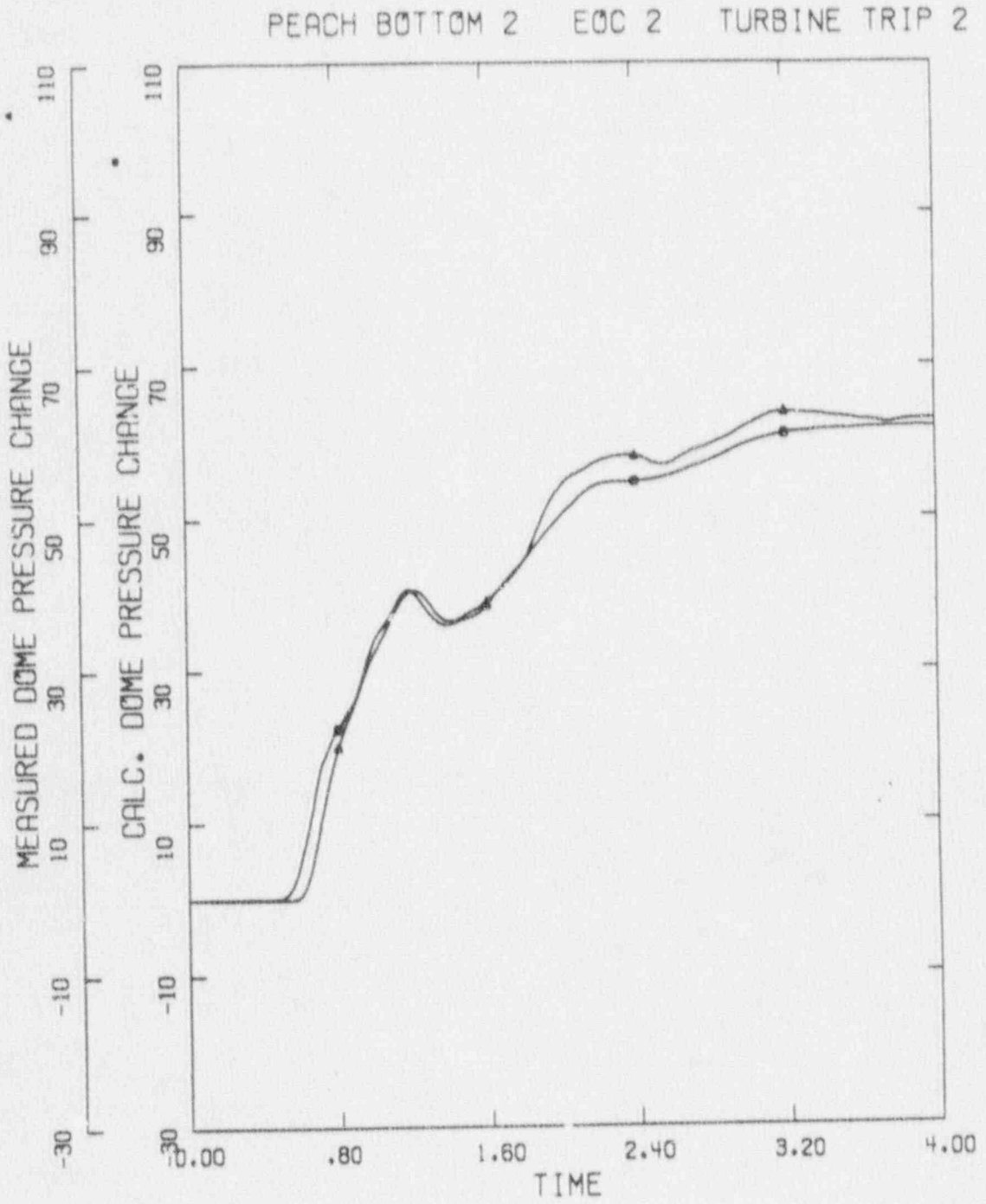

Figure 7.10 Predicted vs Measured TSV Pressure, Peach Bottom Test TT2

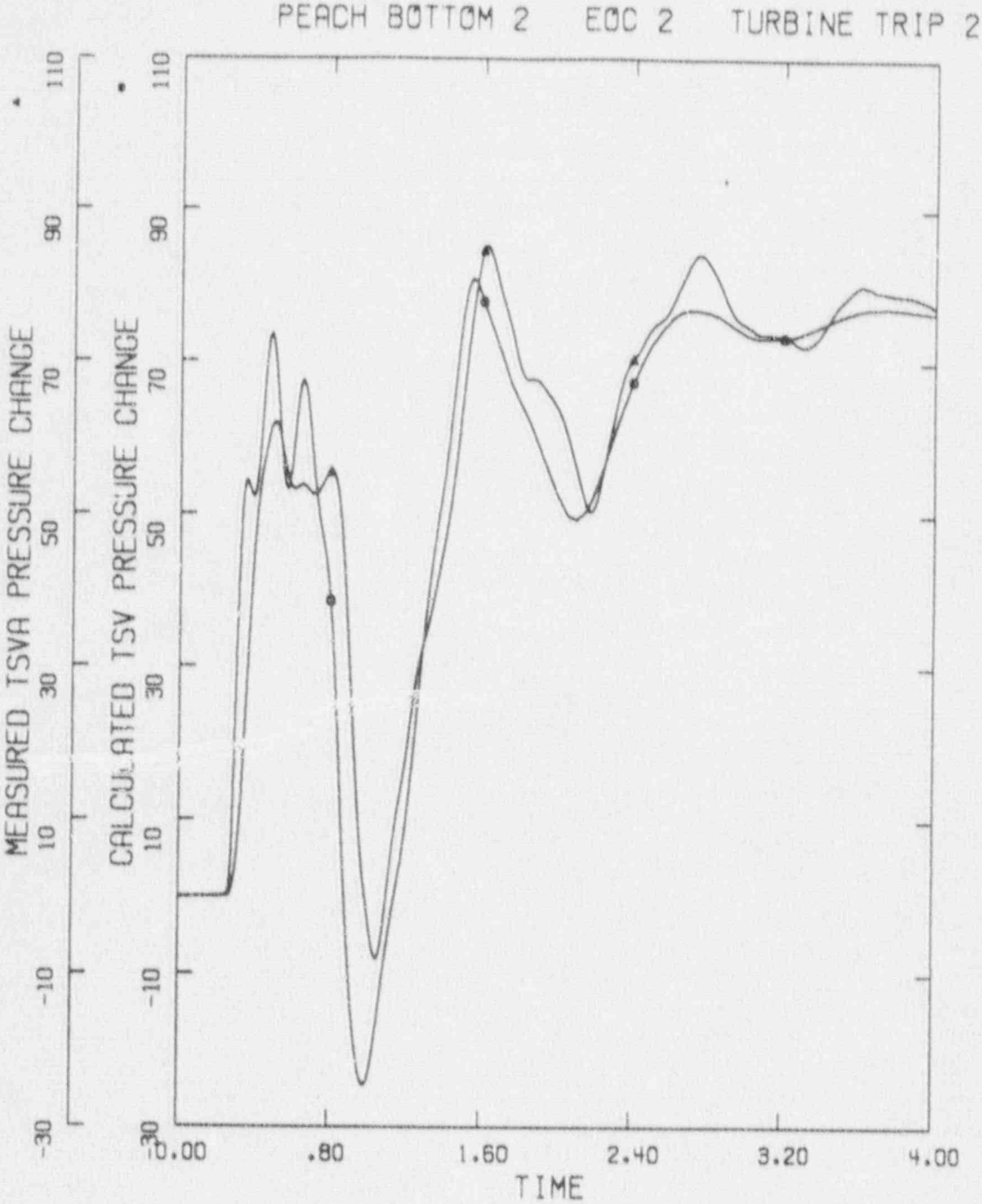

Figure 7.11 Predicted vs Measured Core Inlet Flow, Peach Bottom Test TT2

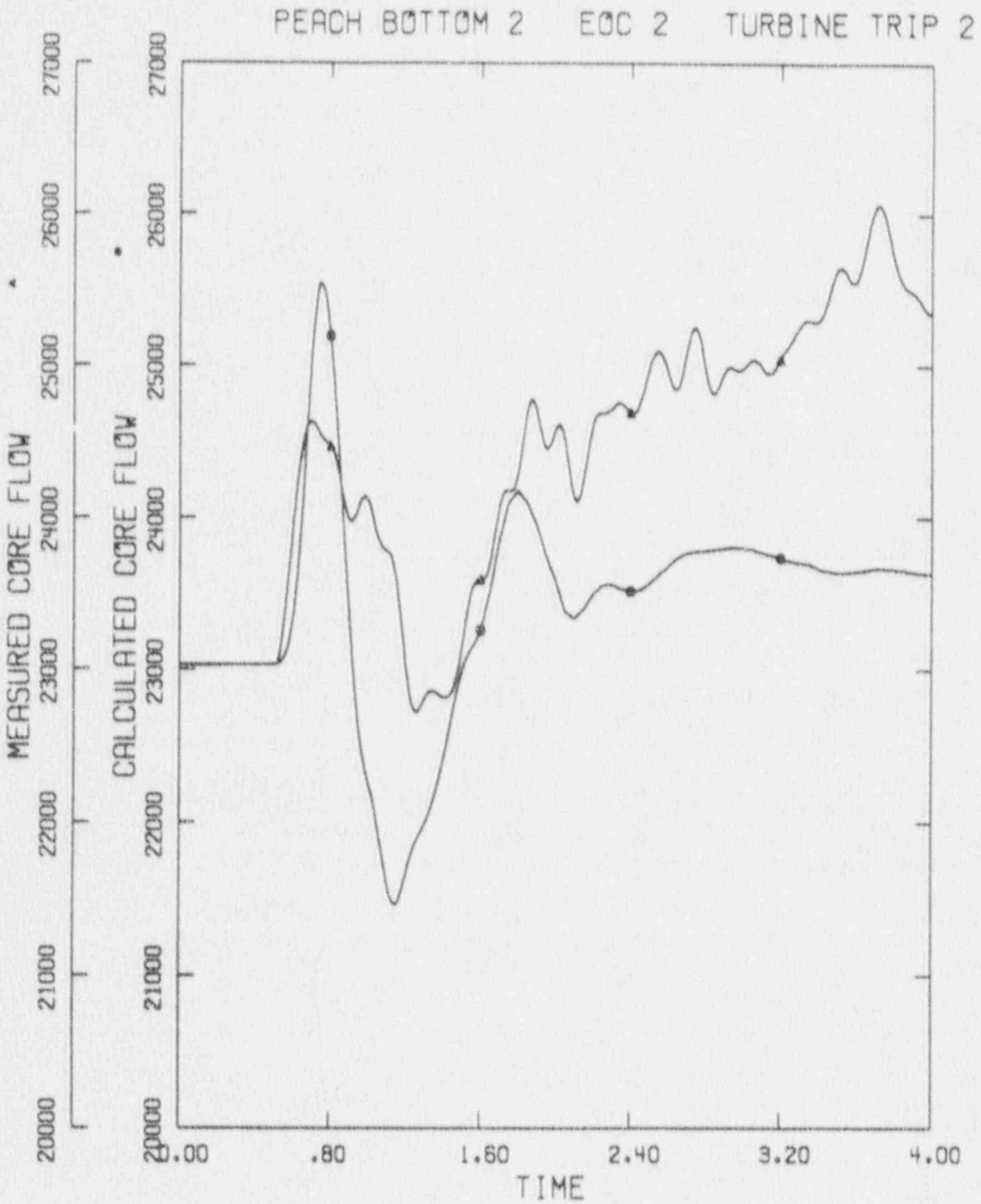

Figure 7.12 Predicted vs Measured Core Average Power, Peach Bottom Test TT3

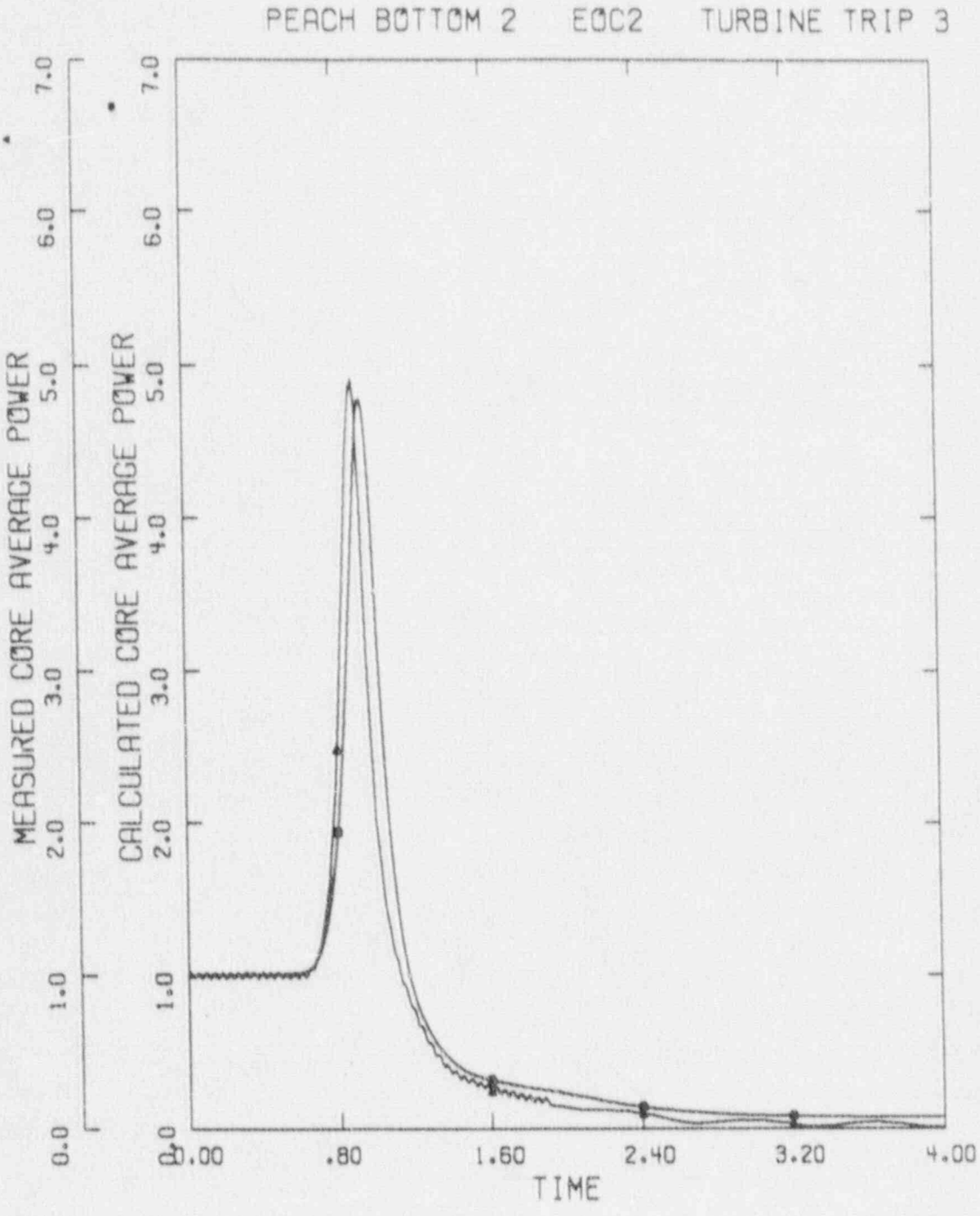

Figure 7.13 Predicted vs Measured Upper Plenum Pressure, Peach Bottom Test TT3

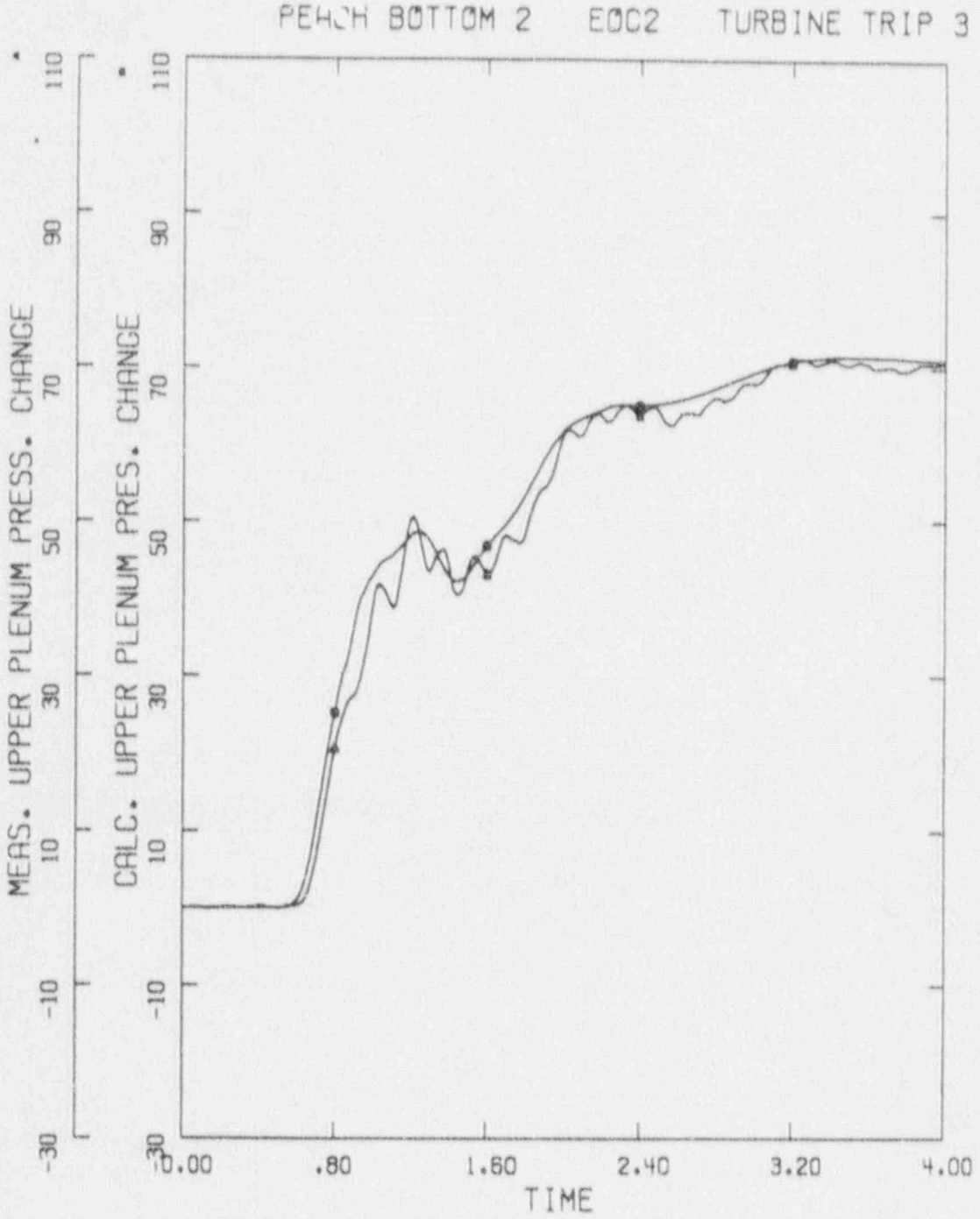

Figure 7.14 Predicted vs Measured Dome Pressure, Peach Bottom Test TT3

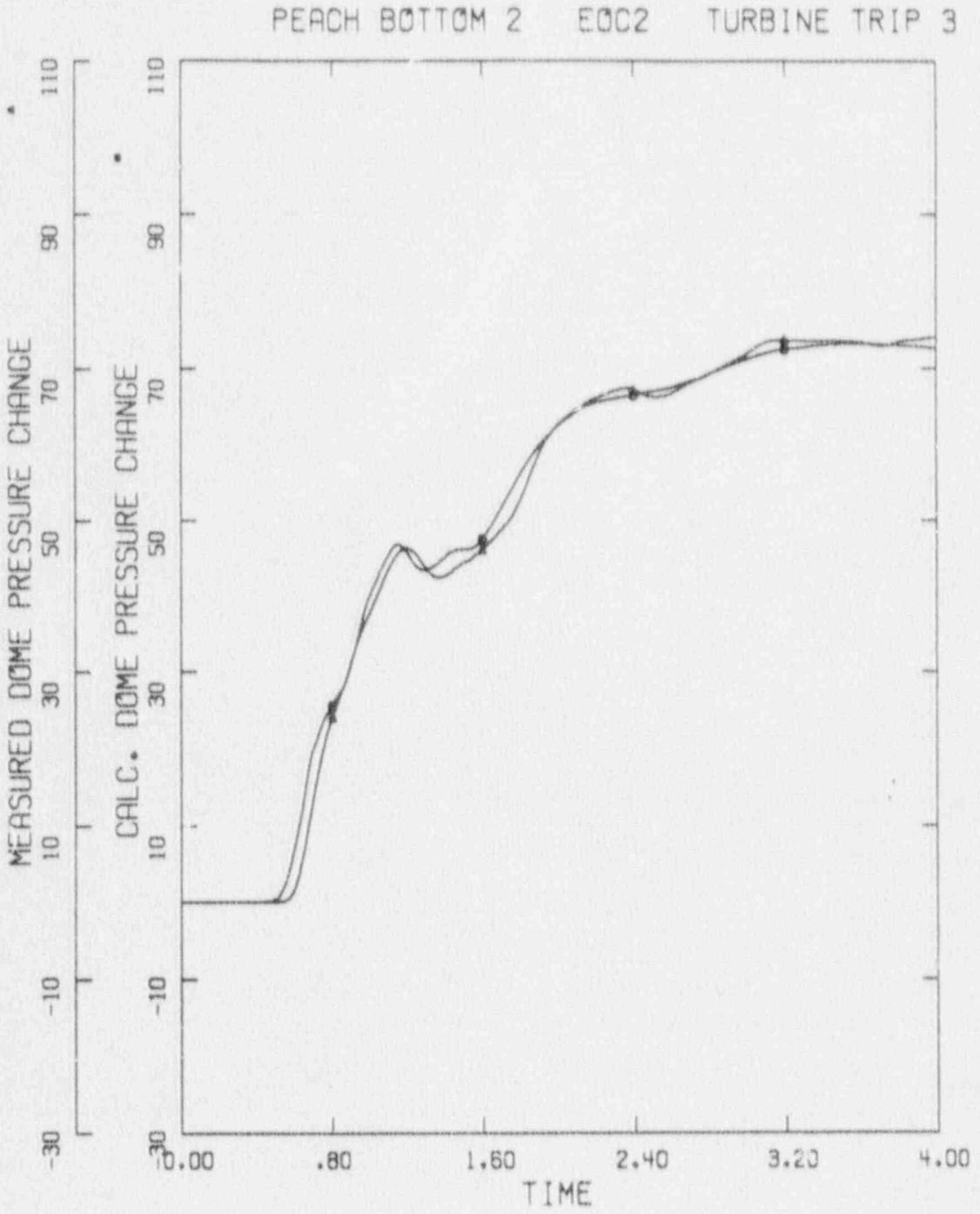

Figure 7.15 Predicted vs Measured TSV Pressure, Peach Bottom Test TT3

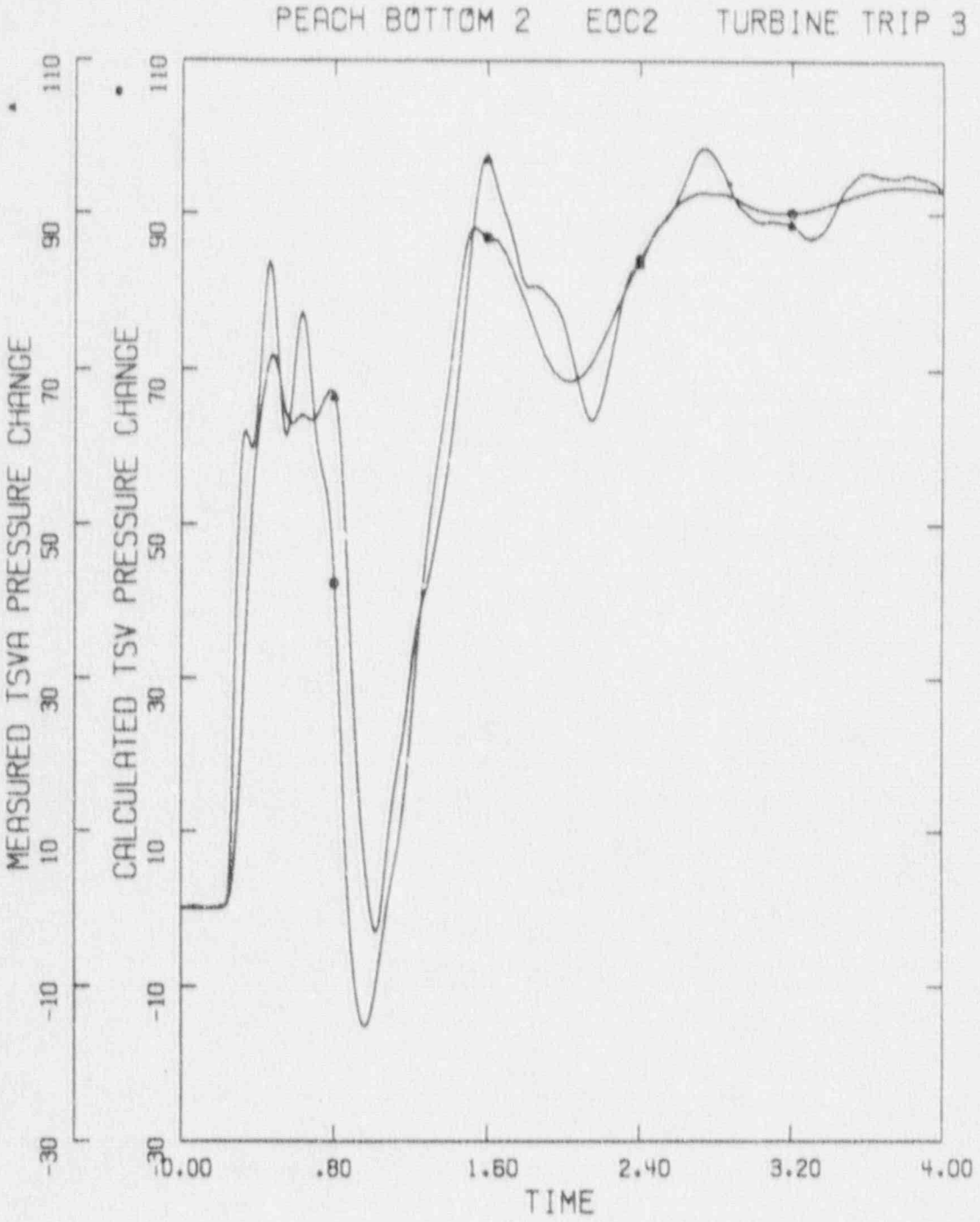

Figure 7.16 Predicted vs Measured Core Inlet Flow, Peach Bottom Test TT3

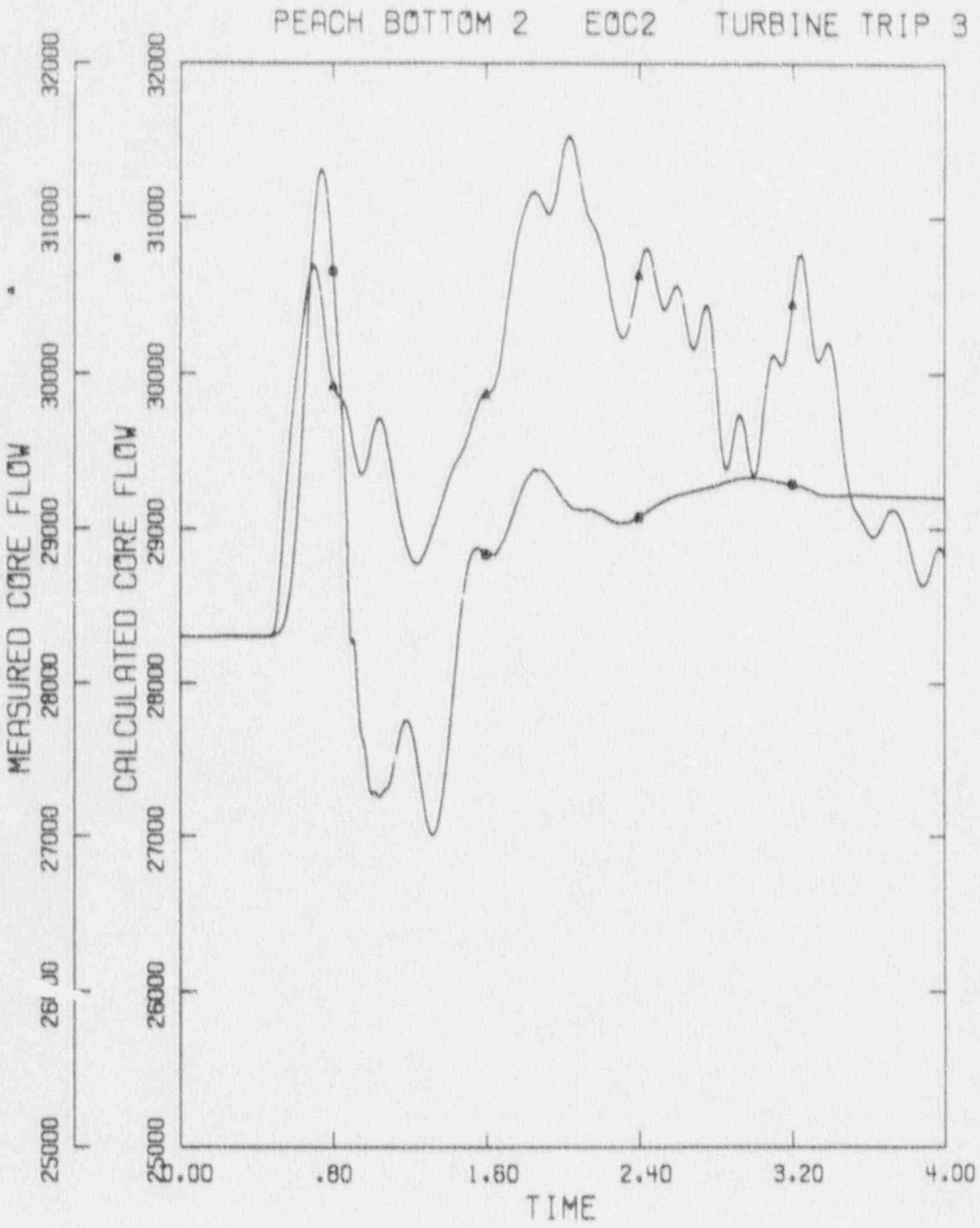

Figure 7.17 Axial Power Distribution, Peach Bottom License Basis Transient

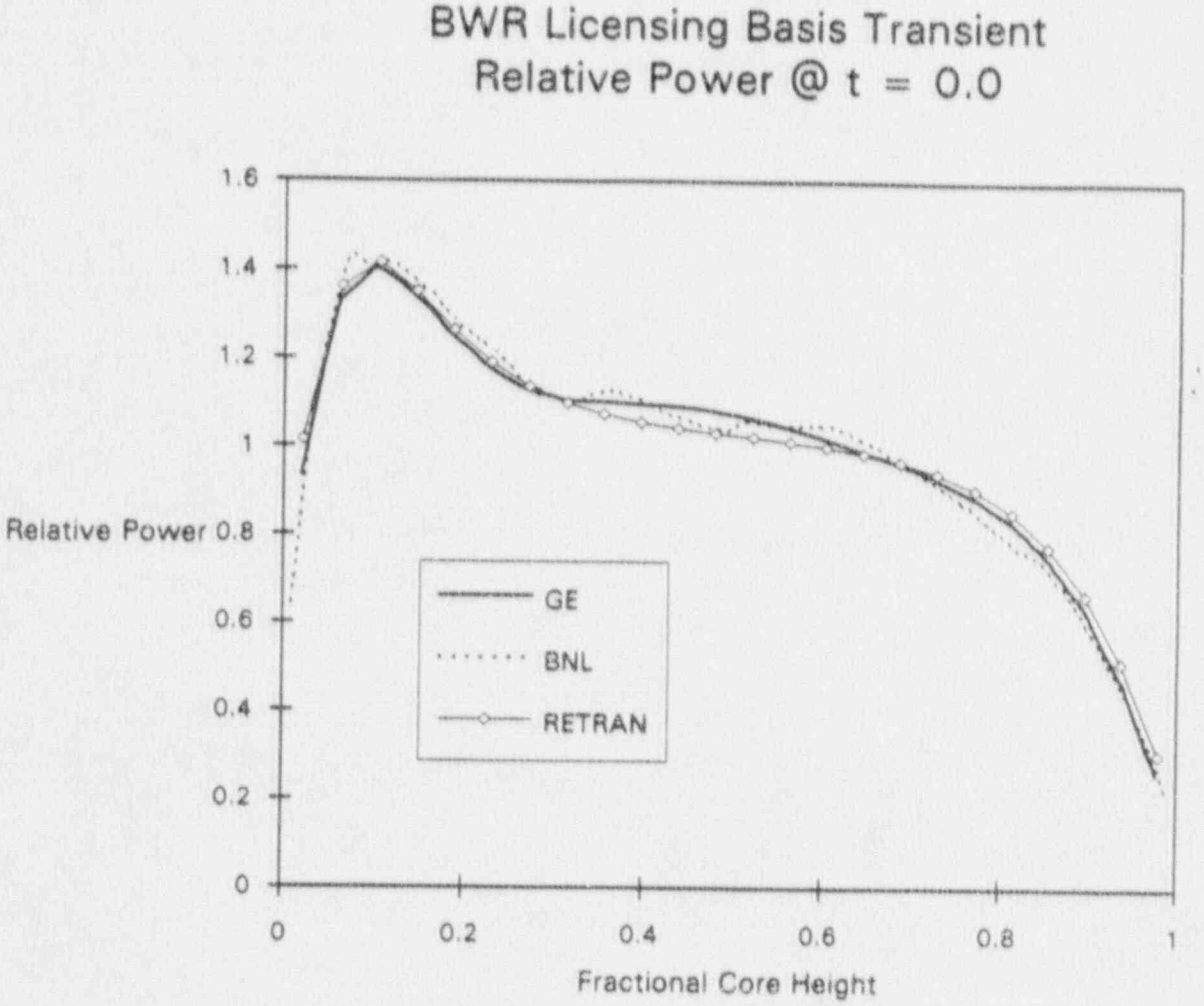

Figure 7.18 Fuel Temperature Distribution, Peach Bottom License Basis Transient

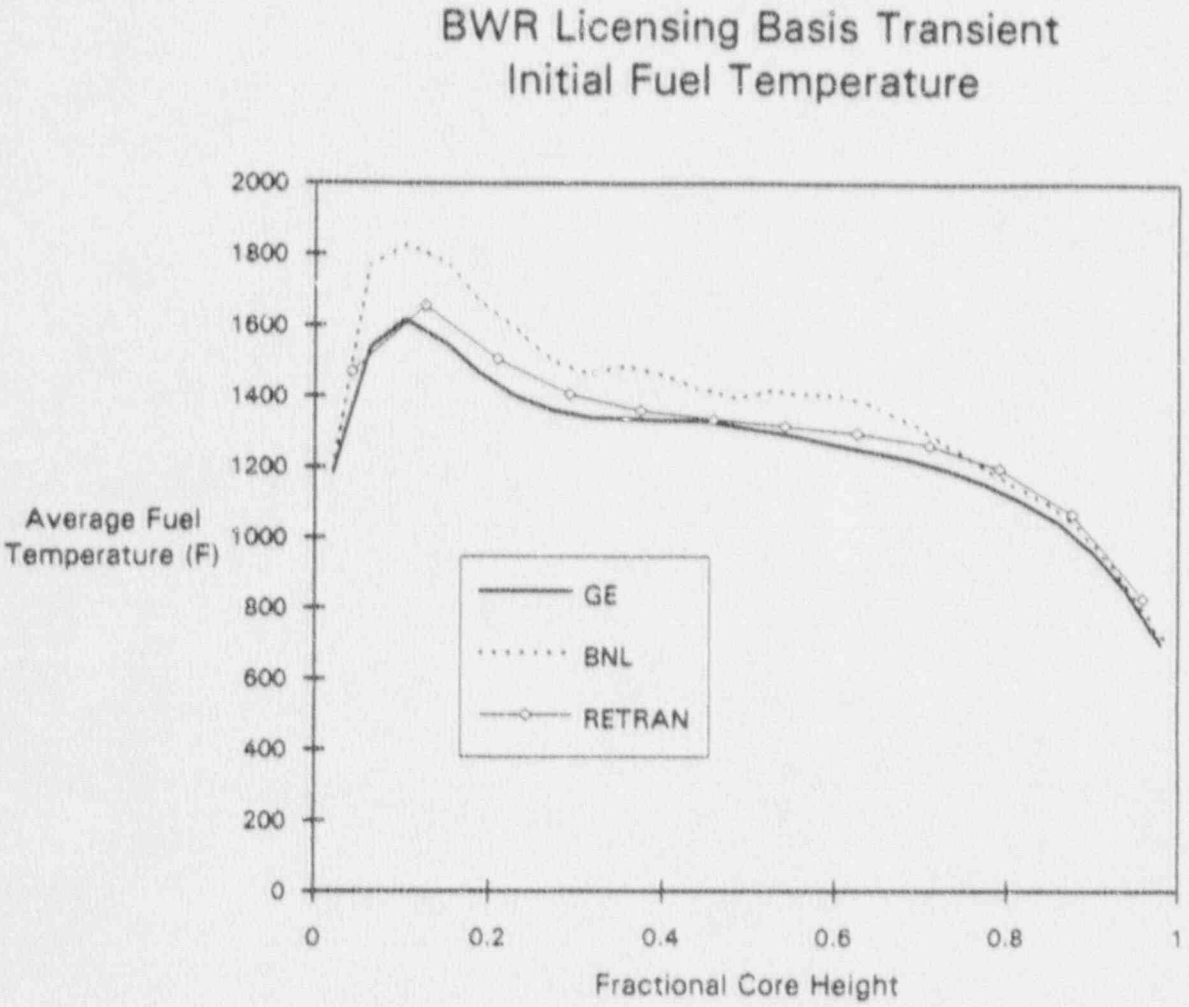

Figure 7.19 Initial Heat Flux Distribution, Peach Bottom License Basis Transient

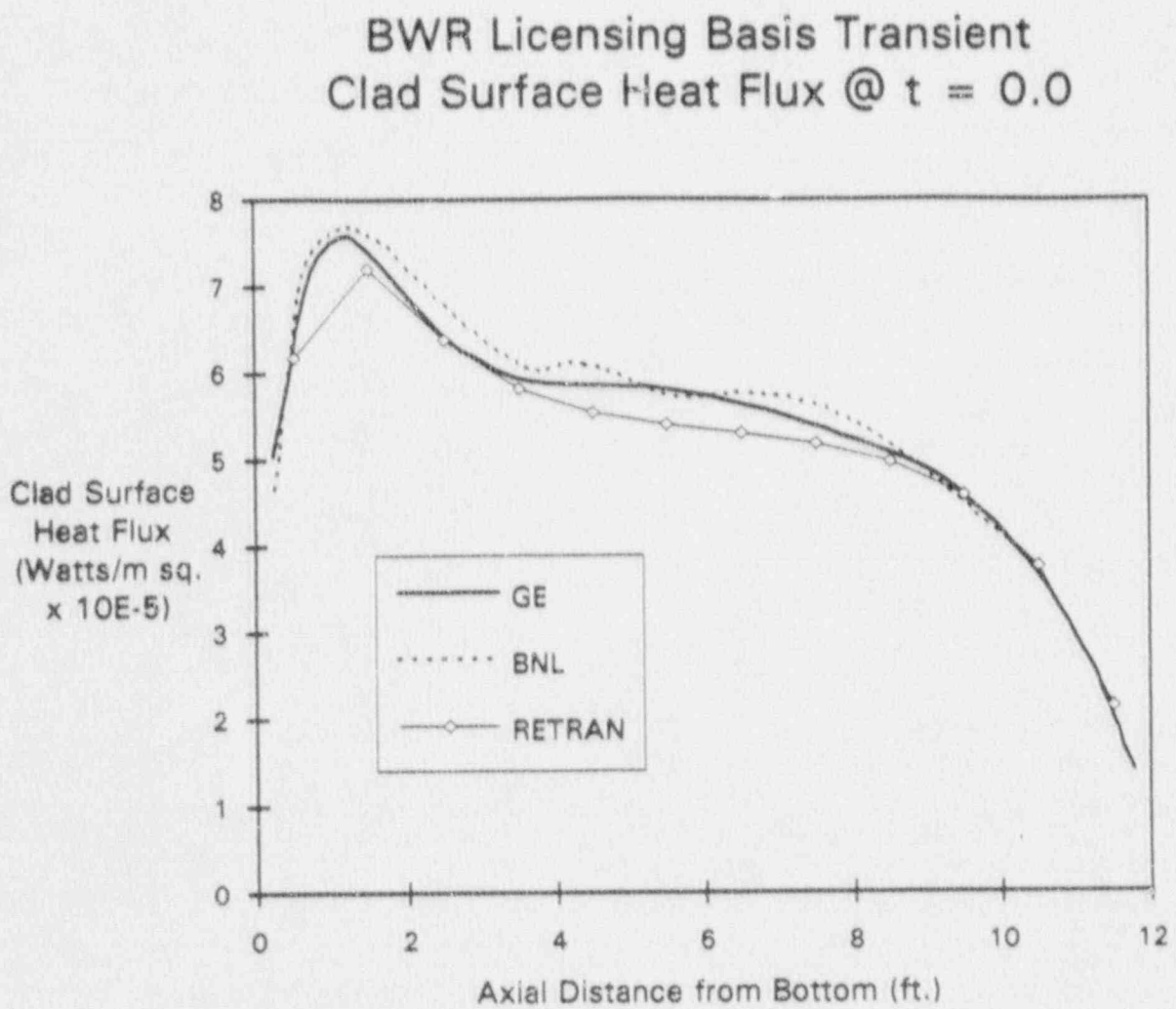

Figure 7.20 Initial Void Distribution, Peach Bottom License Basis Transient

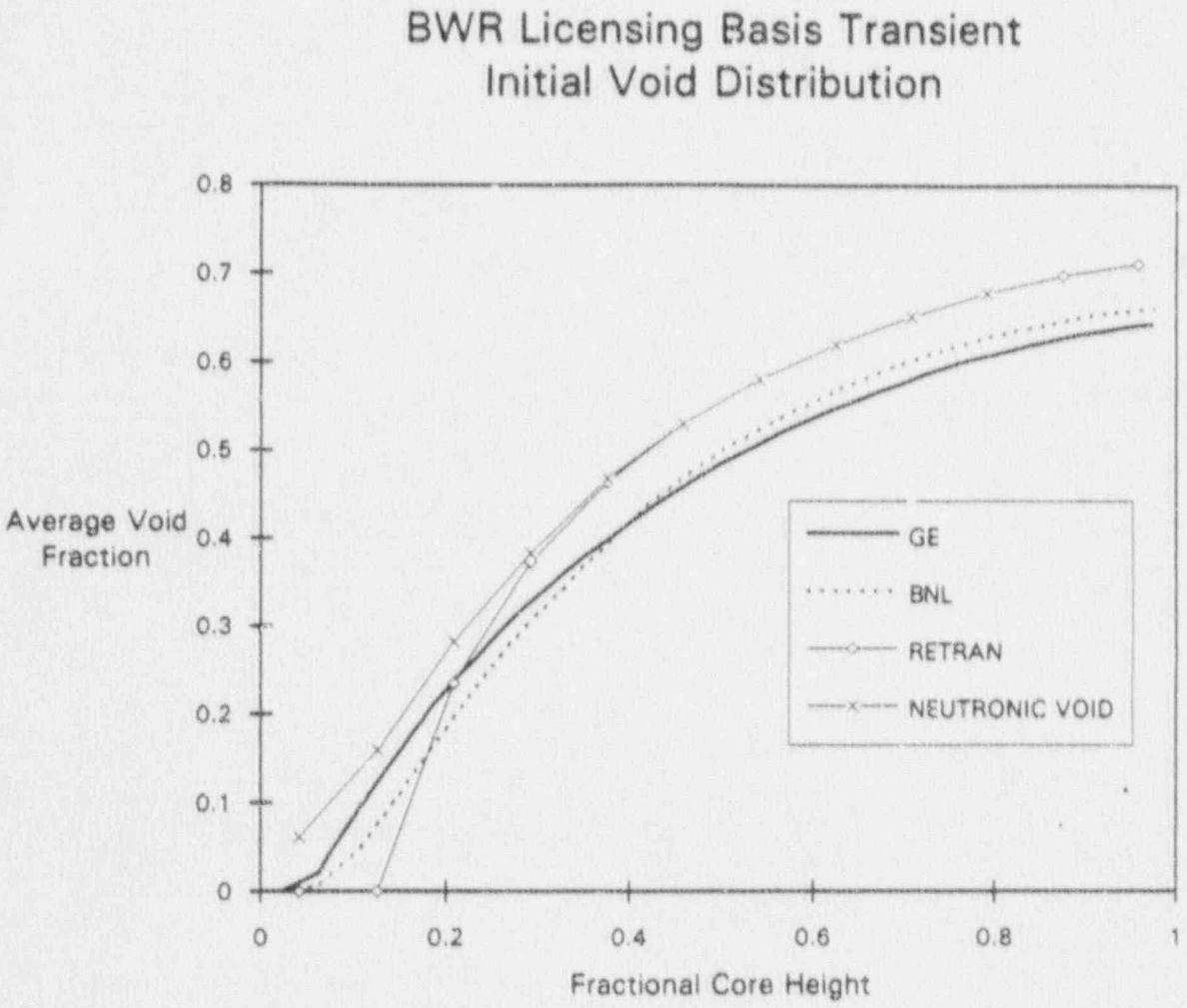

Figure 7.21 Core Average Power, Peach Bottom License Basis Transient

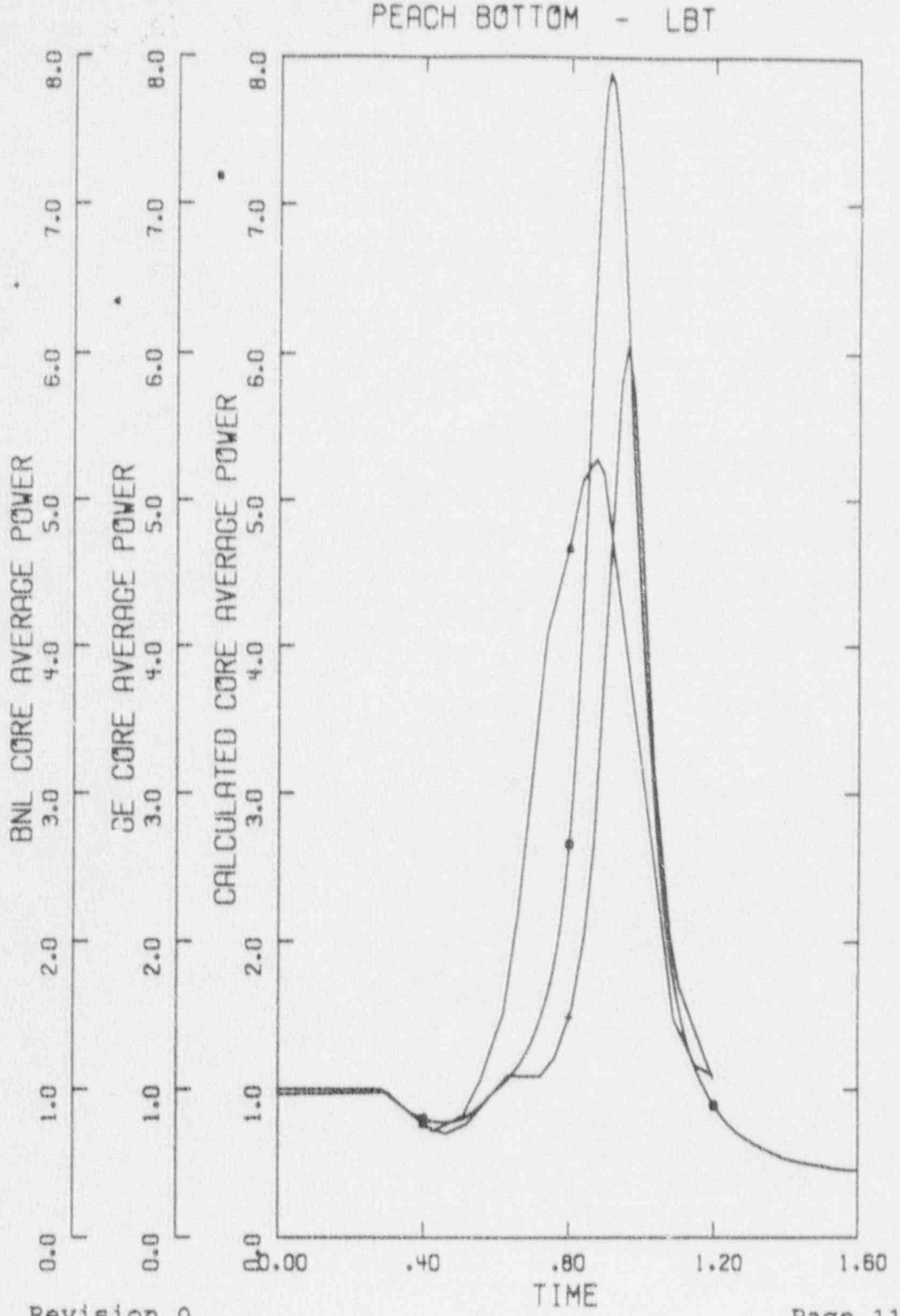

Figure 7.22 Upper Plenum Pressure, Peach Bottom License Basis Transient

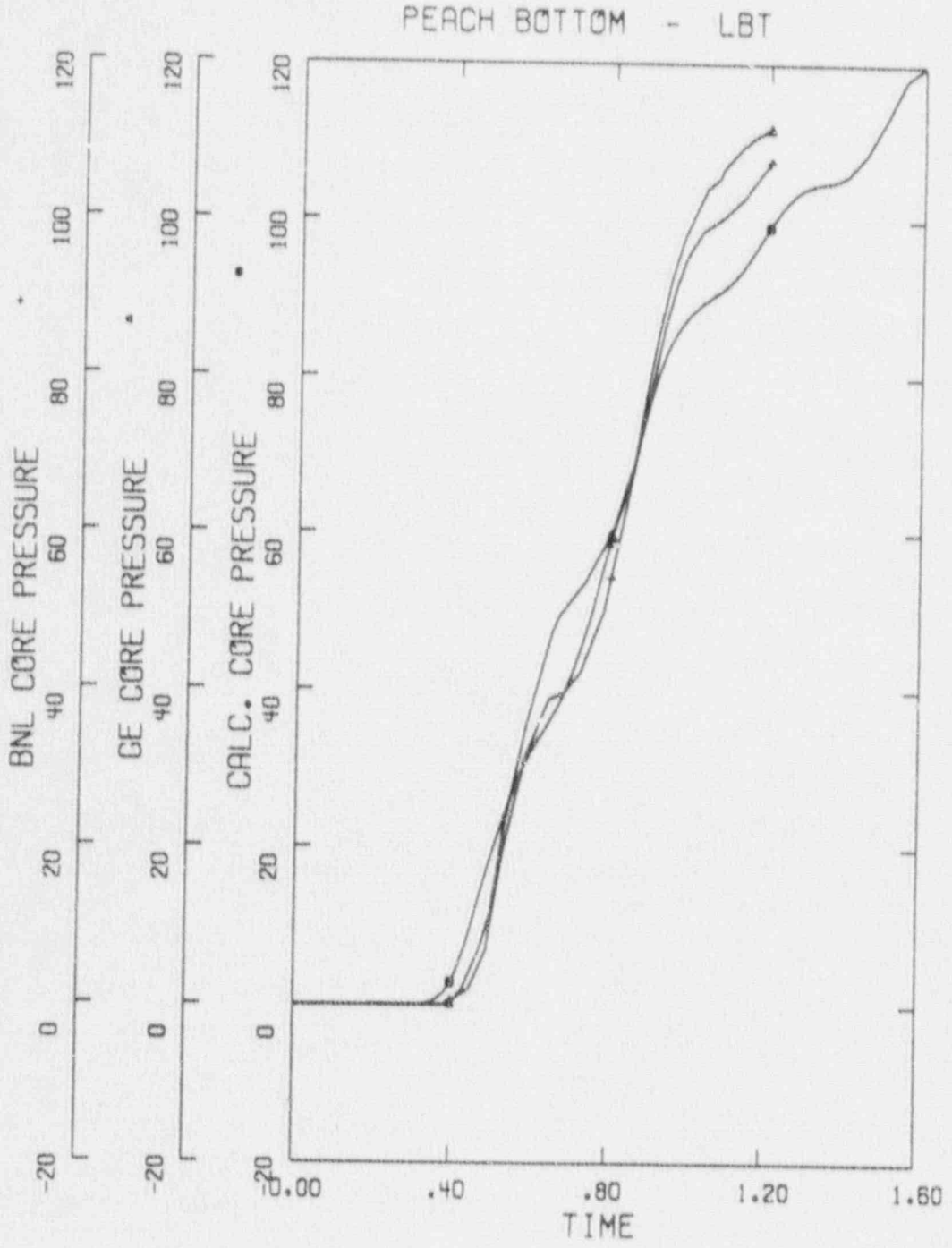

Figure 7.23 Core Inlet Flow, Peach Bottom License Basis Transient

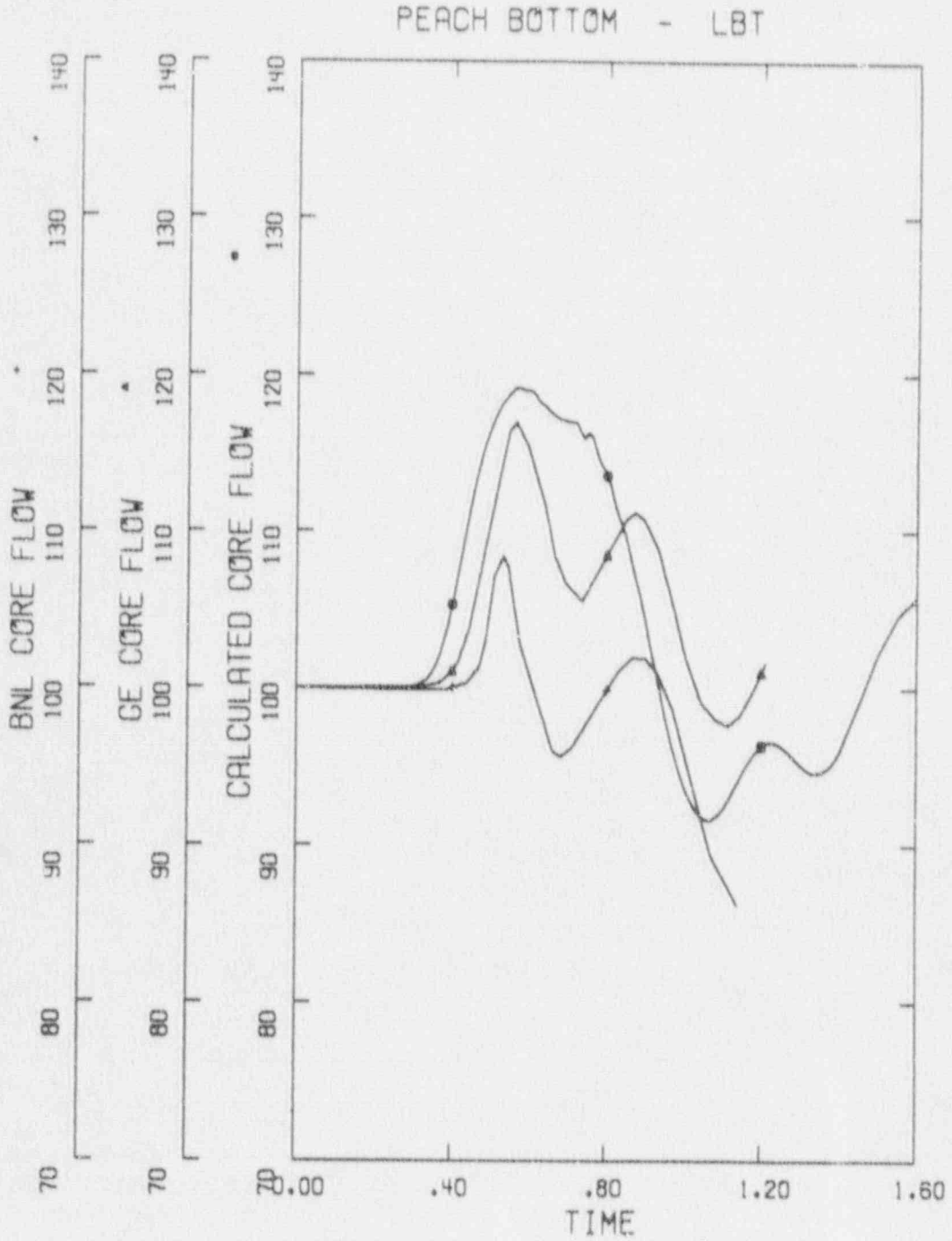

Figure 7.24 Heat Flux Distribution @ t = 0.8, Peach Bottom License Basis Transient

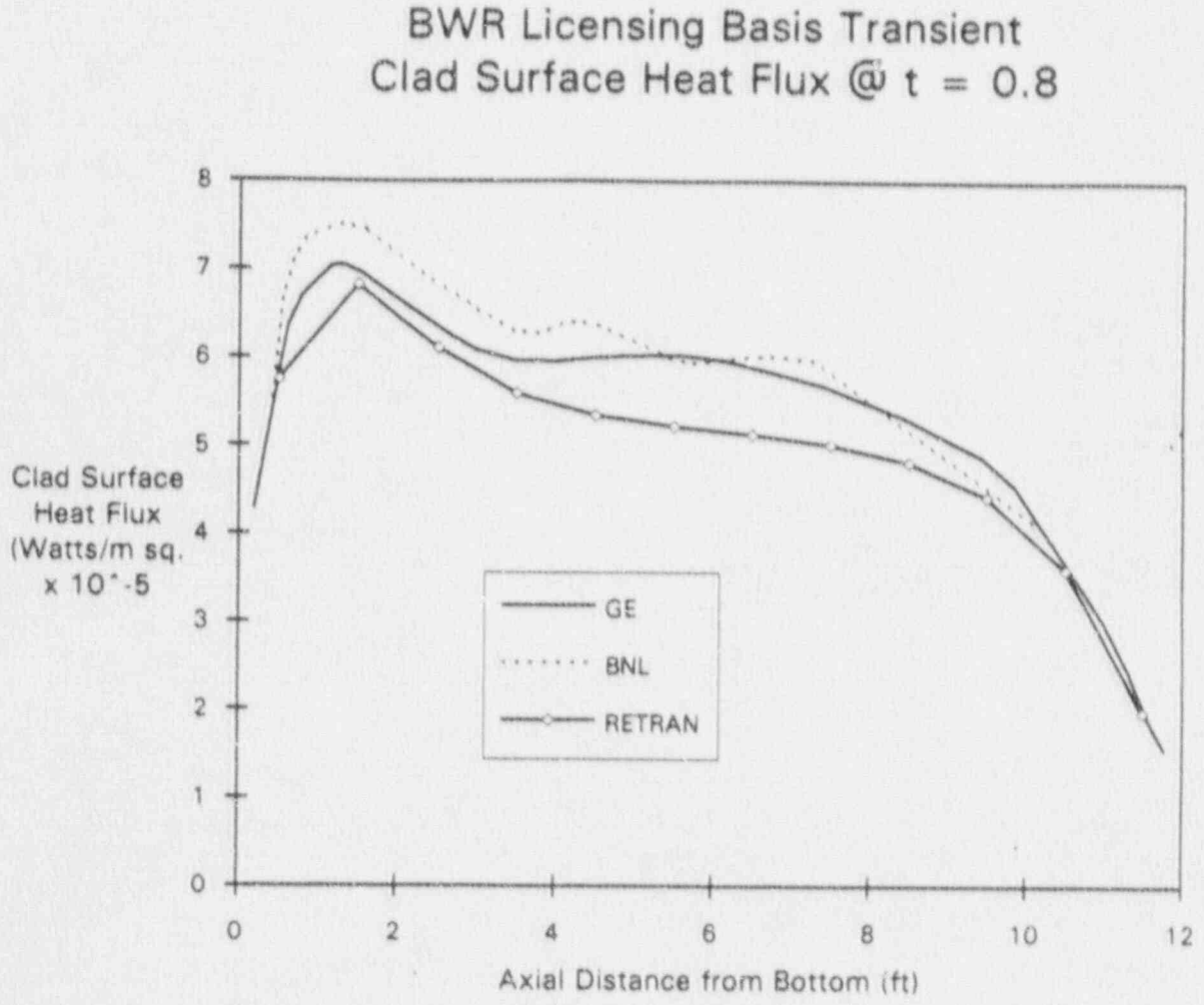

Figure 7.25 Heat Flux Distribution @ t = 1.2, Peach Bottom License Basis Transient

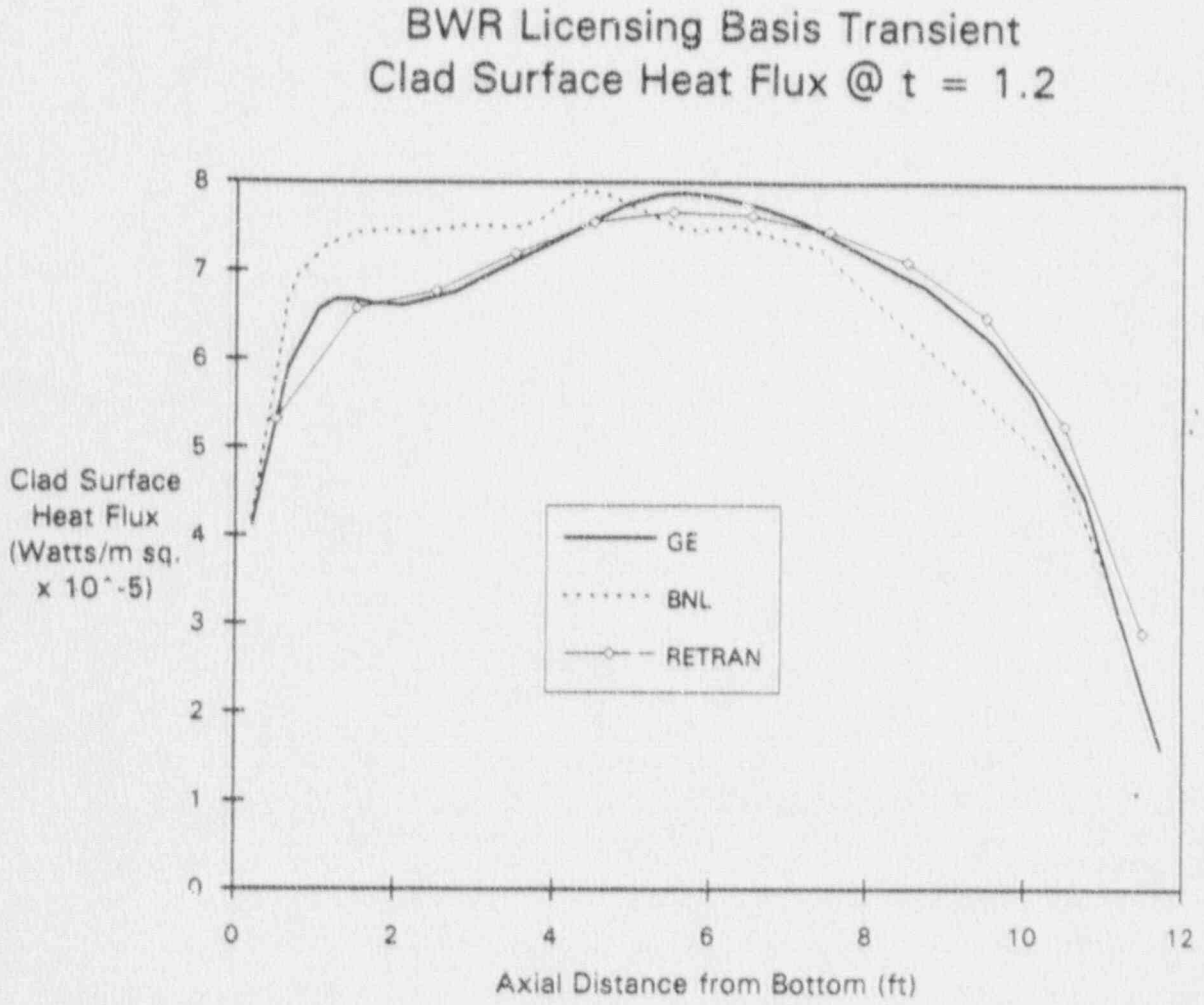

8.0 HOT CHANNEL MODEL

The overall system transient response is calculated with the RETRAN computer code. In the system model, the core is represented by a single, average power channel. The results of the system calculation: neutron flux, core pressure, core flow and inlet enthalpy as a function of time during the transient are used as boundary conditions for the RETRAN hot channel model. The hot channel is executed separately from the systems model to allow a different model to be developed for each mechanically unique fuel design in the RBS core and to facilitate changes to initial conditions such as radial and axial power distribution, gap conductance, etc., which may differ from those used for the system (core average) calculation.

The RETRAN hot channel model geometry represents the in-channel portion of one fuel bundle and the upper plenum. Figure 8.1 is a nodalization diagram of the RBS hot channel model. This model consists of 27 volumes, 27 junctions, 25 conducting heat exchangers and 25 non-conducting heat exchangers. The non-conducting heat

exchangers model the direct power deposition to the coolant.

The forcing functions (boundary conditions) for this model come from the RETRAN systems transient calculation. The hot channel rod conduction power is proportional to the transient neutron flux; as is the power fraction directly deposited in the active coolant due to gamma heating and neutron slowing down. The upper plenum in the hot channel model is a RETRAN time-dependent volume, set to the pressure versus time from the system calculation. The inlet to the hot channel is a RETRAN positive fill, so that the inlet flow and enthalpy may be specified. The inlet enthalpy is taken directly from the systems calculation; the core flow from the systems calculation is multiplied by the fraction of the total flow which enters the active zone of the hot channel.

The flow distribution fraction is calculated by a response surface fit to a series of parametric FIBWR core hydraulic calculations. FIBWR calculates the multi-channel inlet flow distribution, including leakage flows and water tube flows. The independent parameters of this response surface fit are core power, flow, pressure and radial peaking factor. The core flow distribution was

found to be insensitive to the calculated change in inlet enthalpy. By using an inlet flow forcing procedure, rather than a plenum-to-plenum pressure drop forcing function, the potential for inconsistencies between the systems model and the hot channel model from differences in pressure drop models, flow regime options, nodalization, inertia and time step selection are minimized.

In addition to the above forcing functions, the axial power shape and gap conductance must be specified for the hot channel model. An axially averaged representative value of 2315 BTU/hr-ft^2-°F was used in the hot channel analysis. This value was determined by the RBS ESCORE model to be typical of high-powered assemblies of the current fuel design which may be on thermal limits at end-of-cycle conditions. In accordance with the GETAB[17] procedure for BWR/6, a standard 1.4 middle-peaked axial power distribution is used for hot channel analysis. Sensitivity studies have shown that ΔCPR is somewhat dependent on axial power shape, with a top peaked power distribution yielding a higher ΔCPR. However, because a high power assembly will also have high voids, the probability is low that an assembly near thermal limits will be peaked above mid-core.

Output from the RETRAN hot channel model is processed by EDTRAN to determine ΔCPR. This calculation is described in a separate report.

Figure 8.1 RBS RETRAN Hot Channel Nodalization

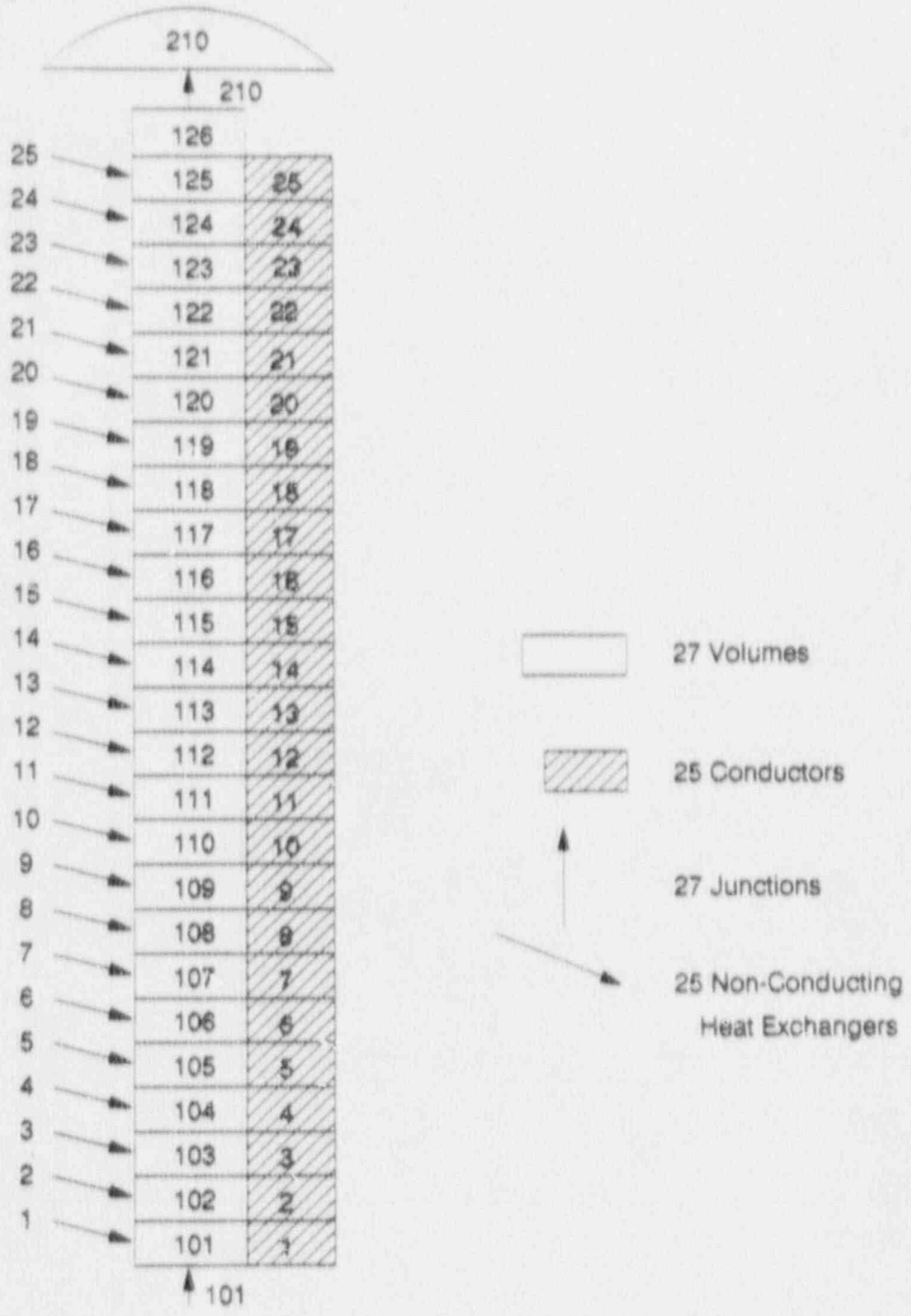

9.0 REFERENCES

1. C.H. Greene, et. al., "Steady State Core Physics Methods for BWR Design and Analysis," **EA-CA-91-0001-M**, Gulf States Utilities Company (1991).

2. A.F. Ansari, et. al., "FIBWR - A Steady-State Core Flow Distribution Code for Boiling Water Reactors," **EPRI NP-1923**, Electric Power Research Institute (1981).

3. A. F. Ansari, et. al., "FIBWR: A Steady-State Core Flow Distribution Code for Boiling Water Reactors, Code Verification and Qualification Report,", **EPRI NP-1923**, Electric Power Research Institute (1987)

4. J. A. McClure and G. C. Gose, "SIMTRAN-E: A SIMULATE-E to RETRAN-02 Datalink", **EPRI NP-5509-CCM**, Electric Power Research Institute (1987).

5. I. B. Fiero, "ESCORE: The EPRI Steady-State Core Reload Evaluator Code", **EPRI NP-4492-CCMP**, Volumes I and II, Electric Power Research Institute (1986).

6. B.J. Gitnick, "Consistent Initialization of Pressure and Flow Parameters for BWR Transient Analysis at Off-Rated Power and Flow Conditions," *Nuclear Technology*, January 1991, pp. 92-104.

7. J.H. McFadden, et. al., "RETRAN-02 - A Program for Transient Thermal-Hydraulic Analysis of Complex Fluid Flow Systems," **EPRI NP-1850-CCM**, Volumes I, II, and III, Electric Power Research Institute (1981).

8. C. S. Brennan, "EDTRAN: A Program for the Editing, Linking and Post Processing of RETRAN Computer Runs", **PSE&G NFU-0090**, Public Service Electric and Gas of New Jersey (1988).

9. General Electric Company, "GEXL-PLUS Correlation Application to BWR/2-6 Reactors, GE6 through GE8 Fuel", **NEDC-31598P**, (1988), Proprietary.

10. D.A. Prelewicz, et. al., "BWR Water Level Modeling," Proceedings: Sixth International RETRAN Conference, Electric Power Research Institute (August 1990), p. 15-1.

11. J.S. Miller, et. al., "RETRAN Simulation of a BWR/6 Load Rejection Transient," Fifth Proceedings of Nuclear Thermal-Hydraulics, ANS Winter Meeting (November 1989), pp. 350-358.

12. L.A. Carmichael and R.O. Niemi, "Transient and Stability Tests at Peach Bottom Atomic Power Station Unit 2 at End of Fuel Cycle 2," **EPRI NP-564**, Electric Power Research Institute (1978).

13. M.S. Lu, et al., "Analysis of Licensing Basis Transients for a BWR/4," **BNL-NUREG-26684**, Brookhaven National Laboratory (1979).

14. K. Hornyik and J. A. Nasser, "RETRAN Analysis of the Turbine Trip Tests at Peach Bottom Atomic Power Station Unit 2 at the End of Cycle 2", **EPRI NP-1076-SR**, Electric Power Research Institute (1979).

15. A.M. Olson, "Methods for Performing BWR Systems Transient Analysis," **PECo-FMS-0004**, Philadelphia Electric Company (1987).

16. "Qualification of the One-Dimensional Core Transient Model for Boiling Water Reactors," **NEDO-24154**, Volume I, General Electric Company (1978).

17. "General Electric Thermal Analysis Basis; Data, Correlation, and Design Application," **NEDO-10958A**, General Electric Company (1977).

APPENDIX A

CALCULATION OF FUEL ROD GAP CONDUCTANCE

List of Tables

List of Figures

CALCULATION OF FUEL ROD GAP CONDUCTANCE

This appendix describes the use of the ESCORE computer program to calculate fuel rod gap conductance for use in RETRAN system and hot channel analyses. The following sections describe the preparation of ESCORE cases.

1.0 ESCORE CALCULATION METHODOLOGY

This section describes the use of the ESCORE computer program to evaluate fuel rod thermal-mechanical effects. The following sections describe the selection of axial power shapes and the determination of the remainder of the ESCORE input.

1.1 AXIAL POWER SHAPE IN ESCORE CALCULATIONS

Fuel rod gap conductance is axially variant, and each nodal value is slightly dependent on the other nodes in the fuel rod via the gas gap temperature. While an

axially dependent gap conductance could be calculated in RETRAN, thermal-mechanical coupling between nodes is not available in the current coding. A utility RETRAN study[1] demonstrated that an axially averaged gap conductance produces nearly the same total heat deposited in the coolant as a function of time as the axially variable gap conductance for typical pressurization events. Selection of conservative gap conductance values for the core average application makes a greater difference in the transient consequences than the use of the axially averaged value. ESCORE calculated values of axially averaged gap conductance are used in the RETRAN system model.

Another study in Reference 1 determined the effect of using an axially averaged gap conductance in the RETRAN hot channel model. For various axial power distributions examined in the study, the axially averaged gap conductance produced equal or higher calculated ΔCPRs than the axially variable gap conductance. An axially averaged gap conductance is therefore used for the hot channel analysis, since higher values of ΔCPR indicate more severe thermal margin effects during transients.

1.2 ESCORE INPUTS

This section describes the preparation of input for the ESCORE gap conductance calculation. Separate input streams are required for system modeling and hot channel modeling because the conservatisms required for each application of the gap conductance are different.

Input parameters which are well characterized physical properties (such as yield strength) are taken at established, nominal values.

Parameters which are controlled within fabrication tolerances are also taken at nominal values when used in the ESCORE analysis. Use of nominal values is appropriate because both the core average and hot bundle calculations represent statistical evaluations of a large number of fuel rods and pellets; the mean values of these parameters will be the nominal values for the material lots. These parameters include grain size, pellet O.D., cladding I.D., and rod pre-pressure.

Other parameters which are not as strongly characterized and do not strongly affect the results as demonstrated by parametric analyses performed by others[1] are also set to their nominal values. These parameters

include fuel pellet densification, fast flux to Linear Heat Generator Rate (LHGR) factor, system pressure, and resonance escape probability.

Axial power distribution and power history strongly affect the results and are chosen at conservative values.

2.0 POWER HISTORY IN ESCORE CALCULATIONS

Fuel rod thermal-mechanical effects are strongly dependent on the irradiation history of the fuel rod. These effects include pellet phenomena (densification, cracking, swelling, and fission gas release), cladding phenomena (embrittlement, creepdown, and pressurization), and interaction phenomena (pellet-cladding interaction and axial stack growth).

2.1 CORE AVERAGE GAP CONDUCTANCE

The core average gap conductance determines how changes in total core power causes changes in heat deposited to the coolant. The high power bundles

contribute more to the core thermal response than low power bundles because high power bundles generally have higher gap conductances than low power bundles. Using all of the bundles in the core and number weighting the bundles underestimates the core average void response.

The gap conductance of an individual fuel rod generally increases with burnup because the width of the gap decreases as the fuel pellet swells and the cladding creeps down toward the pellet. This effect is offset to some extent by decreased conductivity of the fill gas caused by the release of fission products from the material lattice. On a core average basis, pellet cladding contact does not occur and the over prediction of contact conductance by the ESCORE code is not a concern.

The core average gap conductance is based on a statistical weighting of the number of fuel rods operating within a certain power range at various burnup points during each cycle for the various type fuels in the core (i.e. fresh, once burned, and twice burned). The rod average gap conductance is determined for each power interval and then weighted by the fraction of the rods in this interval. Corewide power and exposure distributions

for this analysis are determined in the nuclear design analysis.

An initial burnup interval of 0-3.7 GWd/T is used because this is near the end point of densification where the minimum gap conductance value would be attained. Additional calculations cover subsequent burnup increments of approximately 4 GWd/T to a maximum exposure of approximately 12 GWd/T for the fresh fuel. This defines four statepoints from beginning to end of cycle. Table A-1 presents the power and power history information necessary to determine the core average gap conductance.

The gap conductance value at each kW/ft value within a given statepoint box is determined for each burnup interval or statepoint. This gap conductance value is then weighted by the relative number of rods in each increment to define an overall average value for a statepoint box. That is, considering the fresh fuel, the burn history, as the calculation proceeds from left to right, is made by assuming that the fresh fuel burns at the average value of all the fresh fuel in the core. This procedure is then repeated in burning the history from statepoint 2 to statepoint 3 at the average value between each statepoint. In the case of the once burned

fuel which has a prior burn history before the start of statepoint 1, it is assumed that the prior history is the average obtained by the fresh fuel which was in the previous cycle. The once burned fuel is then burned from statepoint 1 to statepoint 3 at the average value of all the once burned fuel between each statepoint. Similarly, in the case of twice burned fuel which has a prior burn history before the start of statepoint 1, it is assumed that the prior history is the average obtained by the once burnad fuel in the previous cycle. The twice burned fuel is then burned from statepoint 1 to statepoint 3 at the average value of all the twice burned fuel between each statepoint. Finally at the end of each burn point, the power level is stepped to the particular power level of interest. To further illustrate this point a typical core average gap conductance power histogram is shown in Figure A-1 for fuel rods in the 5-6 kW/ft range.

Using the increment-averaged power for the statepoint to statepoint power history and prior cycle averages for the once burned and twice burned fuel results in a very smooth power history for the analysis. Path-dependent effects are minimized by this lack of power fluctuations, resulting in a conservatively low

value of the calculated core average gap conductance. This entire analysis was performed using an end of cycle bottom peaked Haling axial power profile to establish the trend in core average gap conductance with burnup. Since the trend revealed increasing gap conductance with burnup, the calculation was not performed for statepoint 4.

2.2 Hot Channel Gap Conductance

The power history in the hot channel gap conductance calculation is biased to maximize pellet and relocation cracking without excessive fission gas release. The bundle is modeled as a single fuel rod.

The rod operates with the peak node at the Maximum Average Planar Linear Heat Generation Rate (MAPLHGR) limit for the first .001 GWd/T using a top peaked axial power shape. The rod then operates with the peak node at the MAPHLGR limit for the period .001 - .002 GWd/T using a middle-peaked axial power shape. This power history produces substantial pellet cracking and relocation without significant fission gas release. The LHGR is then reduced to the bundle average value and then maintained constant to the second statepoint. The power is then maintained at the average value between state-

point 2 and 3 and so on until the bundle reaches the end of cycle. The axial power profile at the beginning of the statepoint is used across the burn interval and is then changed to the axial power profile at the next statepoint. This procedure is then repeated until statepoint 4 is reached.

Although the bundle average gap conductance for the once and twice burned level may be slightly higher than that obtained for the fresh fuel, it is the fresh fuel that operates at linear heat rates that are of concern for thermal margin evaluations. Only the fresh fuel is considered for determination of the maximum gap conductance. Several potential hot bundles are tracked across the burn cycle to ensure that the maximum gap conductance bundle has been identified.

3.0 ESCORE TECHNICAL EVALUATION CONCERNS

This section describes the use of the ESCORE program for gap conductance analysis. The text specifically addresses technical concerns voiced during the ESCORE regulatory review[2].

3.1 Fuel Rod Radial Power Distribution

Using extreme void distributions (such as a constant value of 0% and 80% along the entire rod), the code was allowed to calculate the resonance escape probability, P. The effect on the predicted gap conductance was very small (<3%). Any uncertainty introduced by the resonance escape probability is more than accounted for in the assumed gap conductance uncertainty of 25% that was used in the ΔCPR calculation.

3.2 Power-to-Melt and Auxiliary Power Calculation

These features of the ESCORE computer code were not used in determining the core average and hot channel gap conductance.

3.3 Fuel Rod Temperature Distribution

In this area, the overprediction of pellet clad contact conductance was addressed. Based on the proce-

dures used in the determining the core average and hot bundle gap conductance, the fuel was not predicted to experience pellet clad contact; although in some cases the predicted hot gap width was as small as 0.15 mil. The overprediction of gap conductance due to pellet clad contact conductance is not a concern for this ESCORE application.

4.0 REFERENCES

1. C.E. Dodge, "Application of Reactor Analysis Methods for BWR Design and Analysis," **PL-NF-90-001**, Pennsylvania Power & Light Company (1990).

2. A.C. Thadani, "Safety Evaluation of Topical Report EPRI NP-5100, 'ESCORE - The EPRI Steady-state Core Reload Evaluator Code: General Description,'", U.S. Nuclear Regulatory Commission (1990).

Table A-1 Example of RBS Cycle Dependent Power Distribution Used to Determine Average Gap Conductance[1]

Fresh Fuel

Rod Power (kW/ft)	BOC	Number of Rods		EOC
	Statepoint 1	Statepoint 2	Statepoint 3	Statepoint
1 - 2	232	0	0	0
2 - 3	1144	80	0	0
3 - 4	64	368	0	0
4 - 5	368	1072	240	0
5 - 6	1136	1128	1736	1832
6 - 7	2376	1848	2376	1744
7 - 8	2304	2728	3040	4568
8 - 9	2848	4340	4752	5248
9 - 10	2848	1876	1296	48
10 - 11	120	0	0	0
Total Number of Rods	13440	13440	13440	13440
Exposure Average (GWd/T)	0.1	3.77	7.53	11.36
Statepoint Instantaneous Average Power	7.1	7.3	7.6	7.6
Burn Average Power - Statepoint to Statepoint	-	7.2	7.45	7.6

Once-Burned Fuel

Rod Power (kW/ft)	BOC	Number of Rods		EOC
	Statepoint 1	Statepoint 2	Statepoint 3	Statepoint 4
3 - 4	96	96	160	256
4 - 5	600	488	832	608
5 - 6	1088	1384	1544	1268
6 - 7	2816	3600	4312	5484
7 - 8	3760	4520	3224	2562
8 - 9	1808	80	96	0
Total Number of Rods	10168	10168	10168	10168
Exposure Average (GWd/T)	12.38	15.83	19.15	22.44
Statepoint Instantaneous Average Power	6.9	6.8	6.4	6.2
Burn Average Power - Statepoint to Statepoint	-	6.85	6.6	6.3
Prior Power	7.4	-	-	-

[1]Power history and distribution taken from core follow analysis output

Table A-1 Example of RBS Cycle Dependent Power Distribution Used to Determine Average Gap Conductance (Continued)

Twice-Burned Fuel

Rod Power (kW/ft)	BOC	Number of Rods		EOC
	Statepoint 1	Statepoint 2	Statepoint 3	Statepoint 4
1 - 2	444	116	396	476
2 - 3	3996	3880	3884	3764
3 - 4	1996	2424	2036	2052
4 - 5	2168	2188	2364	940
5 - 6	2506	2640	2704	4332
6 - 7	3056	3072	3064	3068
7 - 8	464	312	184	0
Total Number of Rods	14632	14632	14632	14632
Exposure Average (GWd/T)	19.82	22.07	24.28	26.51
Statepoint Instantaneous Average Power	4.0	4.6	4.4	4.1
Burn Average Power - Statepoint to Statepoint	-	4.3	4.5	4.25
Prior Power	7.0	-	-	-

TOTAL NUMBER OF FUEL RODS IN CORE: 38240

Figure A-1 Gap Conductance Contribution by Fuel Rods in the 5-6 kW/ft Range

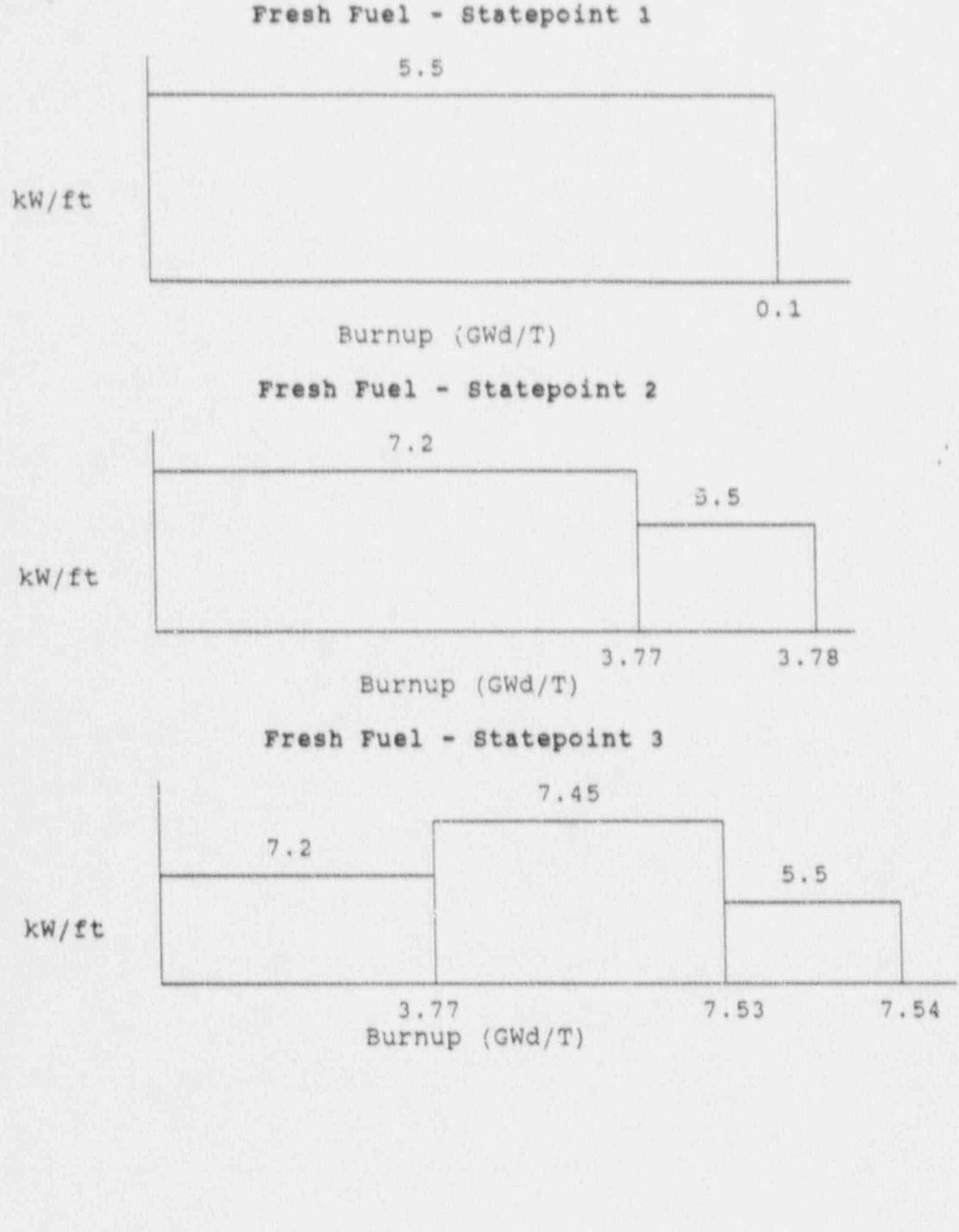

Figure A-1 Gap Conductance Contribution by Fuel Rods in the 5-6 kW/ft Range

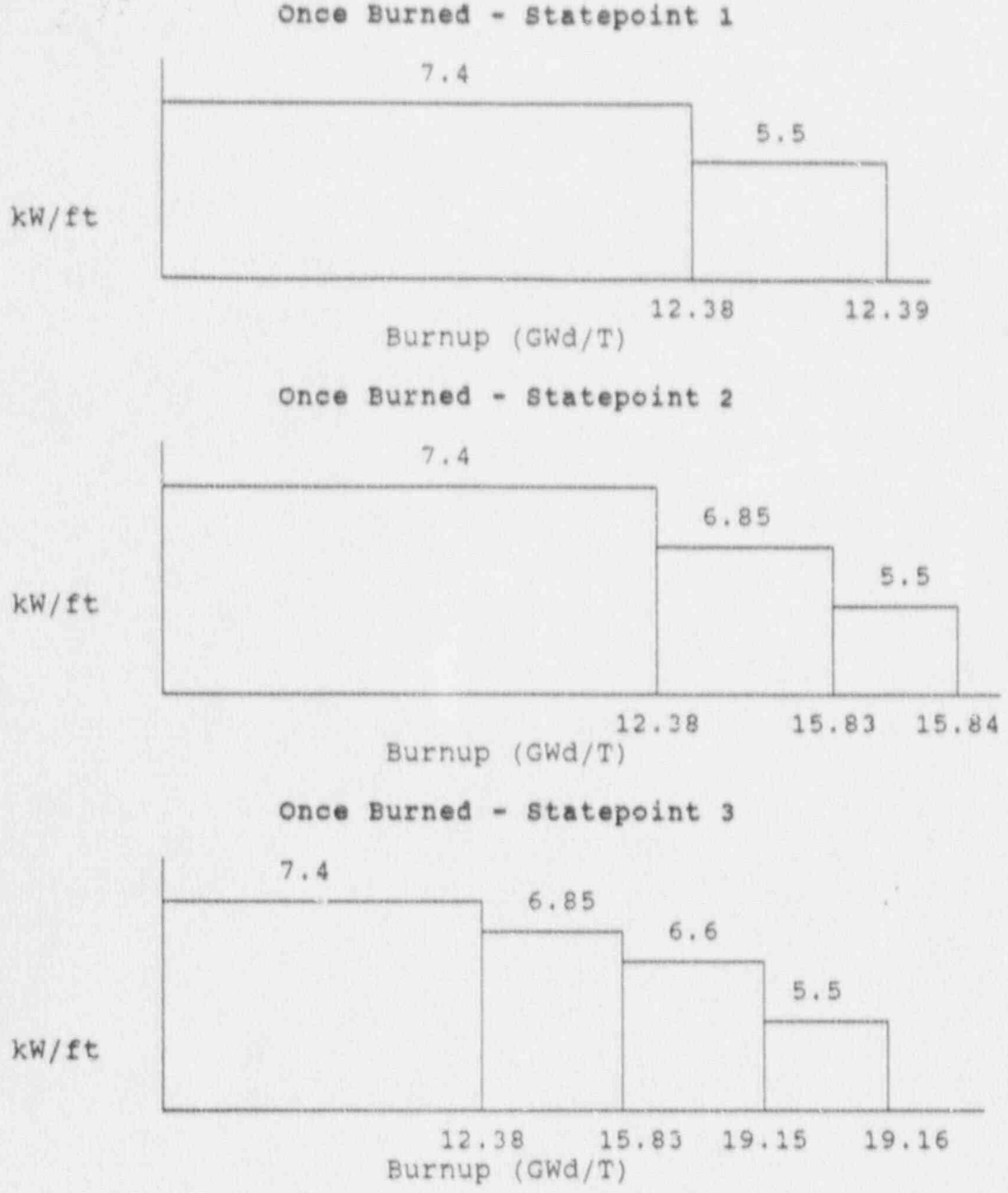

Figure A-1 Gap Conductance Contribution by Fuel Rods in the 5-6 kW/ft Range

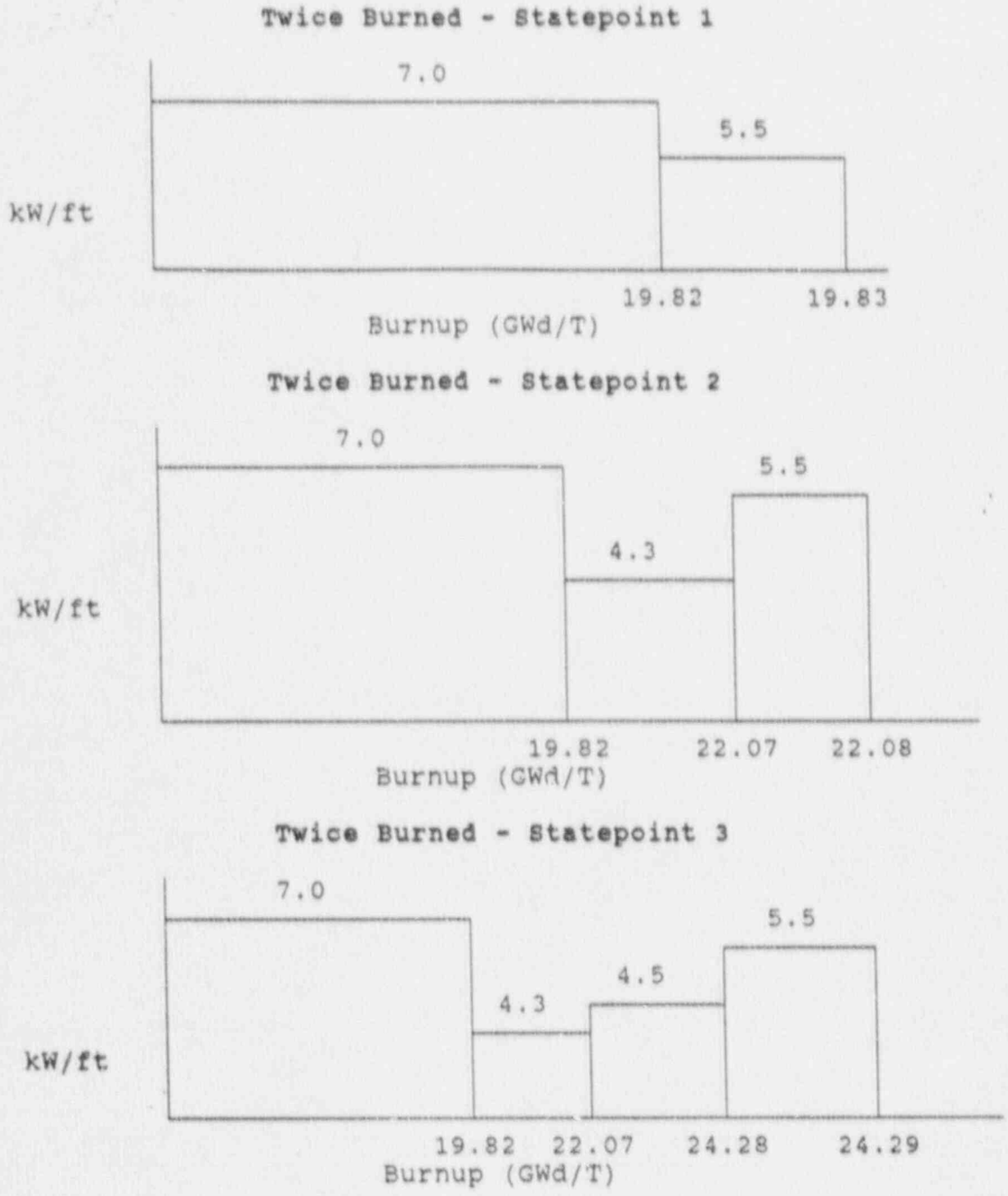

APPENDIX B

ACRONYMS USED IN THE TEXT

ACRONYMS USED IN THE TEXT

ACRONYM	SIGNIFICANCE
AOO	Anticipated Operational Occurrence
APRM	Average Power Range Monitor
BVP	Bypass Valve
BWR	Boiling Water Reactor
CPR	Critical Power Ratio
ΔCPR	Delta-CPR (Change in Critical Power Ratio)
EPRI	Electric Power Research Institute
ERIS	Emergency Response Information System
FCV	Flow Control Valve
GE	General Electric Company
GSU	Gulf States Utilities Company
HFMG	High Frequency Motor Generator
ICPR	Initial Critical Power Ratio
LBT	License Basis Transient
LFMG	Low Frequency Motor Generator
LHGR	Linear Heat Generation Rate
MAPLHGR	Maximum Average Planar Linear Heat Generation Rate
MCPR	Minimum Critical Power Ratio
MSIV	Main Steam Isolation Valve
NBR	Nuclear Boiler Rating

NSSS	Nuclear Steam Supply System
PWR	Pressurized Water Reactor
RBS	River Bend Station
RCPR	Ratio of Critical Power Ratios
SRV	Safety/Relief Valve
TCV	Turbine Control Valve
TSV	Turbine Stop Valve